Cortical Computations during Maintenance of Postural Stability:
Towards a Postural Neuroprosthetic

by

GREGORY DANIEL DISSE

DISSERTATION

Submitted in partial satisfaction of the requirements for the degree of

DOCTOR OF PHILOSOPHY

in

Neuroscience

in the

OFFICE OF GRADUATE STUDIES

of the

UNIVERSITY OF CALIFORNIA

DAVIS

Approved:

_____

Karen Moxon, Chair

_____

Gene Gurkoff

_____

Kiarash Shahlaie

_____

Sergey Stavisky

_____

Zhaodan Kong

Committee in Charge

2023

Dedication

To my fiancée and role model Dr. Sarah Mahdavi,
who has provided inspiration, patience, and adventure,
even from the depths of the hospital basement

and to my parents Greg and Geri Disse,
who have supported me from the start

Acknowledgements

Thank you first and foremost to my advisor Dr. Karen Moxon for introducing me to the world of neuroengineering and for providing guidance, opportunities, and abundant resources throughout this nonlinear scientific adventure. Your passion for science is infectious, and I will be forever grateful for what you have taught me over the last few years.

The entire Moxon Lab has been instrumental to this work. However, I would like to particularly acknowledge Dr. Bharadwaj Nandakumar and Dr. Gary Blumenthal who have been amazing mentors since my first day in the lab, teaching me all of the skills I needed to complete this degree. I could not imagine collecting data during the early, uncertain months of the Covid-19 pandemic with anyone else.

Thank you to each member of my dissertation committee. Dr. Gene Gurkoff, thank you for your guidance over the last six years, serving as my first medical school interviewer, first rotation mentor, chair of my qualifying exam committee, and now a member of my dissertation committee. Dr. Kia Shahlaie, thank you for showing me what it means to be a true neurosurgeon physician-scientist. Dr. Zhaodan Kong, thank you for guiding this non-engineer through concepts of control theory and dynamical systems. Dr. Sergey Stavisky, thank you for your enthusiasm and for exposing me to the inspiring world of human neuroengineering research.

Finally, thank you to my friends, family, and mentors who encouraged me to embark on this journey and who have provided unwavering support along the way. This dissertation would not have been possible without you.

Abstract

Despite advances in our understanding and management of spinal cord injuries (SCI), less than 1% of individuals completely recover by hospital discharge. Restoration of voluntary motor function remains one of the most desired therapeutic outcomes for individuals with these injuries. Brain-machine interfaces (BMI) have been shown to decode neural signals about movement intention and use these signals to control an external device (e.g., a cursor). Since neuronal circuitry remains largely preserved in the spinal cord distal to the injury, using decoded neural signals to control stimulation of the spinal cord itself could allow paralyzed individuals to produce self-directed movements. While the majority of lower limb BMI research has focused on restoring rhythmic locomotor movement patterns and has garnered success as it translates to human clinical trials and device development, all of these approaches have failed to generate completely independent movement in part due to an ability to restore postural stability. Compromised postural control notably increases risks of falls, carrying additional personal physical and financial burden. Therefore, it is necessary to develop a BMI to restore this critical aspect of lower limb function after SCI.

The long-term goal of this work is to develop neuroprosthetic interventions to improve motor function and improve quality of life for individuals with debilitating neurological conditions. The aims of this project specifically were to understand (1) how the cortex – the most ubiquitously used signals in neuroprosthetics – encodes for postural control, (2) the extent to which this information can be decoded to inform BMI design, and, most importantly, (3) whether or not this remains true after traumatic spinal cord injury. We demonstrate that neurons across the sensory and motor cortex convey significant information about postural perturbations, even after two different models of spinal cord injury (moderate contusion and complete transection). This information is encoded in parallel streams by speed-scaling and direction-dependent neural responses. Ground reaction forces, notably those most altered by mediolateral shifts in center of pressure, can be decoded based on

the latent dynamics of the motor cortex, with different perturbation directions requiring unique computations that can be scaled with perturbation speed. After injury, the responsiveness of individual neurons to perturbations and the information conveyed by the neurons that respond is attenuated but remains significantly above chance (and can be further enhanced with physical rehabilitation); however, as a population, cortical dynamics are largely preserved. Thus, the cortex, which is already a target in multiple brain-machine interface trials, should be considered as a control signal for a postural neuroprosthetic.

Table of Contents

List of Figures

Chapter 1 – Introduction

1.1 Brain-machine interfaces to restore motor function after neurological injury

Compromised motor function is a hallmark of many neurological conditions that raises significant quality of life challenges for many individuals. Beyond the obvious physical, economic, and emotional implications[1,2] associated with the inability to walk, grasp, or communicate, immobility poses major secondary health risks. In fact, in spinal cord injury, which often leads to severe motor impairment and immobility, a leading cause of rehospitalization is decubitus ulcers[3] which can be life-threatening, increasing risk for fatal infection or even worsening functional disability. Thus, continuing to restore mobility is critical.

One promising approach to restore function in individuals with such neurological conditions involves functionally bypassing the lesion through brain-machine interfaces (BMI), a technology that continuously records and processes neural signals to ultimately control an effector (e.g., a robotic arm, cursor, exoskeleton, etc.) or even a stimulator to elicit movements from an individual's own musculature. Initially merely science fiction, decades of advances in engineering, mathematics, and computer science have paralleled our growing understanding of the nervous system's circuitry, allowing BMI to enter the realm of translational feasibility with some applications already in clinical use for stroke[4] and epilepsy[5]. While such technology has been developed or conceived for myriad conditions – from improving deep brain stimulation electrodes for Parkinson's disease[6] to regulating

mood in psychiatric conditions[7] – this dissertation focuses specifically on BMIs aimed to restore voluntary movement.

Developing BMI to restore function after paralysis requires an understanding of how the nervous system encodes such movement. Scientists have been trying to determine how the motor cortex encodes for movement and subsequently how to interpret or "decode" these signals for decades. Evarts related the pyramidal tract neural firing rates to spontaneous[8] and conditioned[9] forces from wrist flexion and extension[10], suggesting that more activity in the motor cortex led to more muscle force. Extending this work, Georgopoulos and colleagues suggested that neurons in the motor cortex encode for movement direction, describing a cosine function that related the activity of single neurons in the primary motor cortex of monkeys to the direction in which the monkeys moved their arms[11]. The development of microelectrodes has allowed scientists to record from multiple neurons simultaneously, improving our understanding of how the brain encodes movement. Such findings led to the first demonstrations of animals controlling robotic arms using neural signals recorded directly from the motor cortex in the late nineties[12,13] and ultimately to the first demonstration in humans in 2004, when Matt Nagle, a C3 tetraplegic paralyzed from the neck down, learned to control a prosthetic arm using signal recorded from his motor cortex[14].

To date, the majority of motor BMI research has focused on restoring upper arm reaching and grasping movements[15–24], primarily through the use of an external device. In 2012, the BrainGate research consortium published a study in which they showed that two stroke survivors could learn to control robotic arms for reaching and grasping, with one individual being able to use the arm to drink coffee from a bottle for the first time unaided in almost two decades[17].

While upper limb BMI technologies have seen many successes, far fewer studies have been conducted to develop BMI control of the lower limb[25–28]. Following years of pivotal work investigating how to stimulate the spinal cord to elicit movement in animals and humans with motor impairment[29–32], it has been argued that exclusively delivering such tonic "open-loop" stimulation protocols does not provide maximal therapeutic benefit[33–37]. Meanwhile, phasic stimulation (similar to that provided by supraspinal centers[38,39,48–50,40–47]) leads to more robust recovery of function[28]. While some have shown that motor cortical activity can be used to predict hindlimb and trunk kinematics during locomotion[51] and can theoretically be adequate to control a spinal cord stimulator to induce stepping after injury[52], few have used these signals to control implanted muscle or spinal cord stimulators[27,28,53]. Recently in primates, Capogrosso et al. used hindlimb motor cortical activity to control epidural electrical stimulation to the lumbar spinal cord, restoring weight-bearing locomotion in the affected limb after a unilateral corticospinal tract lesion in the thoracic spinal cord[53]. In the same year, a study in human subjects with motor complete spinal cord injuries showed that half of participants displayed marked improvements in their motor abilities, moving from ASIA-A (no motor or sensory function) or B (no motor function) class spinal cord injuries to ASIA-C (functionally incomplete injury in which over half of key muscles below the injury can generate gravity-eliminated movement) after a year of training with an EEG-controlled lower limb exoskeleton device[54]. Thus, spinal cord neuromodulation protocols to restore locomotion are likely augmented through BMI control.

Despite great strides in restoring the ability to walk, these approaches required walkers or harnesses to provide lateral stability, or simply used a lateral hemisection model that permitted contralateral weight bearing. However, real-world movement requires the ability to respond to

obstacles, uneven terrain, and unexpected postural disturbances through the complex, concerted action of trunk and leg musculature. Minimal work in the brain-machine interface space has focused on this important function. To date, there appears to be one instance of using closed-loop control to improve trunk postural stability. In this case, bilateral kinematics, leg electromyographic signals, and ground reaction forces during continuous stepping controlled a bodyweight support system that controlled trunk orientation online[55]. They observed that proper trunk orientation improved locomotor performance. Thus, while significant progress has been made in recent years demonstrating that the same principles that led to successes in upper limb BMIs can be used for lower limb BMIs, independent lower limb function cannot fully be optimized until mechanisms to improve vertical stability in both stance and during movement are considered.

1.2 The cortex as a target for resorting postural stability

Maintaining upright posture during stance and especially during complex movements requires highly interconnected circuits within the nervous systems (see Appendix for details). Thus, in developing novel technologies to restore this critical function, one could choose from several targets along the neural axis. However, the cortex is an attractive target for several reasons.

First, from an economical perspective, maximizing the signal that can be understood from safely accessible cortical structures has several obvious advantages – especially when years of BMI efforts have used motor cortical signals. While one study controlled spinal cord stimulation with kinematic variables and ground reaction forces[37], the translatability and scalability of this method is limited. In contrast, the majority of motor neuroprosthetics use cortical signals, whether recorded intracranially

or at the surface (e.g., through EEG) as a control signal. Thus, before finding secondary targets that would require additional hardware and possible invasive implantation surgeries, extracting the most signal from a singular target has significant financial and safety incentives.

Second, from a feasibility perspective, the size and location of the cortex compared to many other structures in the nervous system involved in postural control provides many benefits. Its superficial positioning allows for safe, easy surgical access and its size provides a comfortable margin of error for the positioning of microelectrode arrays. While deeper structures (e.g., brainstem nuclei) are heavily involved in postural control, likely even leading to superior information about posture relative to that provided by the cortex, accessing these targets while avoiding damage to closely neighboring structures (such as critical respiratory centers) requires significantly more technical skill and risk.

Third, from a basic science perspective, while the cortex may have a debated role in postural control prior to injury, it is necessary to initiate voluntary, targeted movements. Additionally, studies have demonstrated that the cortex is critical for maintaining the proper recruitment of competing muscle synergies[56] as well as that cortical reorganization or "plasticity" is *necessary* for functional recovery after various neurological injuries. In both human and animal models, it has been shown that the extent of plasticity in the sensorimotor cortex correlates with spontaneous recovery of motor function[31,57–64]. Lesioning the region of the cortex that undergoes significant reorganization in spinally injured rats that undergo physical rehabilitation reverses any recovery of weight supported stepping[65]. Interfacing with this reorganization may thus allow for greater improvements in outcomes for individuals with impaired motor function. Brain-controlled "neuromodulation therapies" have used cortical signals to control deep brain stimulation and epidural electrical stimulation of the spinal

cord. When paired with physical rehabilitation, these technologies have led to enhanced recovery of volitional locomotor function after SCI[66,67].

Combined, these reasons make M1 a compelling region to understand. Thus, by recording ensembles of neurons in the regions of the primary sensory and motor cortices associated with the trunk and the limbs, I examine in this thesis the extent to which the cortex encodes for postural control (Chapter 2) and how two types of injury – complete spinal cord transection and a more clinically-relevant contusion – alter this encoding (Chapters 3 and 4, respectively).

1.3 Employing Population Models to Study Cortical Computations

With respect to motor BMIs, decoding recorded signals from the motor cortex (M1) is complicated by the fact that there is little consensus as to what M1 actually encodes[68]. Over the last fifty years, a "representational" approach to M1 has persisted, with the assumption that M1 simply processes inputs to encode for external kinematic variables[69]. As such, many have attempted to correlate M1 activity with myriad movement parameters[10,70,71]. However, such tuning curves have been shown to change with time[72], arm location[73], posture, and movement speed[72]. In other cases, no such tuning curves have been successfully modeled[72,74,75]. Thus, this traditional representational framework insufficiently captures M1 processes, limiting both basic science questions as well as the translational potential of M1 decoding.

While the neuron is the most basic *structural* unit of the nervous system, combinations of neurons (or a neural ensemble) form the functional units of our complex brains. While systems

neuroscience had focused on the single neuron for the bulk of the 20th century (partly due to technological constraints), it was Donald Hebb and his contemporaries in the 1940s who introduced the then unpopular idea of neural populations as a functional unit[76]. However, the work of Georgopoulos instigated the renaissance of this idea particularly in motor neuroscience, demonstrating that M1 encodes for arm movement direction at the level of populations of single units (rather than at the level of individual units). Such population analyses with respect to motor control have allowed for us to understand the complex, variable internal computations involved in movement preparation and execution[77–79] and have ultimately led to better models of neural dynamics[80–82] and even movement itself[83,84]. Thus, in understanding and ultimately decoding movement generation, understanding the coordinated responses of neural population networks is of critical importance[85].

Various methods of understanding the structure of population activity exist, mostly employing dimensionality reduction techniques that capture a particular aspect of this activity to a certain empirical standard. For example, factor analysis and principal components analysis (PCA) are common methods that capture the greatest shared variance in the data with and without discarding spiking variability in individual neurons. The simplicity of these models is both an advantage and a limitation. Whereas PCA must often be used with trial-averaged data, ignoring trial-to-trial variability, it is incredibly interpretable and ubiquitously used both within and outside the field.

Alternatively, the temporal evolution of neural covariance can also be extracted through dynamical systems[80,82], gaussian process factor analysis[78], or other more complex methods that even allow for comparisons of neural activity between experimental trials. As many have shown that M1 population activity evolves through time[86–91], dynamical systems models have gained popularity in

motor neuroscience. A dynamical system is a physical system in which the state **s** at time **t+1** is a function of its current state at time **t**, additional inputs, and noise. In understanding M1 activity, dynamical systems modeling hypothesizes that the recorded neural activity arises from this latent "neural state". Such modeling has allowed for better predictions of neural activity than models that do not account for such dynamics[80,92–94] and for a deeper understanding of inter-trial variability. While a linear dynamical system cannot capture nonlinearities of the neural system in question like more complex models can (e.g., latent factor analysis via dynamical systems[82], switching linear dynamical systems[95], recurrent switching linear dynamical systems[96], etc.), this simpler approach affords the ability to interpret the underlying system. Finally, while dynamical systems approaches model cortical activity exceptionally well, not all of this activity recorded during behavior directly relates to this behavior. A recently developed approach called preferential subspace identification (PSID)[84] attempts to disentangle the underlying dynamics that are behaviorally relevant from those that are not (e.g., those associated with inputs from other neurons, unrelated internal processes, etc.) and ultimately better predicts behavior. Such unravelling therefore allows for a better understanding of the computations the cortex undergoes during different behaviors. Thus, a dynamical systems model – whether accounting for behavioral dynamics or cortical dynamics in general – better represents the neural processes in the motor cortex, allows for interpretation of differences between individual trials, and outperforms many common decoders.

Therefore, this combined work applies various types of dimensionality and modeling techniques ranging from simple population functions to preferential subspace identification in order to provide insight into how the cortical neurons as ensembles respond to and encode for postural perturbations.

1.4 Dissertation overview

The central hypothesis of this work is that the cortex conveys significant information about unexpected postural perturbations even after spinal cord injury, and that this signal can be used to develop a postural BMI – a key step in ultimately developing a next-generation BMI to improve motor functioning.

Chapter 2 addresses how the cortex is implicated during postural perturbations in the naive (uninjured) animal at both the individual neuron and population levels. This work has recently been accepted for publication in *Cell Reports*, with the authors listed as Gregory D. Disse, Bharadwaj Nandakumar, Francois Pauzin, Gary H. Blumenthal, Jochen Ditterich, Zhaodan Kong, and Karen A. Moxon. I previously presented this work at the 2022 Society for Neuroscience annual meeting (Disse, Nandakumar, and Moxon, 2022). As lead author, my contributions included co-conceiving the study, developing the methodology, performing the experiments with BN and GHB, analyzing the data with BN, FP, and GHB, and writing the manuscript. Professor Moxon provided mentorship throughout the process.

While the ability to understand how the cortex encodes postural control and even decode movement in the uninjured animal is important, the translatability of this concept to a neuroprosthetic is only relevant if these signals can also be interpreted after neurological injury. **Chapter 3** addresses how a complete spinal cord transection, severing all ascending and descending connections between the lumbar spinal cord and supraspinal centers, alters the encoding of postural information. This work is published in the *Journal of Neurophysiology*, with the authors listed as Jaimie

B. Dougherty*, Gregory D. Disse*, Nathaniel R. Bridges, and Karen A. Moxon, where the asterisk represents equal contribution. As co-first author, my contributions included analyzing the data collected by JBD and writing the manuscript.

Chapter 4 addresses the effects of incomplete spinal cord injury on cortical posture dynamics, which is of critical importance when developing a translational application. While the previous chapter addresses the effect of complete spinal transection on cortical encoding, incomplete injuries (e.g., contusions) are significantly more common in the SCI population[97,98]. Additionally, we have demonstrated that animals who undergo longitudinal physical rehabilitation after spinal cord injury show unique cortical reorganization that is associated with improved functional outcomes[65]. Thus, this chapter also assesses the effect of physical rehabilitation on the cortical encoding of posture. This work is currently being prepared for submission with the authors listed as Gregory D. Disse, Bharadwaj Nandakumar, Gary H. Blumenthal, Logan M. Peters, and Karen A. Moxon. As lead author, my contributions included co-conceiving the study, developing the methodology, performing the experiments with BN and GHB; analyzing the data with BN, GHB, and LMP; and writing the manuscript. Professor Moxon provided mentorship throughout the process.

All of this work was supported by the National Institutes of Health Grant R01 NS096971 (Karen Moxon); the National Science Foundation Grant DARE – 1933751 (Karen Moxon); and the National Center for Advancing Translational Sciences, National Institutes of Health—UL1 TR001860 and linked award TL1 TR001861 (Gregory Disse).

1.5 Animal model

A rodent model, specifically adult female Sprague-Dawley (Chapters 2 and 4) and Long Evans (Chapter 3) rats were used for all experiments. As this project focused on understanding postural control, many may question how well the findings from this model translate to bipedal humans. Given that bipedal activity in primates has been estimated to have begun at least 4-6 million years ago[99], one could conclude that these two forms of movement must be vastly different. However, beyond the fact that most individuals with lower limb deficits after neurological injury require assistive devices (e.g., walkers, lateral support beams) to maintain horizontal stability (thus requiring both arms and legs), significant similarities actually exist in the neuroanatomical control of gait and posture between quadrupeds and bipeds. The three supraspinal locomotor regions – the mesencephalic, subthalamic, and cerebellar locomotor center – have been preserved during the transition to bipedal locomotion in the human[100]. A study comparing feline and human postural responses to anteroposterior disturbances when maintaining a quadrupedal stance[101] showed that both species corrected stance primarily with the hindlimbs and used the forelimbs as "supportive struts." From this result, they concluded that the hindlimb-dominated posture control is "probably common and relatively ancient pattern" and, importantly, that "reorganization of the hominid CNS circuitry was probably unnecessary because hindlimb control was already a feature of the system".

Second, regardless of whether the mammal consistently walks on all four limbs or just two, significant work has shown that innate neuronal networks providing the functional units for motor output are conserved across species. During human locomotion, interlimb reflexes in both the arms and legs after cutaneous nerve stimulation are phase modulated during the walking cycle[102]. This has been shown to even have important clinical implications for restoring voluntary movement after

neurotrauma. In case studies of locomotor retraining after SCI, Berhman and Harkema suggested that using the arms for postural and weight-bearing activity may actually inhibit rhythmic stepping with the leg; however, allowing normal reciprocal arm swinging facilitated stepping[103]. Similarly, Kawashima et al showed that in individuals with incomplete cervical injuries, arm activity facilitated leg muscle activity, "shaping" motor output for the legs[104]. Therefore, despite the certain differences between quadrupedal and bipedal locomotion and postural control, significant value can still be given to a quadrupedal animal model.

Finally, the rat was chosen for this study as there is an abundance of work already on the anatomy, physiology, and behavioral science of the effect of spinal cord injury in this model. Rats have similar functional, electrophysiological, and morphological outcomes compared to humans following SCI. Thus, rodents offer well-described reproducible controlled SCI-models, established histological, biochemical, and molecular techniques, readily available behavioral outcome measure assays, and are relatively inexpensive and available to most researchers.

Chapter 2 – Neural ensemble dynamics in trunk and hindlimb sensorimotor cortex encode for the control of postural stability

2.1 Summary

The cortex has a disputed role in monitoring postural equilibrium and intervening in cases of major postural disturbances. Here, we investigate the patterns of neural activity in the cortex that underlie neural dynamics during unexpected perturbations. In both the sensory (S1) and motor (M1) cortices of the rat, unique neuronal classes differentially covaried their response to distinguish different characteristics of applied postural perturbations; however, there was substantial information gain in M1, demonstrating a role for higher-order computations in motor control. A dynamical systems model of M1 activity and forces generated by the limbs revealed that these neuronal classes contribute to a low dimensional manifold comprised of separate subspaces that define different computations depending on the postural responses and are enabled by congruent and incongruent neural firing patterns. These results inform how the cortex engages in postural control, directing work aiming to understand postural instability after neurological disease.

2.2 Introduction

Navigating our surroundings, standing in place, or even quiet sitting require the central nervous system to constantly monitor and coordinate continuous muscle activations. Spinal circuits interface with descending supraspinal signals to inform appropriate motor responses based on

somatosensory, visual, and vestibular inputs [105,106]. While various spinal cord and brainstem circuits have been heavily studied [107–109], the role of the cortex remains debated if not dismissed. Noninvasive recording methods in humans have shown signals linked to the frontocentral cortex that scale with perturbation difficulty as well as aging [110–113]. Despite advances in our ability to directly record neural activity within the cortex especially in animal models, such work with relation to postural control has remained limited. In few such examples, neurons in the rat hindlimb motor cortex responded to postural perturbations, regardless of their predictability [114,115] and ultimately convey information about these disturbances within the first few hundred milliseconds of their onset [114,116]. Given the critical function of cortical circuits for functional recovery after neurological injuries [63–65,117–119], understanding the computations M1 performs during postural control is crucial to optimize recovery of function after injury.

Unfortunately, this limited intracortical work has largely focused on the hindlimb motor cortex and has almost exclusively studied the independent activity of individual neurons. This constrains our understanding of how the cortex encodes for postural information for two reasons. First, postural control requires not only the limbs, but also the active engagement of trunk musculature [120–122]. In humans, trunk contractions modulate corticospinal excitability of the limb muscles and vice versa [123], supporting the close functional and anatomical relationship of the trunk and limb systems. Thus, investigating areas beyond the hindlimb cortex will more adequately explain the cortical postural system. Second, neurons do not function independently. Current recording technologies and analytical techniques have allowed for a deeper comprehension into the computations that populations of cortical neurons employ together as an ensemble (see review in

Gallego et al., 2017) during motor planning and execution [77,86,92,124], as well as during locomotion [125–127]. A significant result of this work has suggested that characterizing the dynamical response of a neural population, rather than simply assessing covariance between neurons, can allow for better predictions of neural activity and, importantly, provide insight into the computations the brain performs during motor tasks. Therefore, to understand the computations undertaken by the cortex during postural control, it is necessary to characterize population dynamics.

Here, we describe the extent to which populations of cortical neurons recorded from the hindlimb and trunk regions within both the primary motor (M1) and sensory (S1) cortices of the rat encode for unexpected postural perturbations. In summary, M1 and S1 conveyed highly redundant information about the different perturbations, accomplished by different neural populations modulating their responses based on the speed and direction of the perturbation. Neurons could be grouped into separate classes characterized by their similar (congruent) or different (incongruent) firing rate statistics [128] in response to different directions of tilt. Presumed higher level computations further increased the information conveyed by M1 relative to S1 while also inhibiting neuronal activity within S1. Preferential subspace identification (PSID), a linear dynamical systems approach that prioritizes the extraction of behaviorally relevant dynamics [84] demonstrated that M1 activity was sufficient to decode the corrective forces generated by the animal to maintain balance. Further investigation into these rotational cortical ensemble dynamics suggested that, depending on the direction of tilt, the neural population activity occupies different regions or "subspaces" within the dynamical state space and that both congruent and incongruent neurons contribute to this divergence. The incorporation of incongruent neurons could explain efforts by the cortex to separate these two

subspaces and contribute to the coordination of unique perturbation-direction specific forces generated by muscular responses (i.e., synergistic flexion and extension of the limbs). These results clarify that cortical computations support higher-order processing related to mechanisms that ensure stability in the state of imbalance.

2.3 Results

2.3.1 Trunk and hindlimb M1 convey more information than trunk and hindlimb S1

To study encoding strategies used by the cortex for postural control, we employed a simple and naturalistic task (Figure 2.1A) in which rats (N=13) had to maintain balance while standing unrestrained on a platform that tilted randomly at two different speeds in each direction in the lateral plane (Figure 2.1B). To maximize the unexpected nature of the task, tilts were delivered at a random "inter-tilt" interval with no additional visual or auditory cues. At the same time, the firing activity of 887 manually-sorted single neurons (68 ± 28 per animal) was recorded using microwire arrays implanted in the trunk and limb representations of the primary sensory cortex (S1) in one hemisphere (n = 388 neurons) and in the trunk and hindlimb representations of the primary motor cortex (M1) in the contralateral hemisphere (n = 499 neurons) based on coordinates from our previous work [129] (Figure 2.1C).

First, to explore differences between the cortical areas in the encoding of postural perturbations, we compared the amount of mutual information in M1 and S1 about the tilts. Overall, the firing patterns of individual M1 neurons at 1.5 seconds after tilt onset (the time by which all

Figure 2.1. Experimental Design.

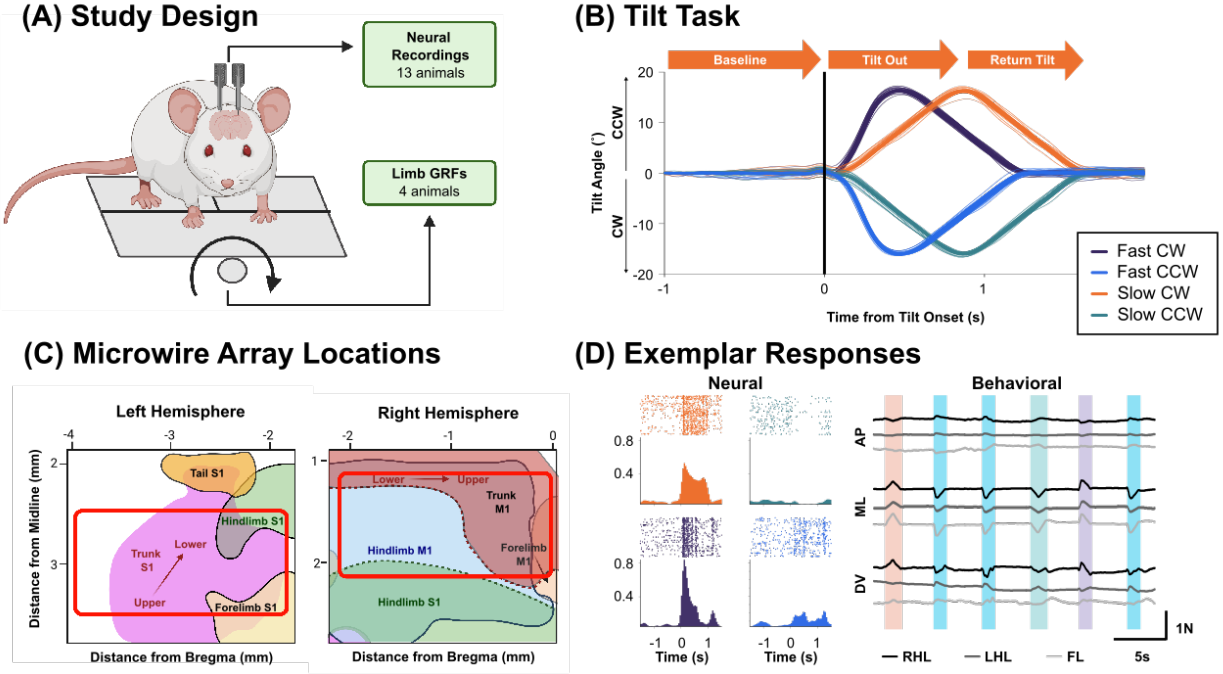

a Tilt task. Animals were placed on a platform with three separate Plexiglas surfaces such that each hindlimb rests on its own surface and both forelimbs rest on the third surface. For a subset of animal, transducers embedded in each platform surface recorded ground reaction forces (GRFs) over time. **b** Four tilt profiles. After a random 2-3 second inter-tilt interval ("Baseline"), the animal was tilted in either the clockwise (CW) or counterclockwise (CCW) direction at either a fast or slow velocity ("Tilt Out"). Once reaching a peak angle, the platform returned to the neutral position at the same velocity for all tilts ("Return Tilt"). Arrows denote "Baseline", "Tilt Out" and "Return Tilt" intervals for Slow CW tilts. **c** Electrode locations in each cortical hemisphere relative to putative sensory (S1) and motor (M1) cortical targets (based on [Nandakumar et al., 2021]). The 32-channel microwire arrays primarily targeted the trunk representation of M1 and S1, with the M1 array implanted slightly more laterally to avoid the superior sagittal sinus. **d** Exemplar neural and behavior (GRF) responses. Neural: peri-event raster plots and histograms (displaying firing probabilities) shown for a single recorded neuron. Behavior: Forces recorded from right hindlimb (RHL), left hindlimb (LHL), and combined forelimb (FL) sensors in the anteroposterior (AP), mediolateral (ML), and dorsoventral (DV) are shown over a sequence of six tilts.

perturbations would be completed) conveyed more information about the perturbation type than those in S1 (Figure 2.2A) [$U = 53868$, $p < 0.0001$]. This remained true at multiple timepoints ranging from 0.1 to 1.5 seconds after tilt onset) (Figure 2.3A). As neurons also employ population coding strategies, we calculated the amount of information conveyed by ensembles of neurons. Since the size

of a population would affect mutual information, we sampled an equally sized random subset of neurons from M1 and S1 and then calculated the population-level information of these regions

Figure 2.2. Significant information gain occurs in M1 compared to S1.

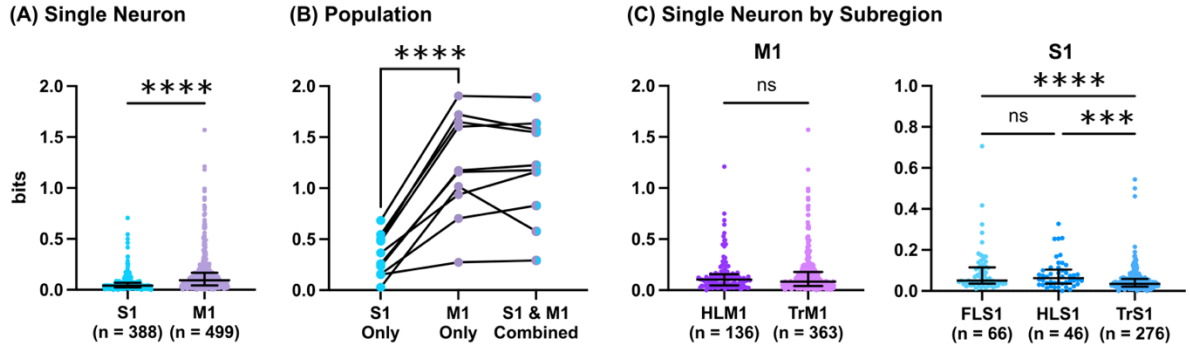

a Single neuron information compared between M1 and S1. **b** Population information for equally sized S1 and M1 when separated and combined. Plotted are means within animal after 1000 permutations of sampling without replacement. Lines connect results for a given animal. **c** Single neuron information when comparing subregions within M1 and S1 separately. (A and C) plot individual neuron values, medians and interquartile. (A-C) ns = Not Significant, ****p<0.0001, ***p<0.001.

separately and together. This was repeated 1000 times with different subsets, and the means of those permutations were analyzed for each animal. Just as at the individual neuron level, M1 conveyed significantly more information than S1 at the population level (Figure 2.2B) [$t(9) = 7.752$, $p < 0.0001$]. Additionally, we observed significant redundancy between the mutual information conveyed by M1 and S1 about the tilts, as the information conveyed by M1 and S1 combined was notably less than the summed information of each region [$t(9) = 4.580$, $p = 0.0012$]. Together, this data demonstrates that M1 has a clear gain in information compared to S1, which could be due to higher-order computations that the brain engages in (e.g., motor planning, sensory gating, efference copy, etc.) during postural control.

To delineate the decoding ability of these two cortical regions more thoroughly, we separated them out into subregions based on previous acute mapping and sensory-evoked potential results [129].

Within M1 (Figure 2.2C), we recorded from hindlimb (HLM1) as well as the trunk musculature (TrM1) regions (n = 136 and n = 363 neurons, respectively). Interestingly, individual neurons in TrM1 conveyed just as much information about the stimulus as neurons in HLM1 [U = 23959, p = 0.6132]. This result highlights the strong functional relationship between these two regions during postural control.

In contrast, within S1 (Figure 2.2C) [H(3) = 28.5, p < 0.0001], the information conveyed by the forelimb (FLS1, n = 66 neurons) and hindlimb (HLS1, n = 46 neurons) regions was comparable [p > 0.9999] and significantly greater than that conveyed by the trunk region (TrS1, n = 276 neurons) [FLS1 v. TrS1, p < 0.0001; HLS1 v. TrS1, p = 0.0006]. This is likely explained by the fact that HLS1 and FLS1 have the benefit of receiving both proprioceptive *and* tactile sensory information (as the limbs are in direct contact with the platform) whereas TrS1 receives predominately proprioceptive information during this task.

Importantly, the fact that M1 conveyed more information than S1 was not simply due to the relatively low information observed in TrS1. When comparing HLM1 and HLS1 neurons only, M1 still conveyed significantly more information than S1 [U = 2255, p = 0.0044] (Figure 2.3B).

Thus, we observed significant differences between the information conveyed by motor and sensory cortex as well as within these respective cortices themselves. Since postural corrections have both a strong sensory and motor component, and since the information in S1 is redundant with the information in M1, the added information in M1 beyond that provided by sensory inputs is likely due to additional internal computations relayed to M1 or even within M1 itself.

Figure 2.3. Further information analyses.

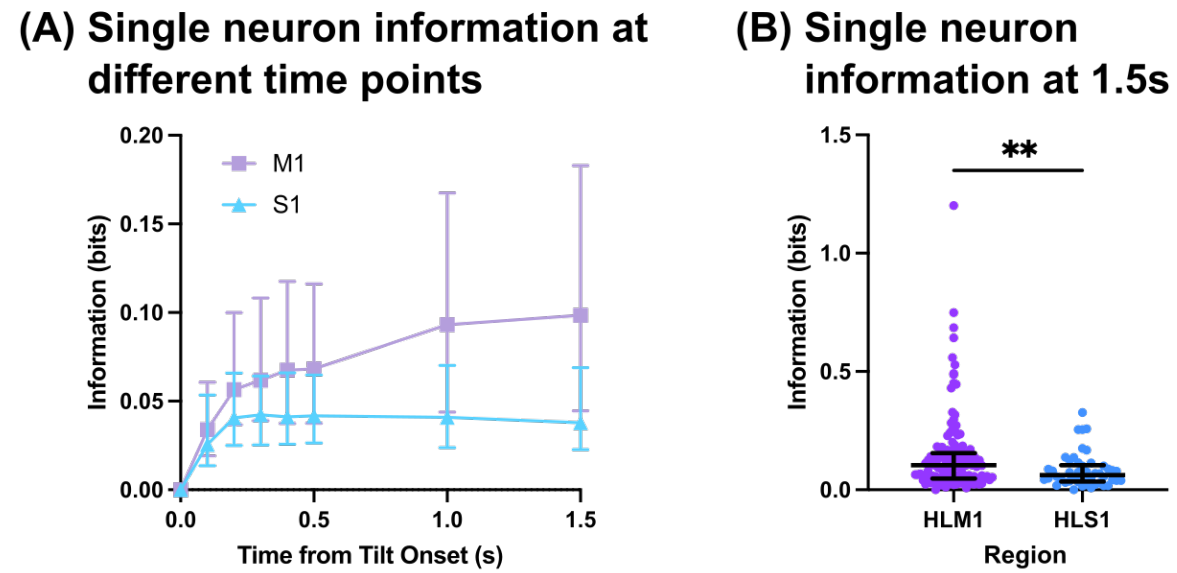

a Information was compared between M1 and S1 using different windows: 100, 200, 300, 400, 500, 1000, and 1500ms after tilt onset. There was a significant effect of hemisphere [$F(1, 879) = 116.6$, $p < 0.0001$, Two-way repeated-measures ANOVA], with M1 conveying more information than S1 at every time point [100ms: $p = 0.0034$; All others: $p < 0.0001$, Sidak post hoc comparisons]. **b** Information was also calculated using only HLM1 and HLS1 neurons [Mann Whitney $U = 2255$, $p = 0.0044$]. **$p < 0.01$. A 50ms bin size was used both all analyses.

2.3.2 Similar covariance patterns in the population response across animals support consistent cortical strategies

Both individual neurons and neural ensembles in M1 and S1 conveyed significant information about the postural perturbations of the task. However, that does not explain *how* these regions encode for these perturbations. We thus sought to uncover the computations that support cortical encoding of postural control at the population level.

Using principal components analysis (PCA), we extracted the three largest sources of covariance in the neural firing activity for each animal. These three principal components captured a significant amount (50-70%) of the variance (Figure 2.4A) and, when examining how each tilt type altered the responses of these components, we observed three common covariance patterns in almost

all animals (Figure 2.4B): (1) a relative increase in activity after tilt onset ("Excitation Component"), (2) a tilt-dependent increase or suppression of activity ("Mixed Component"), and (3) a relative decrease in activity after tilt onset ("Inhibited Component"). Thus, instead of organizing the components by variance explained (e.g., PC1, PC2, and PC3), we categorized the components into one of these three patterns (i.e., Excitation Component, Mixed Component, Inhibited Component). In PC space, the neural population activity diverged in response to the four tilts in a manner highly consistent across animals (Figure 2.4C), suggesting a common strategy across animals for encoding postural signals.

Differences in the responses of Excitation and Mixed Components (Figure 2.4B) to each tilt type suggests that these particular components may encode unique features of the tilt (e.g., speed and direction). The magnitude of excitation in the Excitation Component scaled with the speed of the tilt and the Mixed Component showed either increased or decreased activity based on the tilt's direction. In contrast, modulation of the Inhibited Component appeared independent of tilt type. If excitation and mixed-response covariance patterns supported a mechanism that led to better encoding of tilt-type, we hypothesized that motor cortex neurons would be more heavily weighted in these components than sensory cortex neurons. Thus, we examined how the individual neurons contributed to each of these three components (Figure 2.4D). Indeed, M1 was more heavily weighted in both the Excitation [$U = 74084$, $p < 0.0001$] and Mixed [$U = 50750$, $p = 0.0097$] Components whereas S1 was more heavily weighted in the Inhibited Component [$U = 77245$, $p < 0.0001$]. Of note, within M1, subregions were equally weighted across all three components [Excited: $U = 23089$, $p = 0.1320$; Mixed: $U = 13886$, $p = 0.8528$; Inhibited: $U = 21781$, $p = 0.5540$]. In contrast, in S1, subregions were

Figure 2.4. PCA reveals three common response patterns among animals.

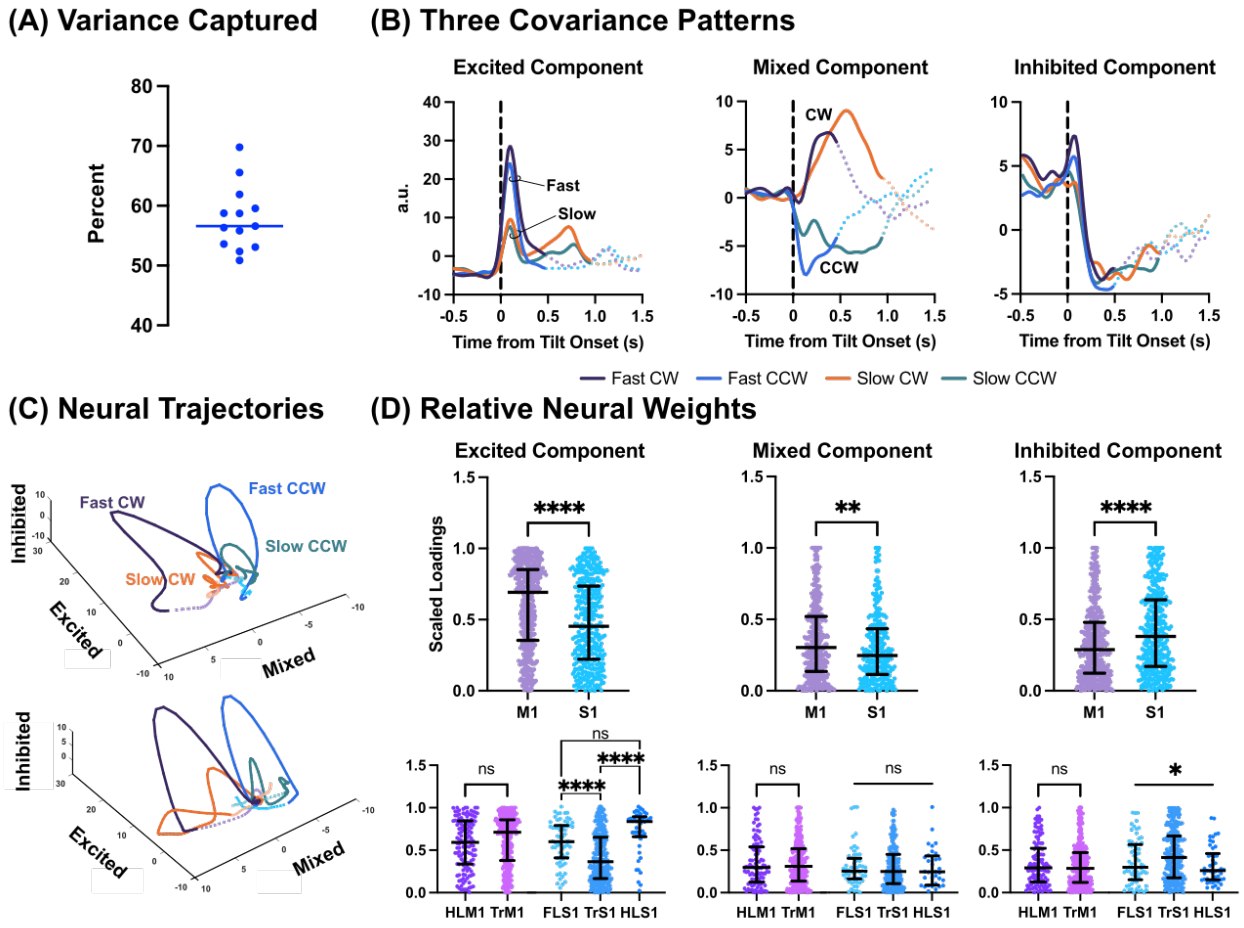

a For each animal, the first three principal components together captured 50.9-69.8% of the variance (median line at 56.6). **b** Responses of exemplar Excited, Mixed, and Inhibited Components to the four tilts. **c** Exemplar projections of neural response into PC space for two animals. **b,c** Solid, darker-colored line represents tilt out; dotted, lighter-colored line represents return tilt. **d** Relative loadings of individual neurons for each Component separated by region and then by M1 and S1 subregion. ns = Not Significant, ****p<0.0001, **p<0.01, *p<0.05.

unequally weighted in the Excitation [$H(3) = 51.37$, $p < 0.0001$] and Inhibition Components [$H(3) = 7.603$, $p = 0.0223$]. This was driven by statically significant differences between the trunk (TrS1) and limb (HLS1 and FLS1) representations in the Excited Component [TrS1 v. FLS1, $p < 0.0001$; TrS1 v. HLS1, $p < 0.0001$; FLS1 v. HLS1, $p = 0.1062$] and a similar trend in the Inhibited Component [TrS1 v. FLS1, $p = 0.1764$; TrS1 v. HLS1, $p = 0.0654$; FLS1 v. HLS1, $p > 0.9999$].

2.3.3 Single neuron activity supports population patterns and differential encoding abilities between cortical regions

The three unique population covariance patterns identified by PCA hinted at a possible mechanism for encoding important perturbation-related information in both M1 and S1. We therefore wanted to determine if similar firing patterns were observed at the individual neuron level. If so, this would suggest cellular-level encoding strategies driving these covariance patterns at the population level. Indeed, we observed neurons that were congruent, showing exclusive increases (excited) or exclusive decreases (inhibited) in activity regardless of tilt direction as well as cells that were incongruent, increasing their response to tilts in one direction and reducing their response to tilts in the opposite direction (mixed) (Examples of individual neurons in Figure 2.5A). Neurons that did not show threshold-crossing responses were considered nonresponsive. Therefore, instead of comparing how different regions contributed to the PCs as in Figure 2.4D, we evaluated the normalized weightings of these particular neuron response types in each of the observed components, where each neuron provided a 0-1 weight to each principal component (Figure 2.5B). As expected, excited neurons were the primary drivers of the excited PC [$H(4) = 365.7$, $p < 0.0001$, Excited v. Inhibited, $p < 0.0001$; Excited v. Mixed, $p < 0.0001$; Excited v. Non-Responsive, $p < 0.0001$], mixed neurons drove the mixed PC [$H(4) = 49.34$, $p < 0.0001$, Mixed v. Excited, $p < 0.0001$; Mixed v. Inhibited, $p < 0.0001$; Mixed v. Non-Responsive, $p < 0.0001$], and inhibited neurons drove the inhibited PC [$H(4) = 184.2$, $p < 0.0001$, Inhibited v. Excited, $p < 0.0001$; Inhibited v. Mixed, $p < 0.0001$; Inhibited v. Non-Responsive, $p < 0.0001$]. We thus observed that these single neuron response types each drive the three largest sources of covariance captured in the neural population observed across animals.

Figure 2.5. Neural response types explain PCA patterns.

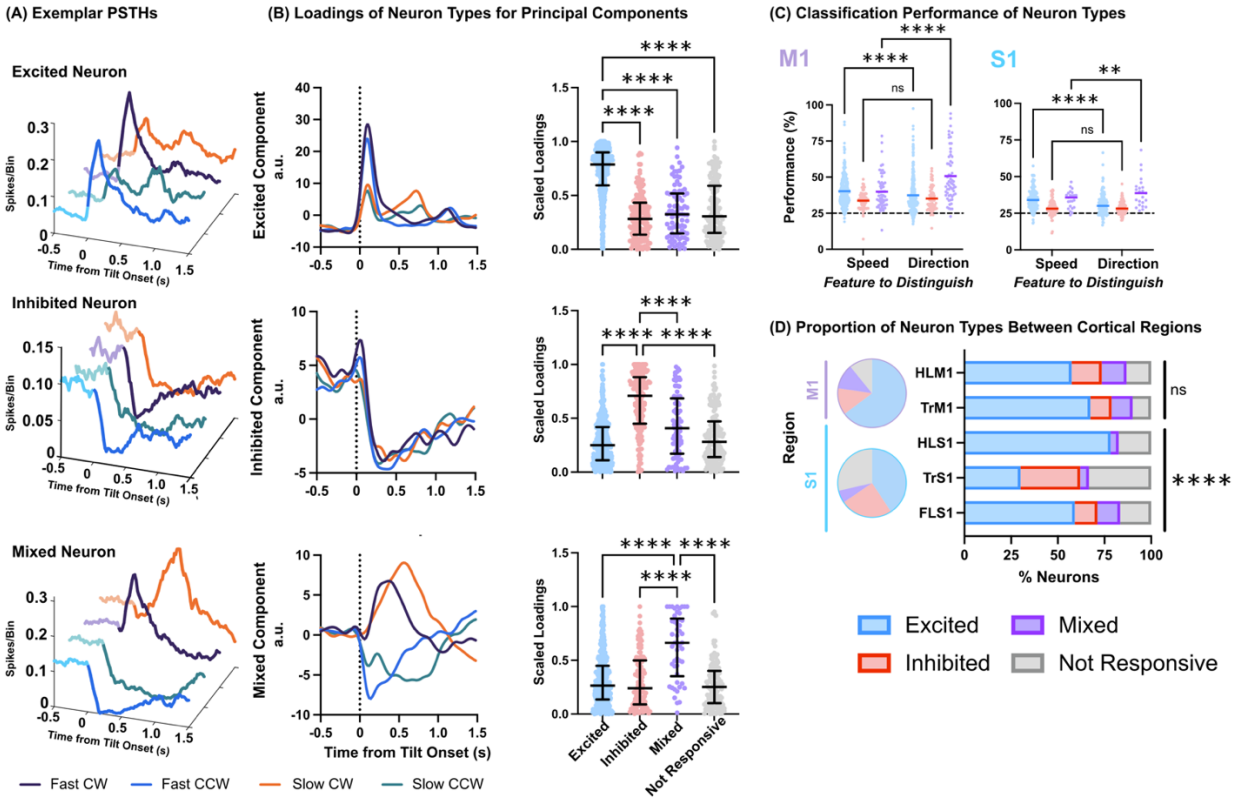

a Exemplar peristimulus time histograms (PSTHs) of one Excited neuron, one Inhibited Neuron, and one Mixed neuron in response to the four tilt types. **b** Relative loadings of individual neurons for each Component separated by neuron response type. Black bars denote medians and whiskers denote interquartile ranges. **c** Performance of neuron response types in encoding tilt speed and tilt direction, separately for M1 and S1. Bars represent medians. **d** Proportion of each cell type in M1 and S1 (left) and then within M1 and S1 subregions. **b-d** ns = Not Significant, ****p<0.0001, **p<0.01.

Since these unique response types were the source of this population covariance, and since we hypothesized these different population covariance patterns carried parallel streams of information about the tilts, we explicitly assessed how well these different classes of neurons defined by these response types can separately encode the speed and direction of different tilts (Figure 2.5C). Within both M1 and S1, when comparing performance based on the parameter being compared (e.g., tilt direction) and the neuron response type, there was a clear effect of neuron type [M1: $F(2,441) = 17.51$,

$p < 0.0001$; S1: $F(2,274) = 26.54$, $p < 0.0001$] and a significant interaction [M1: $F(2,441) = 49.21$, $p < 0.0001$; S1: $F(2,274) = 20.49$, $p < 0.0001$].

In both M1 and S1, excited neurons predicted tilt speed better than tilt direction [M1: $t(441) = 5.075$, $p < 0.0001$; S1: $t(274) = 6.883$, $p < 0.0001$]. In contrast, mixed neurons decoded tilt direction better than tilt speed [M1: $t(441) = 8.475$, $p < 0.0001$; S1: $t(274) = 3.371$, $p = 0.0030$]. In contrast, inhibited neurons performed equally across these two parameters [M1: $t(441) = 1.177$, $p = 0.5610$; S1: $t(274) = 0.024$, $p > 0.9999$], and performed worse than the other neuron types in both measures [M1 Excited v. M1 Inhibited: $t(441) = 3.108$, $p = 0.0060$; M1 Mixed v. M1 Inhibited: $t(441) = 5.864$, $p < 0.0001$; S1 Excited v. S1 Inhibited: $t(274) = 5.570$, $p < 0.0001$; S1 Mixed v. S1 Inhibited: $t(274) = 6.335 < 0.0001$]. Therefore, within this postural task, we uncovered two distinct neural populations responsible for the largest covariance patterns observed at the population level as revealed by PCA that encode for the two salient features of the task (tilt speed and direction). Through speed-scaled excitation and a separate population of neurons with direction-specific excitation or inhibition, the cortex can encode unexpected postural perturbations.

Since we uncovered a clear mechanism that allows the cortex to convey speed and direction information about the tilts, we hypothesized that it was the relative proportions of these neuron types in M1, S1, and their respective subregions that at least partially drove their unequal encoding abilities. While each neuron type existed in both M1 and S1, the distributions of these neurons significantly differed between the two regions [$\chi^2(3) = 87.324$, $p < 0.0001$] (Figure 2.5D). First, a larger proportion of recorded neurons in M1 (89.2%) responded to the task than in S1, with less than 75% of S1 neurons responding to at least one tilt. Second, excitation was the predominant response type in M1, making

up over half of the recorded neurons in M1. Third, M1 had a larger proportion of mixed neurons, whereas S1 had a larger proportion of inhibited neurons. When comparing the subregions within M1 and S1, the distribution of these neuron types was largely homogenous between TrM1 and HLM1 (Figure 2.5D) [$\chi^2(3) = 4.7763$, $p = 0.1889$]. However, S1 regions corresponding to the limbs were much more responsive to the task. Interestingly, TrS1 displayed a uniquely high proportion of inhibited neurons (31.9%) compared to all other recorded regions (0%-16.2%). Since TrS1 is receiving predominately proprioceptive information during this task, this further supports the idea that these inhibited responses reflect sensory gating or the effects of efference copy mechanisms [130–134] during the coordination of complex movements, primarily driven by the proprioceptive system.

2.3.4 Corrective postural movements can be adequately decoded on single-trial basis with a low number of behaviorally relevant dimensions

While we found basic cellular and network-level mechanisms supporting cortical encoding of postural perturbations, the information gain that we observed in M1 motivated us to explore the specific task-related computations M1 conducted throughout the perturbation. State-space modeling using a linear dynamical systems approach allows us to uncover these dynamics of the trunk and hindlimb M1, as well as decode corrective limb responses. We specifically employed preferential subspace identification (PSID) [84] to extract behaviorally-relevant neural dynamics. In a subset of four animals, we recorded the activity in M1 (n = 34-72 neurons) while also capturing changes in ground reaction forces and torques as the animals completed the tilt task. Sensors embedded in the platforms under each hindlimb and the combined forelimbs continuously recorded three-dimensional forces and torques (thus three force and three torque measures per sensor, or 18 behavioral measures per animal).

Figure 2.6. PSID captures behaviorally-relevant dimensions that involve all neuron types.

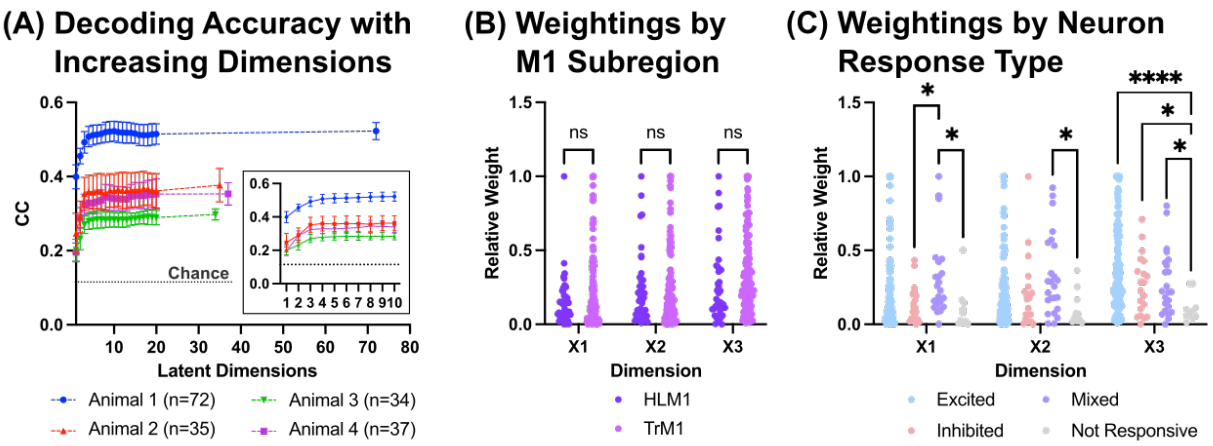

a Results from 5-fold cross-validation showing overall accuracy of decoding 18 force and torque measures based on M1 activity across trials using PSID model with an increasing number of dimensions. Means and standard deviations of 5 cross-validation values plotted. A dimensionality of 1-20 as well as that of the total number of neurons recorded for each animal (n = 34-72) was assessed. Inset shows the decoding accuracy for the first ten dimensions to highlight the elbow curves for each animal. CC = correlation coefficient. **b-c** Relative weights of neurons for each of the three latent dimensions (X1, X2, and X3) derived from a 3D PSID model based on M1 subregion (B) and neural response type (C). Only significance values $p<0.05$ plotted in (C). ns = Not Significant, ****$p<0.0001$, *$p<0.05$.

Through five-fold cross validation, we found that we were able to use M1 activity to decode instantaneous ground reaction forces across trials just as well as using a latent state dimensionality significantly smaller (e.g., 2-4 dimensions) than the dimensionality of the neural activity (Figure 2.6A). When we repeated this modeling using both M1 and S1 activity, S1 neurons minimally contributed to the resultant dynamics (Figure 2.7B) and decoding accuracies were unchanged (Figure 2.7A), supporting our mutual information results. Thus, modeling M1 activity as a low-dimensional, time-invariant linear dynamical system separately for each animal sufficiently captures behaviorally-relevant dynamics that encode for the body's corrective movements (i.e., forces and torques) during a postural task.

Whereas we observed that each of the three distinct response patterns gleaned from PCA were

Figure 2.7. Comparing PSID models with and without S1

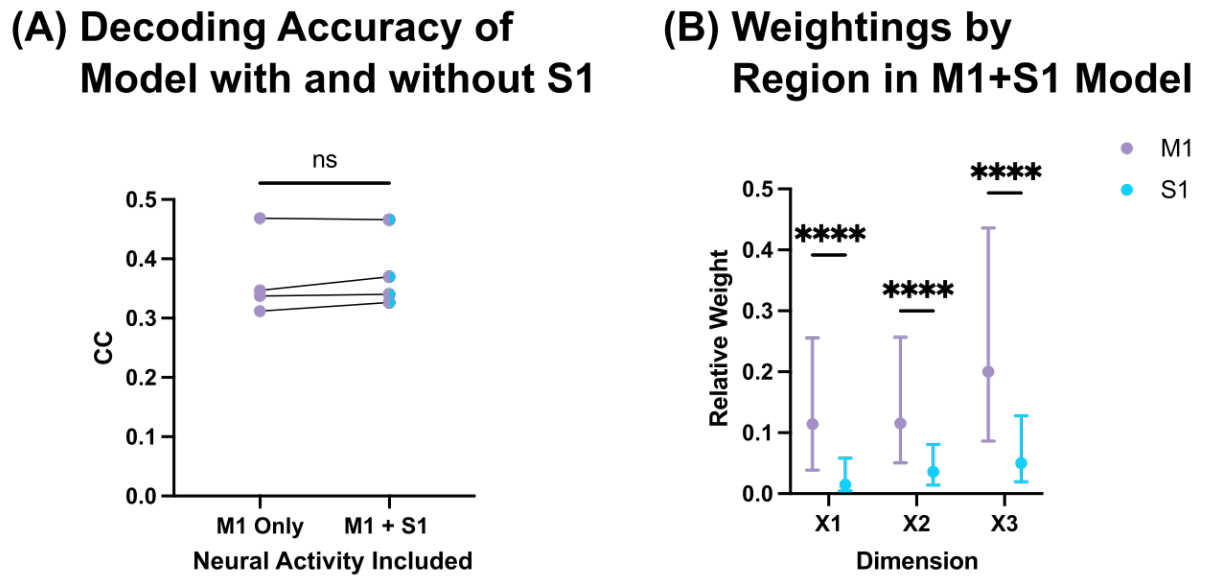

a Decoding accuracy from a three-dimensional model with either M1 alone as the input neural activity or both M1 and S1 neurons as the input activity plotted for each of the four animals [$t(3) = 1.652$, $p = 0.1971$, paired t test]. **b** Relative weights of neurons in M1 and S1 for each of the three latent dimensions (X1, X2, and X3) derived from a 3D PSID model based on M1 and S1 activity. Median and interquartile ranges shown. [Effect of Region: $F(1,310) = 54.18$, $p < 0.0001$, Repeated measures two-way ANOVA; X1: $t(930) = 4.71$, $p < 0.0001$; X2: $t(930) = 4.588$, $p < 0.0001$; X3: $t(930) = 7.925$, $p < 0.0001$, Sidak post-hoc comparisons]. CC = Correlation Coefficient, ns = Not Significant, ****$p < 0.0001$.

driven by the different neuron types, the contribution of neurons to each PSID-derived latent dimension was more evenly distributed, implying PSID captured patterns beyond covariance . We normalized the Cy matrix (the transformation matrix relating observed neural data **y** to the latent dimensions **x**) such that each neuron had a 0-1 weight for each latent dimension. We first examined how neurons from the two M1 subregions were weighted within each latent dimension (Figure 2.6B). While neurons were clearly weighted differently between latent dimensions [Effect of Dimension: $F(1.969, 346.6) = 11.80$, $p < 0.0001$], we saw that the M1 subregions were evenly distributed within each latent dimension [Effect of Region: $F(1,176) = 2.976$, $p = 0.0863$]. Similarly, while the relative weightings of different neuron response types (Figure 2.6C) differed for each of the three latent

dimensions [Effect of Dimension x Response Type: $F(6,348) = 2.960$, $p = 0.0079$], no neuron type or combination of response types dominated a particular dimension. Thus, somewhat intuitively, this linear dynamical systems approach captured a different aspect of how M1 encodes for postural control, in which different neuron types from different M1 subregions work together to encode for behavior.

2.3.5 Neural population dynamics exhibit a low-dimensional structure that suggests higher-order cortical processing

Since a low-dimensional linear dynamical systems model of M1 population activity adequately predicted single-trial postural corrections, we wanted to characterize this underlying latent activity and how it evolved during the different tilts. To do this, we extracted a 2D representation of the neural dynamics for visualization on a single plane representing the top two behaviorally-relevant latent dimensions during both the tilt out and return tilt for all four tilt types (Figure 2.8A). As has been observed in many motor tasks in humans and primates [82,90,92,135], we observed clear rotational dynamics on a single-trial basis.

We additionally observed three notable characteristics of the dynamics. First, when dividing a perturbation into its initial "tilt out" (i.e., from the neutral position to the maximum tilt angle) and the subsequent "return tilt" (i.e., from the maximum tilt angle to the neutral position), one could expect neural dynamics to evolve in at least one of two ways. On the one hand, the cortex could traverse the same region or subspace of the low two-dimensional manifold, during both components, essentially "reversing" its dynamics of the tilt out phase during the return tilt phase. This was observed using PSID during a center-out reaching task with non-human primates [84]. Alternatively, the cortex could

Figure 2.8. Rotational M1 dynamics encode for mediolateral corrective forces.

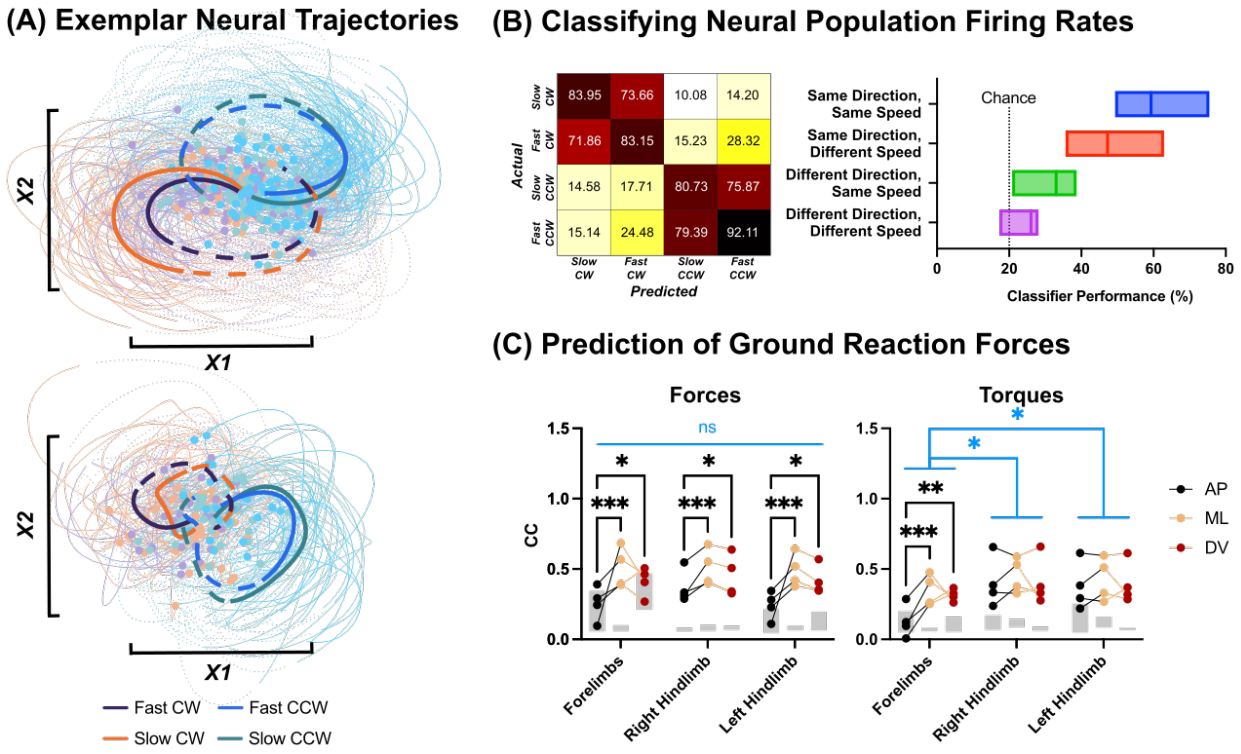

a Exemplar 2D neural trajectories from PSID models for two animals. Dots and thin lines represent individual trials, with the dots indicating the starting point of the trajectory (when the tilt began). Bold lines indicate trial-averaged trajectories for each tilt type, with the solid line indicating "tilt out" and dashed line indicating "return tilt". **b** Neural firing rates during five bins along the neural trajectories were compared to trial-averaged activity for each tilt type. Higher percentages indicate higher similarity. (Left) shows results for one animal. (Right) shows results across animals. **c** The ability to decode ground reaction forces and torques based on M1 activity was assessed using test data. Chance accuracy ranges across all four animals for each measure are shown in light grey. Blue significance bars indicate the effect of sensor; black significance bars indicate effect of directionality. CC = correlation coefficient; ML = mediolateral; DV = dorsoventral; AP = anteroposterior. ns = Not Significant, ***p<0.001, **p<0.01, *p<0.05.

follow a non-overlapping different trajectory back to its original state, utilizing a different subspace, forming a circular trajectory. We observed the latter case, in which the cortex traversed different regions of the latent state space. Thus, even though movement of the platform during the return tilt is simply a reversal of that during the tilt out, the cortex did not simply "reverse" its dynamics. Rather, it

employed unique computations during these two phases of the perturbation to allow the dynamics to follow a continuous path during the entire tilt.

Second, tilts in opposite directions caused M1 dynamics to traverse a separate trajectory for the duration of the tilt. Moreover, the dynamics of tilts in opposite directions are mirror images of each other, orthogonal to the reflection for tilts out versus return tilts. Finally, and most interesting, despite a population of neurons that covary their firing rate in proportion to the speed of the tilt, similar dynamics were seen between fast and slow tilts in a given direction, suggesting possible speed-invariant processing patterns for similar behavioral responses that occur at different timescales.

To clarify that these latent dynamics are a function of the recorded neural firing patterns, we tested whether the observed dynamics, in the two-dimensional subspace, were supported by differences in neural spiking at different time points along the trajectories. For example, if the cortex truly traverses different subspaces during the two phases of the perturbation, the neural firing activity at the time points when the latent activity occupied different areas within the subspace should also be different. We divided the entire duration (binned at 24ms) of the tilt (tilt out and return tilt) into nine epochs, and examined the neural spike counts of the first 24ms bin of each epoch. For each trial of a given tilt type, this generated nine "candidate bins" that were each compared using a leave-one-out method to the trial-averaged spike counts of each of those nine bins ("templates"). The candidate bin was classified into the bin that had the smallest Euclidian distance relative to each template. The percentage of candidate bins that were classified into the correct template bin was then recorded. When comparing the individual trials of a tilt type to the templates of that same tilt type, this

percentage represented how characteristically distinct the spike counts of a given epoch were from the other eight epochs.

This was then repeated comparing the candidate bin of one tilt type's trial to the templates of a different tilt type, and a percentage was calculated in the same way. In this case, a higher classification performance would suggest a strong similarity in the neuronal response patterns – and thus in the ensemble dynamics – across similar phases of the tilt. This process generated a 4x4 grid of percentages for each animal comparing the trials of four tilt types to the templates of each of the four tilt types (Figure 2.8B).

Neural patterns were sufficiently different throughout the phases of the tilt out and back within a specific tilt type (i.e., when the candidate bins and template bins came from the same tilt type) to lead to high classification performance (40-80%). This directly supports our first claim that tilting out causes the cortex to enter different regions of the state space than during the return tilt. We then generated three separate linear mixed effect models to see if changing the speed (Model 1), direction (Model 2), or both speed and direction (Model 3) of the template's tilt type relative to the candidate trial would affect classifier performance – all with the animal as a random effect. The direction of the template's tilt affected performance [Model 1 v. Model 3, χ^2 (1) = 21.68, $p < 0.001$], such that when the candidate tilt and template tilt were in different directions, performance dropped by 23.87 ± 5.59% (standard error). This supports our second observation that tilts in the opposite direction led to unique neural activity at comparable phases of the perturbation and thus diverging neural trajectories. In contrast, the speed of the template's tilt did not significantly affect performance [Model 2 v. Model 3, χ^2 (1) = 5.55, $p = 0.06$]. Thus, neural activity (and thus latent dynamics) during the different phases

of the tilt were highly similar despite different tilt speeds. Therefore, the different regions of the state space visited by our PSID-derived neural trajectories were supported by distinct neural firing activity.

2.3.6 The cortex encodes for changes in center of pressure

Given the fact that the PSID model captured behaviorally relevant dynamics, we sought to evaluate how well each of the different ground reaction forces and torques could be decoded from cortical activity (Figure 2.8C). Whereas the model equally predicted the forces from each limb (i.e., forelimbs v. hindlimbs) [Effect of Sensor: $F(2,6) = 1.100$, $p = 0.3917$], there was a clear effect of directionality on decoding ability [Effect of Direction: $F(2,6) = 8.723$, $p = 0.0168$], forces applied in the mediolateral direction were decoded better than those in the anteroposterior direction [$t(6) = 4.117$, $p = 0.0186$] across animals. In contrast, torques produced by each hindlimb were better decoded than those produced by the combined forelimbs [Effect of Sensor: $F(2,6) = 9.167$, $p = 0.0150$; Forelimbs v. Right Hindlimb: $t(6) = 3.961$, $p = 0.0222$; Forelimbs v. Left Hindlimb: $t(6) = 3.389$, $p = 0.0434$], which was likely driven by the particularly poor performance decoding forelimb torques along the anteroposterior axis relative to the other two axes [Effect of Sensor x Direction: $F(4,12) = 3.359$, $p = 0.0460$; Forelimb anteroposterior v. mediolateral torques: $t(12) = 4.987$, $p = 0.0009$; Forelimb anteroposterior v. dorsoventral torques: $t(12) = 4.193$, $p = 0.0037$]. This bias for decoding the body's reactive forces and torques made along the mediolateral axis is supported by the nature of our task. During the tilt task, the mediolateral aspect of the animal's center of pressure is primarily perturbed, providing data that sufficiently explores the relevant state space to generate a model that can predict forces and torques about the mediolateral direction. We would expect if we had

sufficient data to explore tilts in other directions, the model would have been able to predict the center of pressure in any direction.

2.4 Discussion

Using a naturalistic task that requires complex coordinated movement of the entire body, the present study more thoroughly characterized how the cortex engages in postural control. Beyond demonstrating that the cortex conveys information about postural perturbations, our results show that the motor cortex conveys significantly more information about the tilts than sensory cortex. As would be expected within S1, forelimb and hindlimb S1 convey more information about the tilts than trunk S1 owing to the fact that they carry additional tactile information not conveyed by trunk S1; however, within M1, trunk conveys similar information as the hindlimb region. Considering the similar encoding abilities of the trunk and hindlimb motor cortex as well as their similar response profiles to the task, it is evident that these two regions have homologous encoding strategies, supporting a strong functional coupling between the trunk and hindlimb region that allows for the coordination of muscle synergies during postural control [120,129,136]. Moreover, neurons within both M1 and S1 could be categorized by their firing patterns (i.e., excited, mixed, and inhibited) in response to the perturbations. PCA analysis demonstrated that neurons with similar firing patterns covary together and convey specific information about the features of the tilt (e.g., speed or direction). However, the cortical dynamics relevant to postural control in M1 rely on all three of these neuron types. Additionally, the neural trajectories traversed a different portion of the latent state space during tilt out compared to tilt back, and tilts to the right occupied a separate subspace compared to tilts to

the left – all supported by differences in recorded neural firing activity at these different epochs. However, the cortex employs similar latent dynamics regardless of the tilt's speed, suggesting that the neural computations for slow tilts are similar to those of fast tilts, albeit moving through the state space at different speeds.

2.4.1 The role of neural dynamics in coordinating postural control

The neuroanatomical and functional circuitry involved in postural control is complex. It is generally believed that a distributed network of neural areas in the central nervous systems are involved in postural control, with the particular role of the cortex up for debate. Dietz *et al.* argued that the cortex is involved in coordinating reactive postural adjustments [137]. The present study supports this claim. Using a three-dimensional dynamical systems model of the motor cortex (preferential subspace identification), instantaneous ground reaction forces and torques – particularly those associated with mediolateral shifts in center of pressure – could be decoded from extracted behaviorally-relevant latent activity as the animal was tilted in the lateral direction.

This latent M1 activity followed rotational dynamics, which have primarily been observed in purely voluntary tasks with a motor preparatory phase [82,86,90,92]. Our observation of rotational dynamics in a more *reactionary* task suggests that, whether through intrinsic connectivity or through substantial sensory feedback [138], the motor cortex is actively engaging in the control of posture. Additionally, different dynamics and distinct neural activity were observed during the task's "out" and "back" phases. Thus, the sensorimotor experience during the return tilt is not simply a "reversal" of dynamics during the initial tilt out, but actually requires novel computations associated with the different

muscle activations in response to the different sensory inputs. This is despite the fact that, for the slow tilts at least, the return of the platform is the exact reversal of the outgoing movement of the platform. The need for novel computations is likely driven by differences in the control issues related to maintaining center of mass during tilts out versus during tilts back.

However, differences in the speed of the tilts were handled differently. In this case, whether the tilt is fast or slow, a comparison of trajectory shapes and neural firing activity suggest that the computations are the same with only the timescale adjusted [139–142]. Other work in monkeys has shown that primary and premotor cortices contain significantly more direction-related information than speed-related information at both the individual neuron and population level [143]. This may be because difference in computations related to temporal factors are not handled by a unique set of neural computations [139].

2.4.2 Separate subspaces control activation of extension versus flexion

When examining the dynamics in the low, two-dimensional space, all trajectories in response to these tilts in the lateral plane were within the same manifold supporting the idea of robust neural population dynamics during movement and suggesting that responses to different tilts are part of a family of computations that are similar. Moreover, the firing patterns of both congruent (i.e., excited) and noncongruent (i.e., mixed) cell populations contribute to the path of the trajectories. These results demonstrate a separation of neural activity into different subspaces for tilts in opposite directions, while neural trajectories for tilts in the same direction but at different speeds overlap. Yet, interestingly,

not only are the trajectories for tilts to the right nonoverlapping with trajectories to the left, but even trajectories associated with tilts out differ from those associated with tilts back.

With respect to postural control, the need for separate subspaces can be understood by considering the differences in the muscle synergies elicited [144–146] by distinct shifts in the animal's center of mass [147] when the platform tilts in opposite directions. Our postural task requires coordinated flexion and extension of limbs to maintain balance. Notably, the set of muscles that extend a hindlimb for tilts to the right, for example, would flex for tilts to the left. While there are spinal reflex circuits that respond to brainstem inputs to ensure extensors and flexors work in harmony, the role of the cortex in activating these synergies is much less known and no mechanism has been identified. Cheung *et al.* demonstrated that formerly distinct muscle synergies appear to "merge" in the affected arm after a cortical stroke [56], suggesting a possible role of the cortex in orchestrating the appropriate, harmonious synergy activations. Maintaining the neural computations in different regions of the state-space could be a cortical mechanism to ensure commands for flexion and for extension are not sent to the same muscle groups at the same time.

2.4.3 Mechanisms to control inside versus outside subspace activity

Previous work suggested that confining computations related to separate limbs in separate subspaces was a way to enable muscle activity decoders to ignore signals related to the opposing limb [148], here we show that this phenomenon can occur within limb. Moreover, our data suggest how these computations are maintained in different subspaces specifically by the noncongruent activity of the mixed cells. For tilts in one direction, the activity of a set of mixed cells will be suppressed yet excited

by tilts in the opposite direction, preventing the population response from traversing the inappropriate subspace or undergoing computations that could interfere with the response to the perturbation. This is analogous to previous work related to preparatory versus movement related computations, in which "out of manifold" neural activity is suppressed [79]. The coordinated excitation or inhibition of mixed cells could create divergent dynamics (e.g., driving neural activity into separate subspaces) that ensure the correct series of coordinated limb movements. Further work more directly measuring muscle activity would be needed to support this hypothesis. Thus, our decoding results and array of neural trajectories suggest that the cortex can flexibly coordinate similar postural adjustments at different timescales yet requires unique computations for movements in different directions.

2.4.4 Higher-order processing and differential roles of M1 and S1 in postural control

Given this largely reactionary task, one may find the fact that S1 conveys so much less information than M1 about the perturbation surprising. How does M1 receive more information than is provided to it through sensory input? Our results support the idea that M1 and S1 are also involved in (or at least receive information about) higher-order tasks underlying sensorimotor processing including motor preparation and error detection [149–151]. For example, surface EEG signals attributed to the supplementary motor area in humans during postural perturbations behave similarly to the "error-related negativity" (ERN) observed during erroneous motor movements [152], implying an upstream cortical substrate for error detection during balance [151,153,154].

The information gain in M1 confirms that ongoing control of posture includes substantial additional sensorimotor processing beyond what is supplied by the ascending sensory pathways [155–157].

In order for the body to generate the correct motor output to stabilize balance, sensory information needs to be integrated into these higher-order, task-level computations. In fact, it has been suggested that the muscle synergies activated during postural perturbations are more than simple reflex pathways, as differing sensory input signals that cause similar changes in center of mass will still elicit the same postural responses [147]. Since, the correct motor output is required to stabilize balance, it thus is not so surprising that M1 responses would differ between (and thus convey more information about) the four different perturbation types.

In addition, we observed a significant amount of inhibition in the cortex in response to the perturbation, particularly within Trunk S1. Inhibition defined one of the three largest sources of covariance in cortical activity yet appeared to encode little information about the perturbation. This observed suppression of activity is likely a downstream effect of higher-order cortical computations that gate unnecessary sensory processing in S1. Efference copy, for example, may be used to depress sensory responsiveness during movement through cancelation or gating [130–133]. For example, the auditory cortex shows suppression of excitatory neurons during movement through signals arising from motor cortical regions [134] that facilitate hearing and auditory-guided behaviors. In the present study, the particularly high amount of inhibition that we observed within trunk S1 while the animal maintains balance would suggest that the central nervous system's postural control network is actively gating proprioceptive afferents from the trunk in a similar manner.

2.4.5 Clinical relevance

Taken together, beyond understanding the role of the cortex in postural stability, this work elucidates the role of cortical dynamics during postural perturbations and can be used to understand how to recover postural stability (and thus more robust independent movement) in individuals with various neurological conditions. For example, after complete mid-thoracic spinal cord transection, the rat hindlimb sensorimotor cortex continues to encode for perturbation type [114,116] supporting the potential use of cortical signals after injury to access critical postural control signals.

While injury alters cortical dynamics, it is possible they can be restored, or even new dynamics could be learned to control such technologies. For example, diminished reach function of the contralesional arm following a stroke was correlated with a loss of motor cortical neural trajectories; however, these trajectories then re-emerged after motor recovery [158], supporting the need for additional interventions such as physical rehabilitation. This is likely to be successful since learning to operate a brain-machine interface is also associated with substantial neuroplasticity [13,159–161] that would support the ability of the cortex to control postural corrections through novel mechanisms regardless of initial performance.

2.4.6 Limitations of the study

While this work expands upon the limited literature on cortical engagement of postural control, we must stress its limitations. Our task identified naturalistic responses to postural instability; however, the task only tilted along a single plane such that animals only experienced lateral perturbations. Both behavior and cortical firing patterns have been shown to be altered with modification of the stabilized body positioning [115]. Thus, we cannot fully characterize the receptive fields of individual neurons or

the entire state space explored by cortical populations during postural control. However, given the fact that tilts to the left and right move the cortical state in opposite directions in a speed-invariant manner, we would expect anterior-posterior tilts to move the cortex into two new states orthogonal to the ones described, in line with other work that has shown that neural trajectories follow different paths for different reach conditions in the non-human primate [82]. Additionally, while ground reaction force sensors embedded in the tilting platform allowed us to measure changes in the animal's center of pressure, follow-on work employing more directly measuring the activations of different muscle synergies through electromyography would allow a more thorough understanding of the role of the cortex in postural control.

2.5 Materials and Methods

Animals and Animal Care: All procedures and surgeries were approved by the UC Davis IACUC and followed ARRIVE Guidelines. Experiments were conducted on 13 adult female Sprague Dawley rats (225-250g body weight; Taconic Biosciences). Electrophysiology recordings and the tilt task was conducted in all rats; ground reaction forces were obtained in a subset of four rats. Rats were housed individually on a 12-hour light/dark cycle, with access to food and water ad libitum.

Task: Rats performed the tilt task as described previously [114,116,129]. A platform consisted of three plexiglass plates (one for each hindlimb and one for the combined forelimbs) coupled to a three-phase AC servo motor (Applied Motion Products, USA). Peak velocity, acceleration, and final tilt angle were programmed using SI Programmer™ (Applied Motion Products, USA) on a digital motor drive (SV7-SI-AE, Applied Motion Products, USA), which sent commands to the motor for tilting.

Four tilt profiles were programmed to subject the animal to lateral perturbations of varied speed (slow: 12.5*/s v. fast: 67.9*/s) and direction (left v. right), but to the same final amplitude (16.5°). A custom Python script randomly determined the tilt type (100 trials each), tilt initiation time, the time between tilt trials (varied randomly between 2-3 seconds) and sent those commands to the motor drive. Animals were given 3-4 sessions to become acclimated to proper positioning on the platform and the different tilt types. During recording sessions, the animal was placed on the tilt platform, and the Python program was initiated once the animal adopted the correct body position.

In a subset of animals (n = 4), individual sensors (Mini40-E Transducer; ATI Industrial Automation, USA) were positioned under the three platform plexiglass plates to record three-dimensional forces and torques (18 measures total). GRF data was acquired at 1250 Hz using LabView software, which was filtered offline using a 4^{th} order Butterworth zero-phase low-pass (5 Hz) filter. For each trial, sensor recordings beginning 1.2s before tilt onset and ending 3.6s after tilt onset were extracted and then downsampled by a factor of 30.

Neural recordings during the tilt task: After initial platform acclimation, we performed a sterile surgery during which rats were implanted with 32-channel microwire arrays (arranged in an 8 x 4 configuration with 250 μm resolution; Microprobes, Inc, Gaithersburg, MD, USA) in the cortical infragranular layer (1.3-1.5 mm) of both the right and left hemisphere. We have previously showed that, when averaging the response patterns (e.g., response magnitudes and latencies) of neurons in each hemisphere, tilts in both the ipsilateral and contralateral directions lead to similar responses [114,116]. The procedure was performed under anesthesia via intraperitoneal injection of ketamine (63 mg/kg),

xylazine (6 mg/kg), and acepromazine (0.05 mg/kg). Post operative pain was managed using buprenorphine (0.05 mg/kg), and the animal was allowed at least a week to recover.

The electrode array implanted in the right hemisphere spanned 0-2 mm caudal to bregma and 1.25-2.0 mm lateral to midline, centered around the trunk and hindlimb representations within the rat primary motor cortex (M1). Based on previously published work mapping the trunk representation in the rat M1 [129], the recording electrodes in M1 were grouped based on the region of the body they most likely activated. Ten electrodes between 1-2 mm caudal to bregma and 1.75-2 mm lateral to midline were considered hindlimb M1 (HLM1), as intracortical microstimulation to this region is known to elicit movements in the contralateral hindlimb. The remaining 22 contacts medial and rostral to the HLM1 electrodes were considered trunk M1 (TrM1), as these regions elicit movements in the lower, middle, and upper thoracic musculature upon electrical microstimulation.

The electrode array implanted in the left hemisphere was placed more laterally to capture the primary sensory cortex (S1), spanning 2-3.8mm caudal to bregma and 2.5-3.5mm lateral to midline, with the array inserted at a 9.5° angle to account for the curvature of the brain. The 32 S1 electrode contacts were assigned to hindlimb, forelimb, or trunk S1 subregions (HLS1, FLS1, TrS1, respectively) based on sensory evoked potentials (SEPs) generated in response to 0.5 mA peripheral electrical stimulation (100 1-ms pulses, 0.5 Hz) of the contralateral hindlimb, forelimb, and trunk under 2% isoflurane anesthesia one week after implantation. Briefly, 500 ms of bandpass filtered signal before and after stimulation onset were extracted and averaged to form an SEP. Each electrode in the sensory array was assigned a receptive field center, defined as the body region (i.e., forelimb, hindlimb

or trunk) which, when stimulated, produced the largest SEP negative peak amplitude for that electrode.

Neural signals were amplified and filtered (Multichannel Neuron Acquisition Processor; Plexon Inc, USA) and then manually sorted into single units online (Sort Client; Plexon Inc, USA) prior to beginning the tilt task. Spike times, in addition to the times corresponding to the initiation of a tilt, were then collected as the animal completed the tilt task.

Information Analysis and PSTH-Based Classifier: We assessed the amount of information in the cortex about the tilt type using a PSTH-based classifier [162]. Briefly, in a leave-one-out manner, templates are made by average neural spiking activity (or generating peristimulus time histograms, PSTHs) for each tilt type. The Euclidian distance is then calculated between the left-out trial's neural activity and each tilt type, and the trial is classified as belonging to the tilt type that had the smallest Euclidian distance. This was completed at the individual neuron level and at the population level (where the PSTHs from multiple neurons form the templates). Neural spiking activity was binned at 50ms, as we have seen optimal classifier performance at that resolution in previous work [114,116,129], and 1.5s of neural activity after tilt onset was classified. Classifier performance, as well as mutual information calculated from classifier's confusion matrix, were used to quantify cortical information. For four tilt types, mutual information values could range from 0 bits (implying no relation between neural firing patterns and the different tilt types) to 2 bits (based on the Shannon information formula with four equally likely perturbation types).

To calculate the ability of a neuron to distinguish tilt speed, classifier performance in distinguishing tilts of different speeds in one direction was multiplied by performance distinguishing

tilts of different speeds in the other direction (thus, chance performance was considered 25%). Comparably, to calculate the ability of a neuron to distinguish tilt direction, performance distinguishing tilts of different directions but at the slow speed were multiplied by the performance of that same neuron to distinguish tilts of different directions but at the fast speed.

Finally, to compare population mutual information between M1 and S1, we sampled an equally sized random subset of neurons from M1 and S1. For a given animal, the sample size was the size of the population of the hemisphere with fewer neurons. Using the PSTH-based classifier, we calculated the population-level information of these neuronal subsets separately for each hemisphere and then together (thus, the same neurons used to calculate the individual region mutual information values were used to calculate the combined M1 and S1 mutual information). This was repeated 1000 times with different subsets. The mean values of those permutations were reported and used for additional analyses.

Principal Components Analysis: Neural activity beginning 500 ms before tilt onset and ending 1500 ms after tilt onset was Gaussian smoothed and then averaged within tilt type to form four trial-averaged responses which were then concatenated to form a Neuron x (Event Type x Bin) matrix. The concatenated, trial-averaged response of each neuron was then standardized (z-scored) to avoid PCA results being dominated by high-firing neurons. We used PCA to reduce the dimensionality of the above matrix to three. Since we suspect that various other cognitive processes are occurring beyond those pertinent to the task [84], we chose a dimensionality of three principal components (PCs) to extract the largest sources of variation from the neural activity that would most likely pertain to the task. To

standardize across animals, the same dimensionality was chosen for all animals. PCs 1, 2, and 3 each carried at least 5% of the variance for all animals.

PCA was applied to the neural responses of each animal separately. For each animal, the three components (PCs) were manually sorted into an "Excited", "Inhibited", or "Mixed" Component based on visual assessment. An animal could only have one of each component type. A component was considered "Excited" if its activity after tilt onset increased relative to the baseline period. A component was considered "Inhibited" if activity was reduced relative to the baseline period. A component was considered "Mixed" if it showed increased activity relative to baseline for some tilt types but decreased activity relative to baseline for other tilt types.

The loading (coefficient) matrix was used to determine how different neurons contributed to a given component. Each column of the matrix contains coefficients for one principal component whereas each row corresponds to a given neuron. To allow for comparisons across animals, the values in each column were normalized such that each neuron was given a weight between 0 and 1 for a particular component.

Single Neuron Response Types and Responsiveness: To characterize neural responsiveness, peristimulus time histograms (PSTHs) were built around the start of tilt with a 20ms bin size. Upper and lower response thresholds were defined as 2 standard deviations above and below the average activity in the 500ms prior to tilt onset, respectively. If 5 consecutive bins crossed the upper threshold within 480ms for fast tilts or 960ms for the slow tilts (i.e., the time to the maximum perturbation angle), then the neuron was considered to have an excited response to that tilt type. Conversely, if it crossed the lower threshold, it was considered to have an inhibited response to that tilt

type. If a neuron satisfied both criteria for a given PSTH, its response type was determined manually by visualizing the PSTH.

Based on these responses to individual tilts, a neuron was considered "excited" overall if it had an excited response to at least one tilt type without any inhibited responses to the other three tilt types. If a neuron had an inhibited response to at least one tilt type without any excited responses to other tilt types, it was considered "inhibited." A "mixed" neuron had an excited response to at least one tilt type *and* an inhibited response to at least one other tilt type. Finally, a neuron was considered unresponsive if it did not respond to any of the four tilts.

Preferential Subspace Identification: A MATLAB package (https://github.com/ShanechiLab/PSID) was used to generate our PSID models and evaluate the decoding of behavior (ground reaction forces). Input features (i.e., neural signal and behavior) were parsed into individual trials with a window −0.5 ms to 1.8 ms relative to tilt onset. Due to the sampling rate of the ground reaction force sensors, neural data (putative single unit recordings from the M1 microwire array) was binned at 24 ms. Any unit that fired less than 0.5 Hz during the recording session was not included in the model. The binned spike rates of the remaining units were smoothed using a 100ms Gaussian kernel. Changes in all 3 force and 3 torque values from all 3 sensors (i.e., forelimbs, right hindlimb, and left hindlimb) over these time windows were used as inputs, resulting in 18 behavioral measures. Each behavioral measure was z-scored on a per-trial basis. For each animal, a random 80% of the trials were used for creating the model, determining hyperparameters, and characterizing neural dynamics. The remaining 20% was used to assess the performance of decoding ground reaction forces using M1 activity.

To determine dimensionality and assess decoding accuracy, we set the state dimension empirically by measuring the ability of the model to decode behavior (i.e., how similar model-predicted ground reaction forces were compared to the true observed measures for those same trials) using a five-fold cross validation on the random 80% of trials. After separately concatenating all observed and predicted values for given measure across trials, a correlation coefficient was calculated. This was repeated for all 18 measures, providing a decoding accuracy of each behavioral measure. Overall model prediction accuracy for a given state dimension was assessed by calculating the mean of these 18 correlation coefficients, and this process was repeated while sweeping state dimensions by one from 1 to 20 as well as the total number of included M1 neurons for a given animal. Since the optimal dimensionality was similar across animals (2-4), we chose the same dimensionality for all animals to allow for comparisons. We calculated chance decoding accuracy by shuffling the relationship between neural and behavioral responses, such that a given trial's neural response was matched to a different trial's behavioral response (without shuffling the actual values within a given trial). A model was built, and decoding accuracy was assessed based on this shuffled data. The mean correlation coefficients (both overall and for each of the 18 measures) across 100 iterations of reshuffling was defined as chance accuracy.

Statistics: Statistical analyses were conducted using GraphPad Prism Version 9.4.1 and R. Experimental data were processed offline using MATLAB R2021b (MathWorks). Non-parametric tests were used for all comparisons at the individual neuron level (e.g., information, principal component loadings). Comparisons between two independent variables were done using the Mann-Whitney U Test while comparisons with more than two groups were done with Kruskall-Wallis test,

followed by Dunn's Post Hoc when appropriate. A paired t-test was used to compare population-level information between M1 and S1. Neuron type distributions were compared using a chi-square test. A repeated-measured two-way analysis of variance was used to compare weightings of neurons and decoding accuracy for the PSID dynamical systems modeling, with the Sidak post-hoc test when appropriate. To compare firing rates and trajectories of the four tilts based on the PSID-derived neural trajectory, a linear mixed-effects model was developed, where the two fixed effects were whether the tilts were in the same direction (Yes/No) or the same speed (Yes/No), with the animal ID as the random effect. A chi-square test was used to assess the significance of removing each fixed effect on the model. All figures display individual datapoints, medians, and interquartile ranges unless otherwise specified. ****$p<0.0001$, ***$p<0.001$, **$p<0.01$, *$p<0.05$, ns = Not Significant.

Chapter 3 – Effect of spinal cord injury on neural encoding of spontaneous postural perturbations in the hindlimb sensorimotor cortex

3.1 Summary

Supraspinal signals play a significant role in compensatory responses to postural perturbations. Although the cortex is not necessary for basic postural tasks in intact animals, its role in responding to unexpected postural perturbations after spinal cord injury (SCI) has not been studied. To better understand how SCI impacts cortical encoding of postural perturbations, the activity of single neurons in the hindlimb sensorimotor cortex (HLSMC) was recorded in the rat during unexpected tilts before and after a complete mid-thoracic spinal transection. In a subset of animals, limb ground reaction forces were also collected. HLSMC activity was strongly modulated in response to different tilt profiles. As the velocity of the tilt increased, more information was conveyed by the HLSMC neurons about the perturbation due to increases in both the number of recruited neurons and the magnitude of their responses. SCI led to attenuated and delayed hindlimb ground reaction forces. However, HLSMC neurons remained responsive to tilts after injury but with increased latencies and decreased tuning to slower tilts. Information conveyed by cortical neurons about the tilts was therefore reduced after SCI, requiring more cells to convey the same amount of information as before the transection. Given that reorganization of the hindlimb sensorimotor cortex in response to therapy after complete mid-thoracic SCI is necessary for behavioral recovery, this sustained encoding of

information after SCI could be a substrate for the reorganization that uses sensory information from above the lesion to control trunk muscles that permit weight-supported stepping and postural control.

3.2 Introduction

Maintaining postural stability is critical for recovery of independent locomotion after spinal cord injury (SCI). Efficient control of posture is equally important for standing and walking[163,164] as it is for providing support of voluntary limb movements[165]. Depending on the location and extent of SCI, damage to descending and ascending spinal pathways can result in an impairment of postural control[163]. The behavioral effect of a complete midthoracic lesion of the spinal cord has been well studied[166–170]. Notably, although postural control is reduced after SCI, brief standing episodes have been reported even after injury in some animal models[171,172]. In addition, interventions, including treadmill training[173–176] and epidural electrical stimulation[32], have led to modest improvements in this control. Thus, a more thorough understanding of how the entire neural axis encodes for posture before and after SCI can inform therapies that target the restoration of postural control after SCI.

The effects of SCI on limb responses during various postural disturbances have been studied[45,168,177,178]. Specifically, electromyographic (EMG) recordings in the hindlimbs show increases in response latencies, decreases in response amplitudes, and changes in muscle recruitment strategies after a complete midthoracic transection, suggesting that descending neural circuits from above the lesion are necessary for postural control[168,177]. Partial lesion studies in rabbits have suggested that the ventral spinal pathways (reticulospinal and vestibulospinal tracts) arising from the brainstem are critical for postural control whereas dorsal pathways arising from the cortex and midbrain

(corticospinal and rubrospinal) are less important[43,45,179,180]. Although these brainstem circuits clearly provide important descending control of posture, cortical responses to periodic (predictable) rotations in the frontal plane (tilts) have also been documented in rabbits and cats, both before[115,181–183] and after SCI[45,47,179]. Though cortical activity is not critical for basic postural tasks[109,184] in intact animals, its role increases substantially after spinal cord injury. It has been shown that cortical reorganization[65,185] and sprouting of corticospinal axons[65,186] is associated with recovery of locomotion after injury. More importantly, lesioning the reorganized cortex results in a loss of behavioral improvement achieved after therapy, demonstrating that, in addition to other supraspinal circuits, descending information from the cortex is critical for functional recovery. Therefore, the role of cortical circuits in the encoding of posture and balance is of interest and the impact of spinal cord injury is unknown.

To better understand the impact of SCI on HLSMC encoding of information about postural perturbations, we assessed the hindlimb ground reaction forces, the responses of ensembles of single neurons in the rat HLSMC, and the interaction of the two during an unpredictable tilting task both before and after a complete midthoracic spinal cord transection. In intact animals, when sensory input from the hindlimbs is removed, the response of neurons in the hindlimb sensorimotor cortex (HLSMC) to predictable tilts is greatly attenuated[49]. This would suggest that cortical responses would also be attenuated after complete spinal transection, resulting in a decrease in the encoding of information about the tilt. Alternatively, it is possible that HLSMC reorganization after SCI allows for continued encoding of unpredictable tilts due to inputs from sensory afferents above the level of the lesion. As reported previously, we observed cortical response modulation to different tilt types in intact rats. Cortical neurons encoded information about the initial velocity of the perturbation within

50 ms of the start of tilt, and that the timing and magnitude of the hindlimb ground reaction forces scale with initial tilt velocity. After a complete spinal transection (PostTx), cortical activity was sufficient to determine if a tilt occurred and to provide information about the initial velocity of the tilt. Despite a reduction, this sustained cortical encoding about postural perturbations even after a complete spinal cord transection could inform therapies that target cortical reorganization. In addition, as open-loop spinal stimulation has been shown to improve functional outcome after SCI[47,187–189], how this cortical information could be used to control a spinal prosthetic is discussed.

3.3 Materials and Methods

Ethical Approval: All experiments were performed under approval of the Drexel University Institutional Animal Care and Use Committee, followed established National Institutes of Health guidelines (Protocol 19786), and was conducted in accordance with the Animal Research: Reporting of In Vivo Experiments (ARRIVE) guidelines[190].

Cortical Implantation Surgery: Eight Long Evans rats were trained to tolerate a harness and were acclimated to the task for 1–2 wk. Once adapted to the harness and standing, animals were chronically implanted bilaterally with 16 channel (4 × 4) Teflon-insulated stainless steel microwire arrays (MicroProbes for Life Sciences) in layer V of the hindlimb/trunk sensorimotor cortex (Figure 3.1A) using methods standard in our lab[26,191]. Of note, there is an almost complete overlap of hindlimb sensory and motor cortices in the rat[192]. As the electrode was lowered, neural activity was preamplified, bandpass filtered between 100 Hz and 8 kHz, and digitized with data acquisition hardware (National Instruments, Austin, TX). Digitized raw signal and waveforms were displayed on a computer with

Figure 3.1. Experimental design

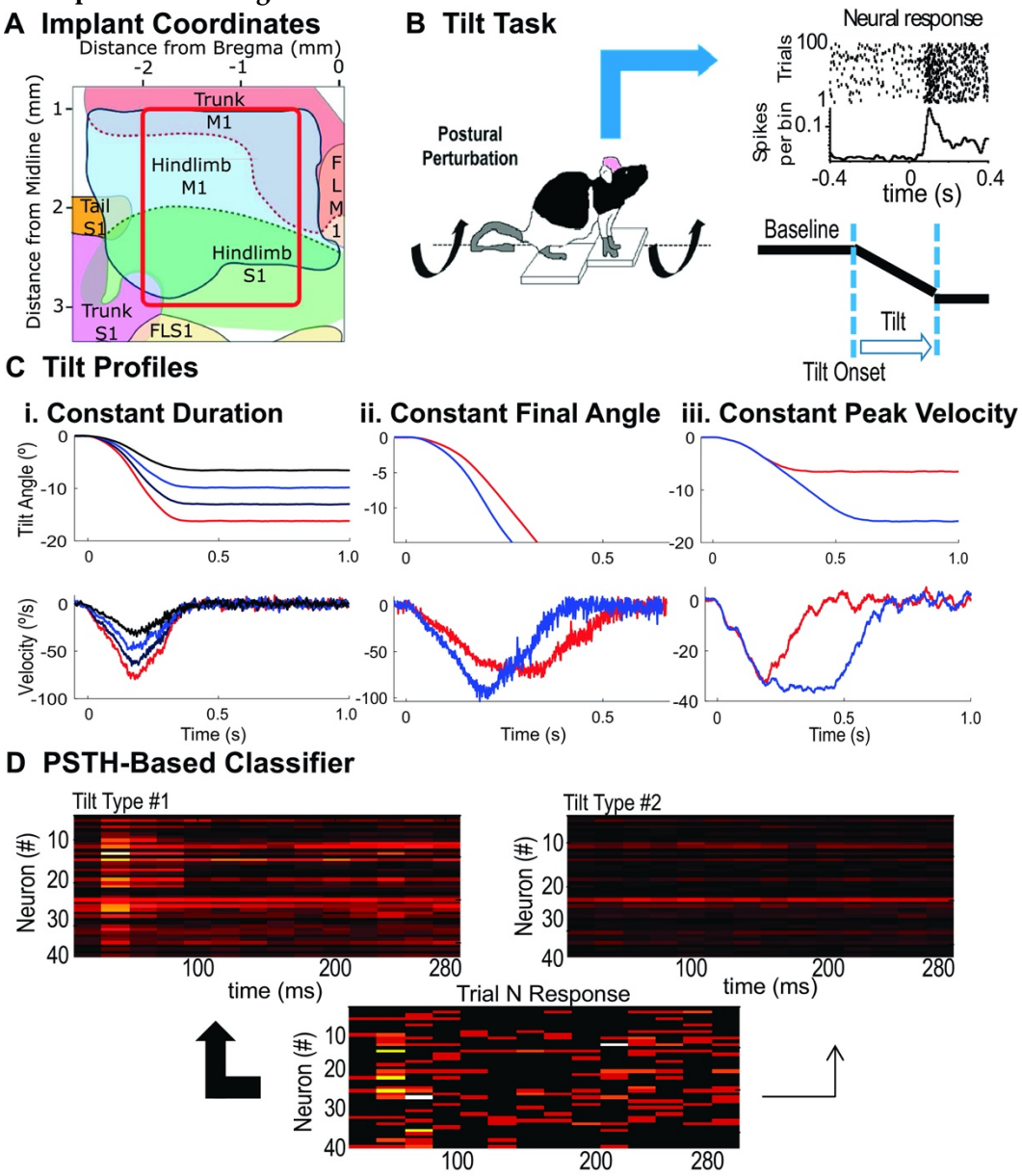

a Location of the bilaterally implanted cortical arrays[129] centered over the exclusive hindlimb motor cortex (M1) with some overlap with trunk motor (M1) cortex medially and hindlimb sensory (S1) cortex laterally. **b** At baseline, the animal stands on a platform with left hindlimb, right hindlimb, and forelimb force sensors. The platform makes unpredictable tilts of varying speed and direction in the horizontal plane described in C. Neuron spiking activity is recorded throughout task, and an exemplar neuron's raster plot and PSTH for a specific tilt is shown. **c** Platform angle (top) and velocity (bottom) profiles for the 8 different tilt types in one direction: 4 "constant duration tilts" with varying final angle and peak velocity (i), 2 "constant final angle tilts" with varying duration and peak velocity (ii), and 2 "constant peak velocity tilts" of varying duration and final angle (iii). **d** PSTH templates are generated for every neuron from over at least 100 of each tilt or baseline epoch. The PSTH from an individual trial is then compared with each template bin by bin, and the single trial is classified as belonging to the template with the most similarity (in this case, Tilt Type #2).

recorder software (Plexon Inc, Dallas, TX) and also monitored on an oscilloscope and made audible through speakers. The array was lowered in 20-μm increments, no faster than 60 μm/min. At each 20-μm step, sensory responsiveness was assessed by tapping a blunt tip probe over cutaneous surfaces. Neurons predominately responding to hindlimb stimulation ensured proper electrode position in the hindlimb sensorimotor cortex[129,193]. Once characteristically large amplitude layer V neurons were visualized on a majority of the channels (at a depth of 1.3–1.6 mm), the array was cemented in place. All surgical procedures were performed under general anesthesia (2%–3% isoflurane in O2) via orotracheal intubation. Pain was managed using buprenorphine SR LAB (0.5 mg/kg; Wildlife Pharmaceuticals Inc.), and animals were given at least a week to recover from the surgery.

Spinal Transection Surgery: After intact (PreTx) recordings were complete, animals underwent a complete spinal transection procedure at T8, identical to the methods in previous studies[26,191]. In brief, animals were given prophylactic antibiotics (enrofloxacin 5 mg/kg) and were anesthetized with an induction dose of 4% isoflurane followed by maintenance at 1.5%–2% isoflurane. A laminectomy was performed at T8/T9. Microdissecting scissors were used to remove the dura, and the cord was transected with iridectomy scissors immediately followed by aspiration. Two surgeons confirmed the lesion visually under ×20 magnification. The muscle and skin were sutured in layers with 4-0 non-dissolving suture. Animals were treated with an analgesic (buprenorphine 0.05 mg/kg), given 10 mL saline, and placed on a heating pad until recovery. After transection, animals were kept on a heating pad and received ongoing care including bladder expression 2–3 times daily, antibiotics, and fluids as needed. Transected animals were given 1 week of recovery before PostTx recordings were performed. All PostTx recordings were collected within 3 weeks of the injury.

Tilt Task: The tilt task is shown in Figure 3.1B. Rats stood in a neutral position on a platform consisting of three Plasti Dip (Plasti Dip International) coated plexiglass plates (one for each hindlimb and for the forelimbs collectively) coupled to a high-performance brushless AC servo motor (J0400-301-4-000, Applied Motion Products). The animal wore a pelvic harness attached to a body weight support system at the pelvis. No vertical weight support was provided PreTx, allowing the animal to freely adjust posture, make small steps, and shift body weight. PostTx, approximately 50% of the weight was supported vertically at the pelvis.

The platform rotated in the frontal plane, remained at the peak angle for approximately 1 s, then returned to the neutral position while the neural response to the perturbation was recorded. The platform remained in a neutral position for a random intertrial interval of 2–3 s. Tilt type was randomized within a recording session using LabVIEW (2015, National Instruments), and direction was reversed during a subsequent recording session. Several tilt types were programmed using Si Programmer (v. 2.7.22, Applied Motion Products) on a digital motor drive (SV7-SI-AE, Applied Motion Products). Start of tilt was defined as the time at which the platform started to move.

Tilt Types: Eight tilt types were classified based on their duration, final tilt angle, and peak velocity. A set of four “constant duration tilts" varied in peak velocity and final tilt angle while maintaining the same duration from tilt onset to maximum angle (Figure 3.1Ci). In addition, two “constant angle tilts" modified the peak velocity and duration of the tilt, but they reached the same maximum angle (Figure 3.1Cii). Finally, two “constant velocity tilts" modified the final angle and duration of the tilt with the same peak velocity (Figure 3.1Ciii). For five of the animals, all tilt types

were recorded in the same session with the same population of neurons. For a subset of three animals, only the two "constant final angle tilts" were recorded.

Ground Reaction Forces: Ground reaction forces were measured for the subset of three animals. Original Equipment Manufacturer (OEM)-style single point load cells (LCAE-600 G; Omega) positioned underneath the platform plexiglass plates quantified hindlimb and forelimb ground reaction forces (GRFs). Data were acquired using LabVIEW software (1,000 samples/s), which was filtered offline using a 2nd order Butterworth zero-phase low-pass filter. Sensor data were normalized to a period found in the 200-ms time window before the start of each tilt. Positive values indicate additional loading onto the sensor.

Single Neuron Recordings: Populations of single units were recorded simultaneously during the tilting task using methods standard in our lab[26,191]. In brief, before every session, neurons were sorted online (Sort Client, Plexon Inc.). First, the neural activity was played over speakers to identify whether neurons were present. An oscilloscope was used to confirm neural activity. The oscilloscope, waveforms, and the first two principal components were used to sort the cells (typically 1 or 2 per channel, occasionally 3). A Multichannel Acquisition Processor (MAP, Plexon Inc, Dallas, TX) was used to record from multiple single neurons during each recording session and to record event timestamps. Offline, neurons were categorized as single units if less than 0.5% of spiking occurred in the first 1 ms of the interspike interval histogram (Offline Sorter, Plexon Inc.). All other units were discarded. Waveforms were checked for consistency over the course of the experiment.

To determine cell responsiveness, peristimulus time histograms (PSTHs) were built around the start of tilt (±300 ms) with a 2 ms bin in a manner similar to our previous work[26,194]. Background

activity was defined in the 300 ms before the start of tilt, when the platform had been in the neutral position for a minimum of 1 s. Threshold was defined as the average background activity plus 1.65 times the standard deviation. If five bins (10 ms), with no more than 10 ms separating them, crossed the threshold, then response was compared to an equivalent background window. If they were significantly different (paired *t* test, $P < 0.05$), the cell was classified as responsive, and the characteristics of the response were found.

Analysis of Ground Reaction Forces: For three animals, differences in GRFs were compared between fast and slow tilts and between injury states using a two-way analysis of variance. Peak forces generated during the tilt were averaged for different tilt types before and after SCI.

Neural Response Profiles: The number of responsive neurons and the response characteristics of those neurons were evaluated between each tilt type and before and after spinal cord injury using two-way analysis of variance or *t* tests as appropriate. Using the PSTHs, response characteristics were defined by both the timing and magnitude of the response. The first and last bins to cross threshold were defined as the "first and last bin latencies," respectively. "Response duration" was the difference between the last and first bin latencies. "Response magnitude" was defined as the sum of the spikes in all the bins between the first and last bin latencies, divided by the total number of trials after subtracting the average background activity. "Response firing rate" (in Hz) was therefore the response magnitude divided by the duration of the response in seconds. If a neuron responded to multiple tilt types, only the case with the largest response magnitude was used such that each neuron only contributed one observation to analyses.

Neuron Classification: For the four constant-duration tilts (Figure 3.1Ci), neurons were classified based on the number of tilts which elicited a significant response. A "selective" neuron responded to a single tilt type only, a "nonselective" neuron responded to more than one but less than four tilts, and a "scaled" neuron responded to all four tilt types.

Relating Ground Reaction Forces to Neural Responses: To summarize the effect of SCI, changes in the average firing rate of neurons during a tilt were correlated to the change in GRF during the tilt. The data were normalized to the start of tilt and the change in firing rate was plotted against the change in GRF for different tilt types and injury conditions in the clockwise and counterclockwise direction (Figure 3.5).

Information Analysis: Information was quantified using a PSTH-based method[162]. In short, PSTHs were generated to find the average response profile (100 trials) of each neuron to each event. In a leave-on-out manner, individual trials were compared with the average response (generated without the single trial) and the difference between the single trial and the average profiles was calculated in a bin-bin comparison (see Figure 3.1D). The single trial was classified as either a particular tilt response or a background response by identifying the profile with the smallest difference from the single trial. Performance was expressed as the percentage of correctly classified trials. The information was calculated using Shannon's information formula, formally defined as:

$$I(s;r) = s,rP(r,s)\log 2P(r,s)P(r)P(s)$$

where *P(r)*, *P(s)*, and *P(r,s)* correspond to the probability of the tilt-perturbation response *r*, the tilt perturbation stimulus *s*, and their joint probability, respectively. *I(s;r)*, which is measured in bits, was calculated for each neuron using the actual and predicted tilt type confusion matrix generated when

applying the classifier. Residual bias for *I(s;r)* was then estimated using a bootstrapping procedure by pairing the trial response and tilt types in a randomized order—effectively eliminating their associations. This bootstrapping procedure was performed 20 times and the calculated bias was subtracted from *I(s;r)* such that 0 bits is chance.

To establish the bin size that resulted in the maximal PSTH classifier performance, a range of bin sizes between 2 and 280 ms were considered. The optimal bin size was determined to be 20 ms across animals, consistent with our previous work[116], so this bin size was used for all information analyses.

Tilt Detection: Trials from tilt profiles in which the severity of the perturbation (changing velocity and peak angle but keeping duration constant, Figure 3.1Ci) were used for detection and discrimination analyses. To determine if neurons could detect any tilt severity from standing in a neutral position, responses of neurons to each of the four constant duration tilts (Figure 3.1Ci) were compared with their firing rates at stance (baseline) and thus single trials were classified as either a tilt or baseline. To account for differing neuron numbers between animals and conditions, information was calculated 20 times with a random sampling of 34 neurons. This number was chosen as it represented the total number of neurons for the animal with the least number of discernable neurons. The effects of tilt severity and injury on information were compared using a two-way analysis of variance.

Tilt Discrimination: An important feature of proper postural control is the ability to discriminate between different perturbation types. For tilt discrimination analyses, single trials were classified as being from one of the four tilt profiles. As with tilt detection analyses, information and

performance were calculated from the averages obtained from twenty iterations using 34 randomly selected neurons.

To further explore the encoding for discrimination, the following analyses were performed. First, a set number of randomly selected neurons (from 4 to 34 neurons) was used to determine how population size affected information (neuron dropping). To determine how quickly information was conveyed to the hindlimb sensorimotor cortex, information was calculated with an incremental increase in the event window, from the first 20 ms after tilt onset to 280 ms after tilt onset. For both analysis types, information and performance were calculated 20 times using a different sampling of neurons.

For information and neuron analysis, five animals were tested PreTx condition with two sessions each for a total of 10 recordings. Four of those animals were then evaluated similarly PostTx for a total of eight recordings. For ground reaction force analysis, three animals were tested PreTx and PostTx. All reported values are means ± standard error.

3.4 Results

3.4.1 Ground reaction force magnitude and timing scale with tilt severity and injury

To assess the impact of SCI on the response of the hindlimbs to unexpected tilts in the lateral plane, ground reaction forces (GRF) in response to each hindlimb and to both forelimbs together were collected during the two tilts of constant final angle (varying duration and peak velocity; refer to Figure 3.1Cii, constant angle tilts) before and after the SCI (Figure 3.2A). As described in previous

Figure 3.2. Ground reaction forces during tilts

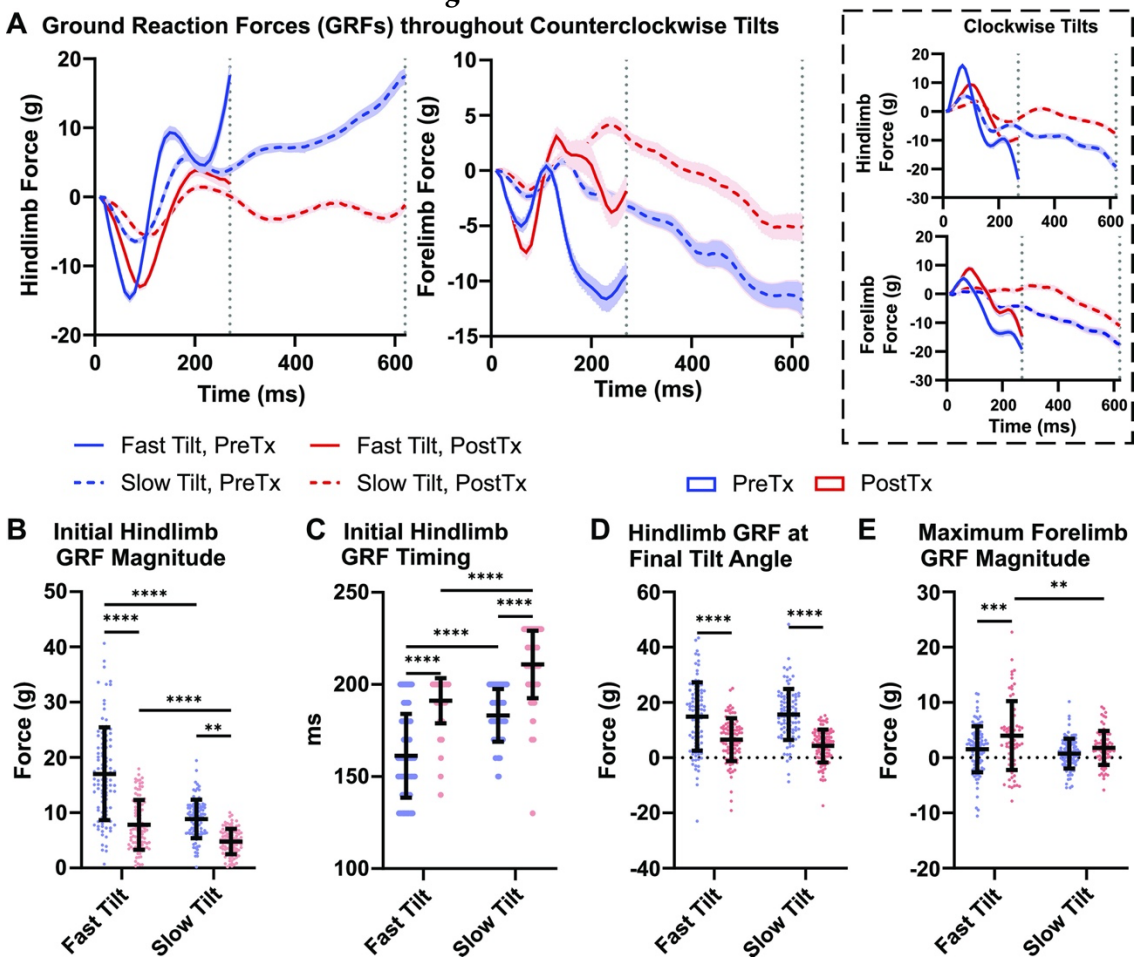

Negative forces imply unloading whereas positive forces imply loading. **a** Average force measured in the left hindlimb (left) and both forelimbs (right) by the sensor for fast (270 ms) and slow (620 ms) constant-angle tilts from tilt onset to the maximum tilt angle in the counterclockwise direction over 100 trials for a single animal. Forces are normalized such that each trial begins with 0 N of force. Shaded areas represent the standard error of the mean. Dotted vertical lines represent the time at which the platform reaches the maximum tilt angle for fast (270 ms) and slow (620 ms) tilts. Inset shows the same animal's forces for tilts in the clockwise direction. **b** The average maximum force applied to the left hindlimb force detector between approximately 100–200 ms during counterclockwise tilts. **c** The timing of maximum force applied to the hindlimb force detector in B. **d** the magnitude of the force applied to the hindlimb force detector during tilt at the end of the tilt (when the tilt platform achieves its maximum angle). E: forelimb forces were also evaluated. The maximum loading force applied to the forelimb force detector was calculated and compared across tilt types and Tx status. Note: only one sensor was used for forelimb force measurements, and animals' weight was partially supported by a trunk harness PostTx. Means and standard deviations are plotted over 99 individual trial data points both Pre- and PostTx. ****P < 0.001, ***P < 0.001, **P < 0.01 (Bonferroni corrected). Tx, spinal transection.

work[116], before SCI, counterclockwise tilts in healthy animals begin with the platform pushing into the right hindlimb and away from the left hindlimb in the first 100 ms, leading to an unloading of

force from the left hindlimb sensor. The next 100 ms is characterized by an active correction of the animal's center of mass, during which the animal extends the left hindlimb and flexes the right hindlimb to shift the center of mass over the base of support. This causes a subsequent increase in the ground reaction forces measured in the left hindlimb sensor. The converse is true for clockwise tilts (data not shown). As expected, the measured GRF of the combined forelimbs is much less than that observed in a single hindlimb since the shifting of the weight is conserved. Nonetheless, the weight on the forelimbs, as measured by the GRF, is unloaded as the tilt is initiated, resulting in an overall reduction in total GRF at the peak of the tilt, suggesting a shift of the center of mass to the hindlimbs.

After SCI, the initial response to the tilt, as the platform moves away from the paw, is similar to the response PreTx. As the platform moves away from the paw, the GRF is reduced. Presumably, spinal circuits below the level of the lesion contribute to a reflex response where the limb is extended resulting in a restoration of GRF. However, unlike in the PreTx response, the GRF in the PostTx condition simply returns to the same force seen at stance, such that the extended position of the paw does not exert any force greater than what was exerted in the neutral position as a harness provided additional support and some of this weight shifted to the forepaw.

To quantify these differences, the forces generated by the hindlimb at the start and end of the faster tilts were compared with those for slower tilts before and after injury. As expected, the initial force was significantly greater for faster tilts [effect of tilt type: $F(1,390) = 113.6$, $P < 0.0001$] and this force was reduced after injury [effect of injury: $F(1,390) = 160.6$, $P < 0.0001$) regardless of the tilt type (Figure 3.2B). However, the difference in force between tilt types was attenuated after SCI [interaction: $F(1,390) = 23.87$, $P < 0.0001$]. Furthermore, regardless of injury status, rats initiated a

correction of their center of mass more quickly during faster tilts [effect of tilt type: $F(1,392) = 142.2$, $P < 0.0001$; interaction $F(1,392) = 0.41$, $P = 0.53$] but these corrections were significantly delayed after injury [effect of injury: $F(1,392) = 272.2$, $P < 0.0001$; Figure 3.2C].

Thus, to stabilize the center of mass within the first 200 ms of the onset of the tilt, the response of the hindlimbs to faster tilts was quicker and more robust than those to slower tilts whereas the response after SCI was delayed and attenuated regardless of tilt type. To assess the impact of tilt type and injury on the final postural adjustment, the forces applied at the maximum angle of the tilt were compared (Figure 3.2D).

As expected, as the final angle was the same, there was no effect of tilt type on the final force generated by the hindlimbs [$F(1,392) = 0.71$, $P = 0.40$], but there was a significant attenuation of this force with injury [$F(1,392) = 115.7$, $P < 0.0001$]. Thus, despite differences in the magnitude and timing of the initial force applied during the tilts PreTx, the animal ultimately applies the same force at the maximum angle of the tilt. After injury, these relationships remain, but the force is attenuated. In an effort to stabilize their center of mass, some of this force is transferred to the forelimbs [Figure 3.2E; effect of tilt type: $F(1,338) = 10.81$, $P = 0.001$; effect of injury: $F(1,338) = 14.83$, $P = 0.0001$; interaction: $F(1,338) = 0.12$, $P = 0.12$], whereas the remainder is taken up by the harness. Thus, after spinal cord injury, the center of mass of the animal shifts forward as more weight is on the forelimbs at the peak of the tilt.

3.4.2 An increasing number of neurons respond to tilts of increasing severity

Neuronal responses to a larger set of tilt types were evaluated to assess the impact of SCI on the encoding of the postural shifts described in Figure 3.2. Populations of single neurons were recorded while animals were subjected to eight different rotations in the frontal plane at random intervals. These tilts maintained either constant duration, constant final angle, or constant peak velocity (Figure 3.1C). For neurons with a significant response to at least one tilt type, their response profiles (response magnitude, duration of response, and latency of response) were compared across tilt types and between Pre and PostTx. The number of cells that responded, or responsive neurons, were different depending on the tilt type [$F(7,63) = 22.00$, $P < 0.0001$]. This change in responsive neurons was observed if the peak velocity was changed but not if the peak velocity was held constant (Figure 3.3A). Thus, more neurons were recruited into the response primarily when the severity of the tilt was increased.

After complete spinal transection (PostTx), there was a trend toward an overall reduction in responsive neurons [$F(1,9) = 4.986$, $P = 0.0524$]. This was observed despite an unchanged number of discriminable neurons PostTx [paired t test, $t(3) = 1.140$, $P = 0.34$]. However, just as in the PreTx condition, neuron recruitment remained tuned to tilt severity (changes in peak velocity).

3.4.3 Duration of neuronal responses are increased with increasing severity of tilt

The magnitude of the response was similarly modulated by tilt type [$F(7,1524) = 0.014$, $P = 0.0142$] with increasing spikes per tilt with increasing severity but no change in number of spikes when severity was held constant. Interestingly, there was no effect of injury on the magnitude of the response, suggesting that information about the tilt is reaching the brain despite the injury [$F(1,1524)$

Figure 3.3 Neuron response profiles for all tilt types Pre- and PostTx.

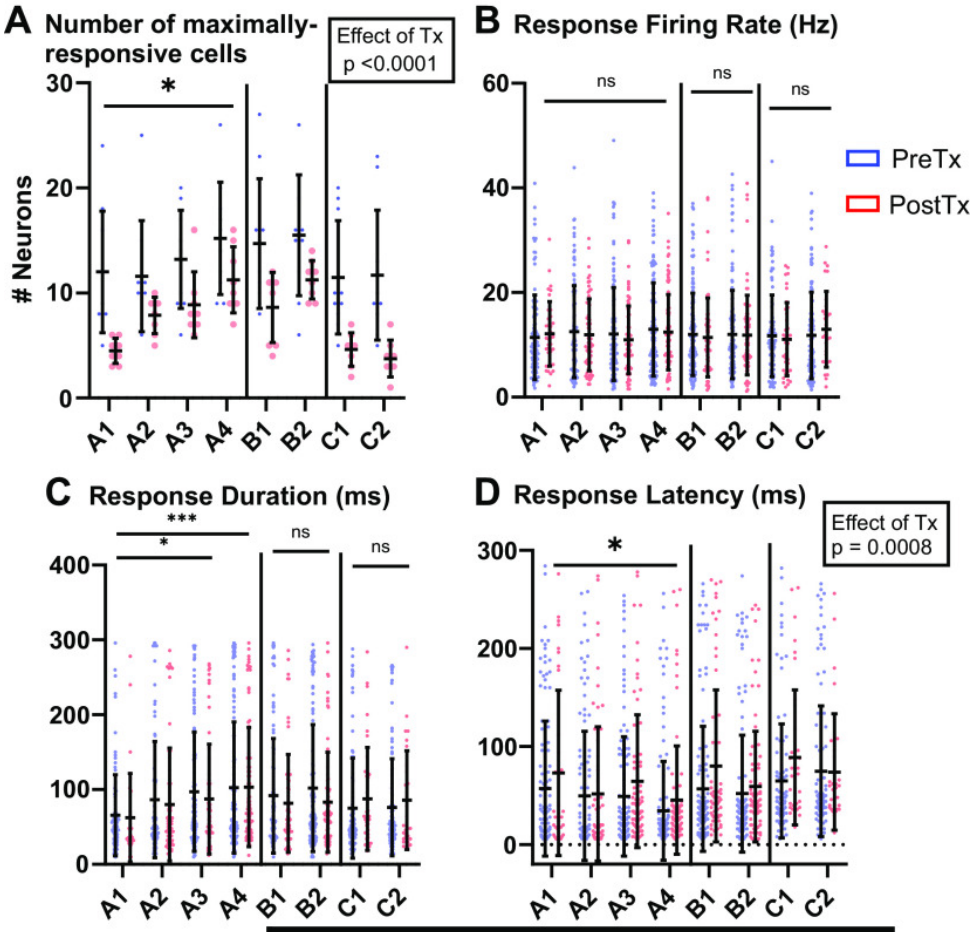

Parameter	Tilt	A1	A2	A3	A4	B1	B2	C1	C2
	Dur. (ms)	**280**	**280**	**280**	**280**	258	198	310	574
	Final Angle (◦)	6.6	9.7	13.5	16.6	**11.2**	**11.2**	6.6	16.3
	Peak Vel(◦/s)	32.4	47.4	63.0	77.7	68.9	91.5	**32.4**	**32.4**

For tilts of different duration, final angle, and peak velocity profiles (see Inset table), the number of neurons and their average response metrics were calculated and compared. If a neuron responded to more than one tilt type, it was only included in the tilt type that led to its largest response. **a** Average number of neurons per animal responsive to each tilt type Pre- (n = 10) and PostTx (n = 8). **b** Average neuron firing rate (in Hz) throughout response. **c** Average duration of neuronal response. **d** Average latency of response onset, defined as the time at which the first bin surpasses threshold. Inset: table defining the tilt types for A–D. Means and standard deviations are plotted over individual data points representing animals in A or individual neurons in B–D. Total neuron numbers for each tilt type (in B–D): A1 (PreTx: 120; PostTx: 36), A2 (PreTx: 116; PostTx: 63), A3 (PreTx:132; PostTx: 71), A4 (PreTx: 152; PostTx: 90), B1 (PreTx: 147; PostTx: 69), B2 (PreTx: 155; PostTx: 90), C1 (PreTx: 115; PostTx: 37), C2 (PreTx: 117; PostTx: 30). ***P < 0.001, *P < 0.05 (Bonferroni corrected). Tx, spinal transection.

= 0.394, P = 0.536]. However, for both Pre- and PostTx conditions, the change in response magnitude for more severe tilts was not due to changes in firing rates [F(7,1524) = 0.81, P = 0.815; Figure 3.3B] but rather to increases in response durations [F(7,1524) = 0.749, P = 0.0009; Figure 3.3C]. Therefore, increases in the severity of the tilt resulted in an increase in the duration of the response both pre- and post-SCI, regardless of the duration of the tilt.

3.4.4 Responses to tilts are delayed, but not attenuated, after transection

Interestingly, response latencies were dependent on the severity of the tilt, similar to the duration of the response (Figure 3.3D). Furthermore, despite SCI having no impact on the firing rate or magnitude and duration of response, injury delayed the timing of the response (Figure 3.3D). In fact, after injury, the response onset, was significantly delayed by about 10 ms [first bin latency: PreTx: 54.1 ± 62.3 ms and PostTx: 63.7 ± 67.1 ms, F(1,1524) = 11.22, P = 0.0008].

In summary, as the severity of the tilt increased, the number of responding neurons and duration of the response increased while the latency of the response shifted earlier without a change in firing rate. These findings emphasize the importance of the severity of the tilt on the neural response. Post-SCI, the severity of tilt had a similar impact on the neural response, but the response was shifted later without impact on the magnitude of the response. Therefore, in an unexpected postural perturbation, neurons in the hindlimb sensorimotor cortex respond to the severity of the tilt even in the absence of sensory feedback from the hindlimbs. The shift in latency after SCI suggests this response in the hindlimbs is due to sensory information about the tilt coming from the upper trunk and forelimbs.

Figure 3.4. Neuron response classification.

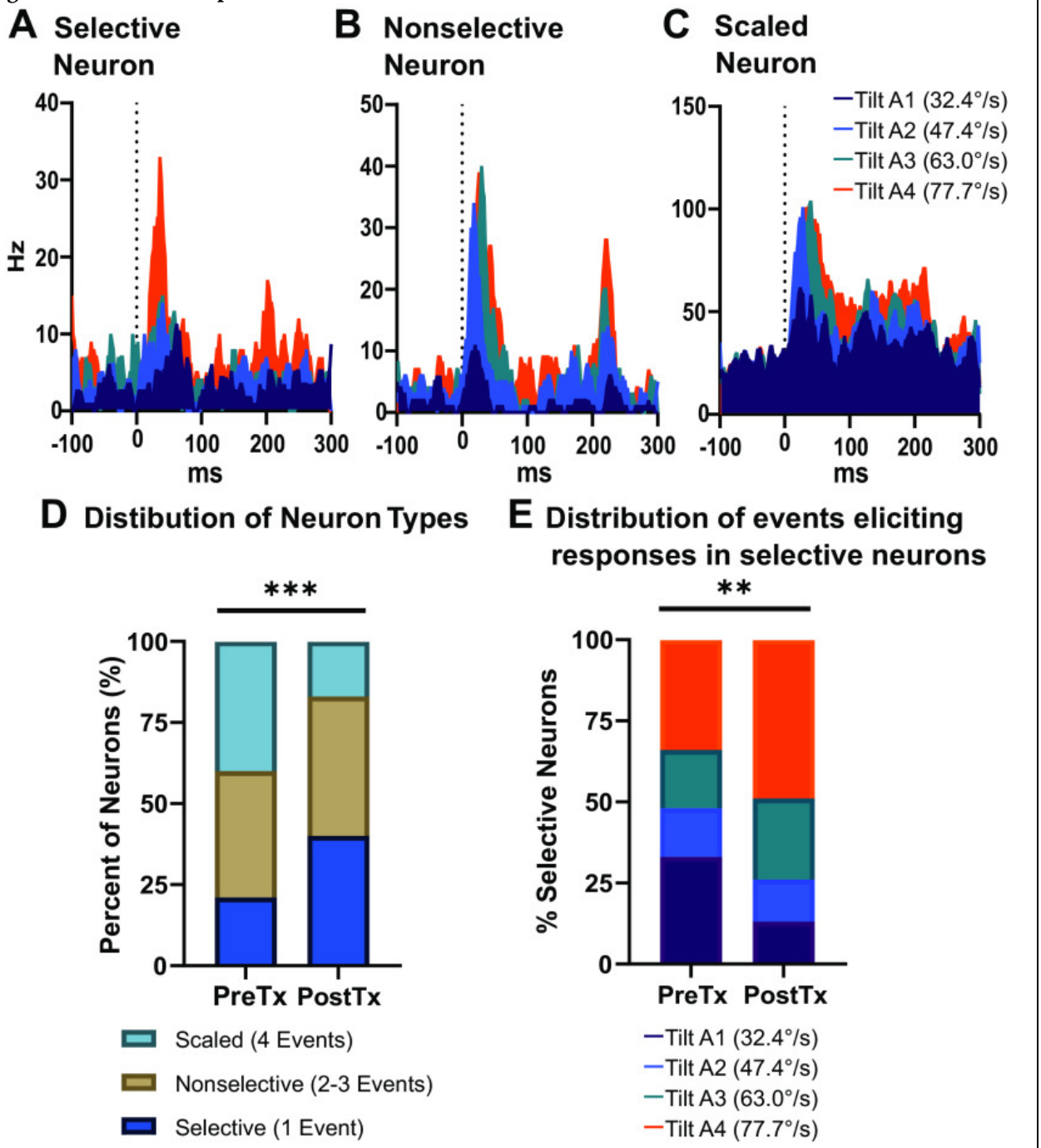

For the four tilts of constant duration but increasing peak velocity and tilt angle, neurons were categorized as being selective, nonselective, or scaled. **a-c** Exemplar peristimulus time histograms of neurons for each classification type, where **a** represents a neuron responsive to only one tilt type, **b** represents a neuron responsive to 2–3 tilt types, and **c** represents a scaled neuron, or a neuron responsive to all four tilt types. **d** Distribution of each neuron type before and after Tx. **e** Distribution of preferred event for all selective neurons before and after Tx. ***P < 0.001, **P < 0.01. Tx, spinal transection.

3.4.5 Some neurons scale their responses to tilts of increasing severity

To further explore the responsiveness of neurons to tilts of increasing severity (peak velocity), neurons were classified into three classes depending on the range of tilts they responded to (out of four possible tilts): 1) selective, neurons responsive to only one tilt type; 2) nonselective, neurons responsive to two to three tilt types; or 3) scaled, responsive to all four tilts (examples seen in Figure 3.4A–C, respectively).

In addition to delayed response to tilt after transection, there was a shift in the classification of neurons (Figure 3.4D), with a decrease in the proportion of scaled neurons (39.6%–17.0%), an increase in the proportion of selective neurons (21.4%–39.7%), and a modest increase in nonselective neurons (39.1%–43.3%) [$\chi 2(2) = 16.06$, $P = 0.0003$]. This shift occurred due to a reduced response to the least severe tilts PostTx. In fact, when classifying the selective neurons by the tilt to which they responded (Figure 3.4E), there was a significant change in these proportions [$\chi 2(3) = 12.69$, $P = 0.0054$], with the biggest change being a reduction in the number of cells uniquely responsive to the lowest severity tilt (33% v. 13%). Thus, this reduction in scaled neurons is likely due to the fact that neurons previously responsive to all tilts may no longer respond to the mildest tilts after injury, leading to a classification as either a selective (responding to one tilt type) or non-selective (responding to 2–3 tilt types) neuron.

3.4.6 Impact of SCI on neuronal dynamics during tilt

To visualize the impact of SCI on the change in firing rate of the population of neurons during tilt, the average response of neurons during each tilt was plotted against the change in GRF. Examining the left hindlimb during clockwise and counterclockwise tilts, the GRF changes first,

Figure 3.5. Relating average neural firing rate to hindlimb ground reaction forces throughout tilts

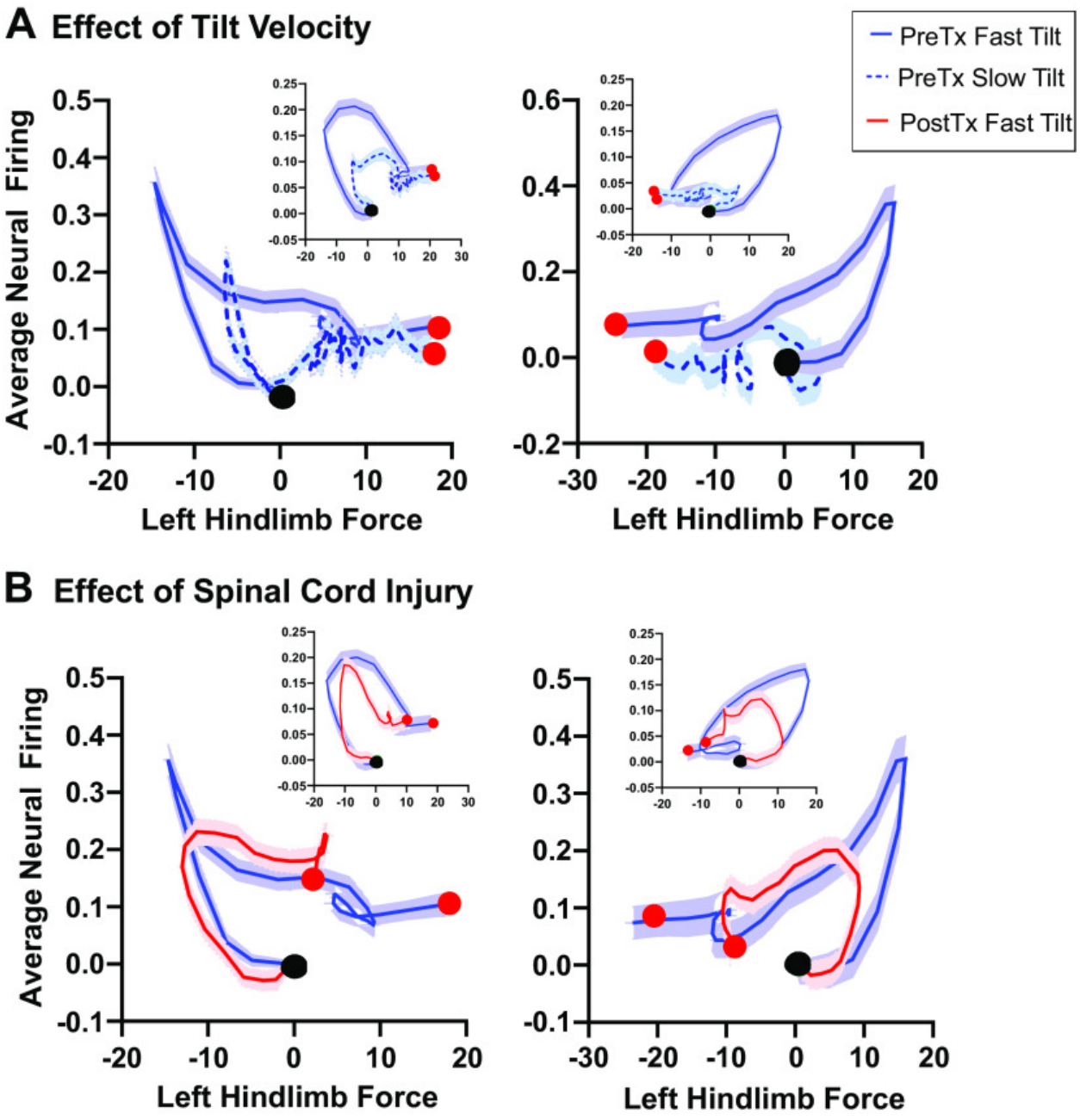

Trial-averaged left hindlimb ground reaction forces and neural firing rates (calculated as average spikes across all responsive neurons per 10 ms bin) are plotted for tilts in the counterclockwise (left plots) and clockwise (right plots) directions from the time of tilt onset (black dot) to the time of maximum tilt angle (red dot) for a single animal. A second animal's results are inset for comparison. Force and neural firing rate were zeroed at the start of tilt. **a** Comparison between fast and slow velocity tilts in the PreTx condition in the counterclockwise (left) and clockwise (right) directions. **b** Comparison between fast tilts in the Pre- and PostTx condition for the same animals in the clockwise (left) and counterclockwise (right) directions. Tx, spinal transection.

before the increase in average firing rate (Figure 3.5A). Then, the firing rate peaks at about the same time as the peak unloading of the limb due to the movement of the platform. As the limb begins to exert a restorative force to stabilize the animal's center of mass, the firing rate of the population starts to decline but does not quite return to baseline before the GRF reaches its maximum restorative force. For less severe tilts, this trajectory pattern is simply scaled down. As the population of cells are the same for the clockwise and counterclockwise tilts, these data suggest that in each hemisphere, a subset of cells are responding to the contralateral limb's extension while others are responding to the contralateral limb's flexion. After injury, the loading, unloading, and final restorative forces are attenuated, likely due to the harness support and the shift of weight to the forelimbs, and the neuronal firing rate is also reduced (Figure 3.5B), resulting in a similar shaped trajectory, albeit reduced in size.

3.4.7 Neurons encode for the detection of tilt

As neurons respond to the tilt even after a complete spinal transection and changes in the severity of the tilt (peak velocity) are the greatest drivers of that response, we wanted to gain insight into how these neurons encode information about the tilt. Specifically, we investigated how neurons encode for the occurrence of a tilt (i.e., is the platform stationary or has it tilted?) and the magnitude of the severity of the tilt (i.e., what was the peak velocity?) as well as the effect, if any, of SCI on that encoding. The first step to evaluate the encoding of tilt was to quantify the information that a tilt occurred (tilt detection) using a fixed number of neurons (Figure 3.6A).

As expected from the increase in the number of responsive neurons and the increase in the magnitude of their response with increasing severity, the information that a tilt occurred within the

Figure 3.6. Information in the hindlimb cortex about tilts

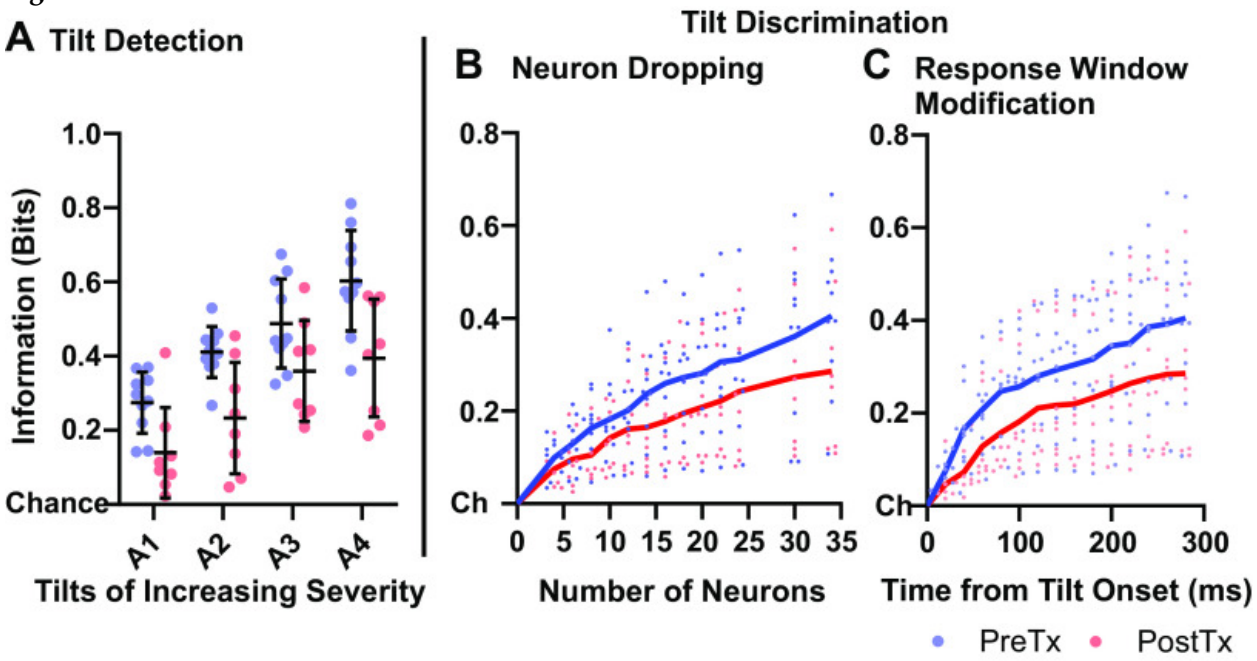

Information about tilt detection and tilt discrimination were each calculated using the PSTH classifier (see material and methods) for the four constant duration tilts of increasing peak velocity and final angle. **a** Tilt detection, or the ability to distinguish stance from the tilt, increased as a function of tilt severity ($P < 0.0001$) in both the Pre- and PostTx condition, even with a significant decrease in information PostTx ($P < 0.0001$). This was despite standardizing the number of neurons in all tilt and Tx states. Means and standard deviations plotted over individual data points. **b-c** Tilt discrimination, or the ability to differentiate one tilt type from the other three, increased with adding more neurons ($P < 0.0001$; **b**) as well as with using a set number of neurons but increasing the length of recording supplied to the classifier ($P < 0.0001$; **c**). Both instances demonstrated a reduction in information PostTx ($P < 0.0001$ and $P < 0.0001$), respectively. For both **b** and **c**, solid line represents the change in mean for each condition, plotted over data points for individual animals (PreTx n = 10; PostTx n = 8). PSTH, peristimulus time histogram; Tx, spinal transection.

HLSMC increased with the severity of the tilt both PreTx (0.27 for least severe to 0.60 bits for most severe), and PostTx [0.14 bits for least severe to 0.39 bits for most severe tilts; $F(3,64)=18.93$, $P < 0.0001$]. After transection, the information about tilt detection was significantly reduced [$F(1,64) = 31.03$, $P < 0.0001$, interaction: $F(3,64) = 0.42$, $P = 0.7406$]. As the number of neurons used to compare PostTx to PreTx was the same, this reduction in information is unlikely to be due exclusively to the trend toward fewer responsive neurons PostTx.

3.4.8 Neurons convey considerable information about tilt type both pre- and post-SCI

Though the detection that a tilt occurred is the first step in understanding how neurons encode for postural responses, of greater interest is discriminating between different types of tilts as the severity of the tilt increased, which would suggest the information necessary to determine the postural adjustments that need to be made to maintain balance. As expected, the ability of populations of neurons to discriminate between tilt types was dependent on both the number of neurons used [Figure 3.6B; $F(12,208) = 8.22$, $P < 0.0001$] and the amount of time that passed from tilt onset [Figure 3.6C; $F(13,224) = 7.56$, $P < 0.0001$]. For the same sized population, a significant reduction in information was observed after transection compared to before [neuron dropping: $F(1,208) = 19.56$, $P < 0.0001$; window size: $F(1, 224) = 27.60$, $P < 0.0001$]. When comparing the number of neurons used (Figure 3.6B), as few as twelve neurons were able to convey at least 0.2 bits of information about tilt detection in the PreTx condition. PostTx, 20 neurons were needed to convey comparable levels of information, likely arising from the decreases in cells with responses to less severe tilts after spinal cord transection. Thus, the nervous system can compensate for the loss in information about postural perturbations by recruiting more neurons into the task after SCI. As expected, as the window of time after the tilt onset used to calculate the information increased (Figure 3.6B), information about tilt discrimination increased. PreTx, the population of neurons conveyed a considerable amount of information (more than 0.2 bits) about the tilt type within the first 60 ms of the tilt. After injury, an additional 60 ms were needed (120 ms) after tilt onset to reach similar information levels, consistent with the delayed neuronal responses seen PostTx. Information continued to increase over time for

both PreTx and PostTx conditions, with information reaching 0.40 bits PreTx and 0.29 bits PostTx within 300 ms.

Therefore, as with tilt detection, both the reduction in the number of responding neurons PostTx and differences in the firing patterns of neurons contribute to the loss of information about the discrimination between different types of tilts after SCI.

3.5 Discussion

Although weight-bearing and stereotypic locomotor movements can be restored following a complete spinal injury through activation of spinal circuits below the lesion[29,187,195–199], there is a need to ensure adequate postural stability[57,116,194,200]. An understanding of how the brain encodes for this stabilization before and after spinal cord injury could be used for the design of therapeutic interventions that aim to enhance postural responses and decrease the morbidity and mortality associated with fall incidence. The data presented here suggest that the hindlimb sensorimotor cortex (HLSMC) encodes information about the severity of an unexpected perturbation by changing the number of responsive neurons and altering the duration, but not firing rate, of their responses. Moreover, after a mid-thoracic spinal cord transection, which prevents sensory information from the hindlimbs reaching supraspinal levels, information about the tilt continues to be encoded in the HLSMC with similar, albeit delayed, neural response dynamics.

3.5.1 Role of afferent feedback and effects of spinal cord injury on the encoding of postural responses in unexpected perturbations

The work presented here, in which animals were subjected to perturbations that were unexpected in timing and severity both before and after spinal cord injury, can be compared with previous studies on behavioral and neuronal responses to predictable tilts in the frontal plane[115,181]. In the previous studies using intact rabbits or cats, the animals compensate for the tilt by extending the limb when the platform moves down and flexing the limb when it moves up. Although we recorded ground reaction forces (GRFs) and not limb kinematics or trunk movements from a subset of animals, our animals behaved similarly to shift their center of mass over their base of support, maintaining an upright position and preventing falling. The use of kinematics in future studies will allow for a better assessment of post-transection behavior, as weight-supporting harnesses undoubtedly affected the ground reaction forces after SCI. With respect to neural responses, we observed unique responses in the HLSMC to unexpected tilts, just as cortical modulation was previously observed in response to tilts in both rabbits[182] and cats[115].

Despite these similarities, there are key differences that distinguish our work. First, in cats[115], the activity of pyramidal tract neurons in the hindlimb motor cortex was almost exclusively correlated with extension of the contralateral limb. In the present study, when the tilt was unexpected, cells responded to both extension and flexion, suggesting a more robust response to unexpected tilts. Second, the peak firing rate in response to unexpected tilts for intact rats was over 30 Hz, about double the rate of those previously reported[115]. This would suggest that unexpected perturbations create greater cortical responses. This is consistent with EEG and TMS studies in humans showing that the magnitudes of evoked cortical responses and postural muscle activations are greater during expected compared to expected postural perturbations[201–205].

Third, we observed a sustained cortical response to tilts even after removal of hindlimb afferents. This is in contrast with previous work that showed that suspending a hindlimb during platform tilts (and thus removing its sensory inputs) led to a strong attenuation of the response in the contralateral hindlimb motor cortex[49]. In the current study, however, a complete mid-thoracic spinal transection that removed all sensory input from below the lesion simply caused a delayed neural response to unpredictable tilts in the HLSMC but had no effect on the magnitude of the response. The unexpected tilts in this work better reflect instantaneous loss of balance and provide insight into the role of the cortex during a more complex balance task. Furthermore, this work clarifies that even after a complete spinal transection, neurons in the cortex still organize to convey information about the perturbation. It is important to note that, while our microelectrode arrays were chronically implanted in the HLSMC, we do not assume that the same neurons are being recorded pre-and post-SCI. Therefore, our conclusions are limited to the average responses of neurons in the HLSMC at these two time points.

This responsiveness in the absence of ascending sensory feedback from the hindlimbs likely originates from sensory signals from forelimb and trunk afferents caudal to the injury as well as inputs from the visual and vestibular system. It has been shown that limb somatosensory afferents are processed and even converge subcortically in the spinal cord and brainstem before reaching the cortex[206–209]. Activity from the forelimbs is likely transmitted to the deafferented hindlimb cortex producing sufficient activation to discriminate the severity of the tilt, with the delay reflecting the additional time needed to reach firing thresholds due to the loss of hindlimb afferent inputs. Although the majority of hindlimb sensorimotor cortex cells respond to stimulation of the contralateral

hindlimb, forelimb afferents also send inputs to the hindlimb sensorimotor cortex. Therefore, neurons in the "hindlimb" representation have been shown to respond to forelimb stimulation and vice versa[193]. In addition, a network of HLSMC neurons that are normally active in response to forelimb movements could be contributing to the responses we observed in the deafferented cortex. This would be in line with the work by Karayannidou et al. , in which a subset of cortical neurons followed the forelimbs more closely when the forelimbs and hindlimbs were tilted out of phase[49].

3.5.2 Neuronal encoding of tilt

Neurons have been shown to encode for multiple sensory and motor events by scaling their firing rate to a parameter of the movement. For example, using multiple linear regressions, cells in the motor cortex have been shown to modulate their firing rate depending on the speed, direction, position, and acceleration of arm trajectory[210]. Moreover, neurons in the motor cortex have been shown to increase their firing rate with finger velocity in a center-out task[211]. In sensory systems, cortical firing rate has been shown to increase with speed of whisker deflection[212]. Our findings extend this scaling of neuronal activity to the hindlimb cortex during postural events and show that the magnitude of the response is scaled to the severity of the tilt, encoding not only that a tilt occurred, but the severity of the tilt.

Therefore, not surprisingly, the information that a tilt occurred increased as the severity of the tilt increased. We show that this is certainly due to the increase in neuronal response magnitude as intensity of tilt increases (e.g., scaling), as holding the number of responsive neurons constant resulted in more information for greater intensity tilts. Of course, the central nervous system (CNS) has access

to the information from additional neurons that respond, and it is likely that this information is used by the CNS to make appropriate postural adjustments in response to the tilt. A likely explanation for the greater number of neurons responding as the intensity of the tilt increases is the need to activate more motor neurons, in turn activating more muscle groups, to maintain balance in response to larger perturbations.

Spinal cord injury reduces the amount of information about tilt detection and tilt discrimination, even when neuron numbers were held constant. This reduction in information suggests that recruiting more neurons into the task is one strategy to ameliorate any loss of information after SCI. After complete mid-thoracic spinal cord transection, neurons in the HLSMC are more likely to both respond to forelimb stimulation and also activate trunk musculature after regular physical rehabilitation[65]. This cortical plasticity has been shown to improve behavioral outcome, as lesioning this reorganized cortex reduced gains in weight-supported stepping achieved by animals that received therapy[65]. Therefore, therapeutic interventions that support reorganization would be expected to further improve outcome, and therapy along the entire neural axis, including the cortex – is likely necessary to optimize outcome after SCI[213–217].

Finally, the sustained encoding of postural information after SCI observed in this study (with respect to both stimulus detection as well as discrimination) has important translational implications for the field of neuroengineering. Despite playing a less significant role in postural control than other supraspinal centers in the brainstem, this study has demonstrated that the cortex can serve as a source of information about postural perturbations after SCI. Brain-machine interfaces can be developed

using cortical signals to augment postural control, such as through spinal or peripheral nerve stimulation to support functional recovery after spinal cord injury.

Chapter 4 – Cortical population dynamics during postural control are preserved after spinal cord injury

4.1 Summary

Human and animal subjects with various neurological conditions are capable of controlling neuroprosthetics using their own cortical signals with surprising ease, even years after loss of sensorimotor function. However, the underlying neural computations that explain this phenomenon have not been elucidated. Employing a clinically relevant rodent model of spinal cord injury, we assessed the extent to which both single-neuron and population-level dynamics in the trunk and hindlimb representations in the motor cortex were affected by injury as well as subsequent physical rehabilitation therapy. Surprisingly, while spinal cord injury led to significant postural deficits and a reduction in cortical encoding about postural disturbances on a single neuron level that were both modestly attenuated with regular physical therapy, the dynamics of neural populations continued to sufficiently predict the animal's desired position in space. Additionally, despite significant changes in behavior and single-neuron dynamics, these population dynamics remained stable for months after injury – providing not only evidence of the cortex's maintained role in postural control after injury, but a possible explanation for neuroprosthetic learning after neurological injury.

4.2 Introduction

Various neurological conditions (e.g., spinal cord injury, amyotrophic lateral sclerosis) sever the communication between the brain and motor outputs, leading to severe, debilitating motor deficits. Brain-machine interfaces aim to restore this disconnect by creating a functional bypass to improve motor function. Substantial work has sought to decode cortical signals to restore arm movement[15,24], speech[135], and lower limb function[27,28,53].

Despite large scale reorganization across the neural axis and impaired sensorimotor function associated with neurological conditions such as spinal cord injury[57,63,65], individuals have the remarkable capacity to quickly learn to map their neural signals to idealized movement[16,19,27,53,116,218] – even when such movements have been impaired for years. In order for individuals to achieve such proficiency after injury, we hypothesized that the cortical computations related to movement generation must be sufficiently stable even after significant neurological injury. If true, this would help explain the success of decoding movement from an injured nervous system.

Dynamics of neural populations in the uninjured cortex are governed by rich underlying structure[77,85,86,92,124] that exhibit long-term stability[219] and even commonality between individuals[125]. However, it is unknown the extent to which significant changes to sensory inputs and impaired motor output would affect such stability. Thus, we sought to not only evaluate the stability of cortical motor control signals after injury, but also if such cortical computations can be found specifically for postural control, as the ability to fully restore independent lower limb function remains limited by the fact that such neuroprosthetic work often fails to account for postural instability. We previously showed that in uninjured animals, the cortex undergoes unique computations on the population level to coordinate the body's response to different perturbations. While limited work has evaluated the

effect of such injuries on the response patterns of individual cortical neurons[114], the effect of injury on population level dynamics remains unknown.

After characterizing the effect of a clinically relevant moderate contusion injury on postural stability, we recorded the single-neuron activity in the primary motor cortex (M1) while rats maintained balance on a randomly tilting platform. As physical rehabilitation has been shown to be critical for the motor improvement after spinal cord injury[65] and is thus standard in the longitudinal care of SCI, a subset of animals underwent additionally treadmill training so we could assess the influence of exercise therapy on these cortical processes.

After injury animals exhibit both behavioral postural impairments as well as a reduction in the responsiveness and perturbation-specific modulation of individual neurons in the motor cortex. Physical rehabilitation therapy attenuates both of these effects and is therefore associated with moderately improved functional outcome. However, despite these changes in behavior and cortical responsiveness, cortical population dynamics remain consistent with those observed prior to injury for at least two months after injury. These results may explain how individuals can successfully learn to control neuroprosthetics after neurological injury while also providing evidence that the cortex can also be used as a control signal to restore postural stability after spinal cord injury.

4.3 Results

4.3.1 Treadmill therapy prevents the reduction of postural stability observed after moderate contusion

After completing a series of pre-injury behavioral assessments, rats received a moderate spinal contusion injury at vertebral level T10 and were randomly assigned to either an exercise therapy or control group. One week after injury, animals assigned to the exercise therapy group underwent thirty minutes of treadmill walking therapy five days a week for eight weeks. Control animals were administered a "sham" therapy in which they were placed on a stationary treadmill for the same amount of time.

Moderate contusion led to significant motor impairment that moderately resolved over subsequent weeks independent of experimental group [$F(1, 34) = 0.06$, p 0.804] as measured by the BBB scale[220]. One week after injury, 46% of animals displayed little to no hindlimb movements with the remaining 54% showing occasional intervals of uncoordinated stepping (Scores = 7.3±1.9). In contrast, nine weeks after injury, all animals had regained some degree of stepping, with 53% displaying intervals of uncoordinated stepping and 47% recovering forelimb and hindlimb coordination (Scores = 14.9±3.3).

However, since the BBB score does not exhaustively assess all aspects of gait (e.g., temporal dynamics), we performed an automated gait analysis (Fig. 4.1a) and compared the quality of stepping between animals who received regular therapy (n = 5-7) and those who did not (n = 8-14) prior to injury and then three, five, seven, nine weeks after injury. Linear discriminant analysis (LDA) was used to identify gait parameters that maximize the separability between classes (e.g., therapy v. non-therapy). Separately for each session (pre-injury and then weeks 3, 5, 7, and 9 post-injury), an LDA model was built using a leave-one-out approach and the remaining trial was then classified as either belonging to a therapy or control animal. Whereas therapy and non-therapy trials could not be

distinguished pre-injury and in the early weeks post-injury, classification accuracy rose above chance levels in later weeks, suggesting exercise altered the manner by which animals walked after injury (Fig. 4.1b).

Figure 4.1. Stepping characteristics over time.

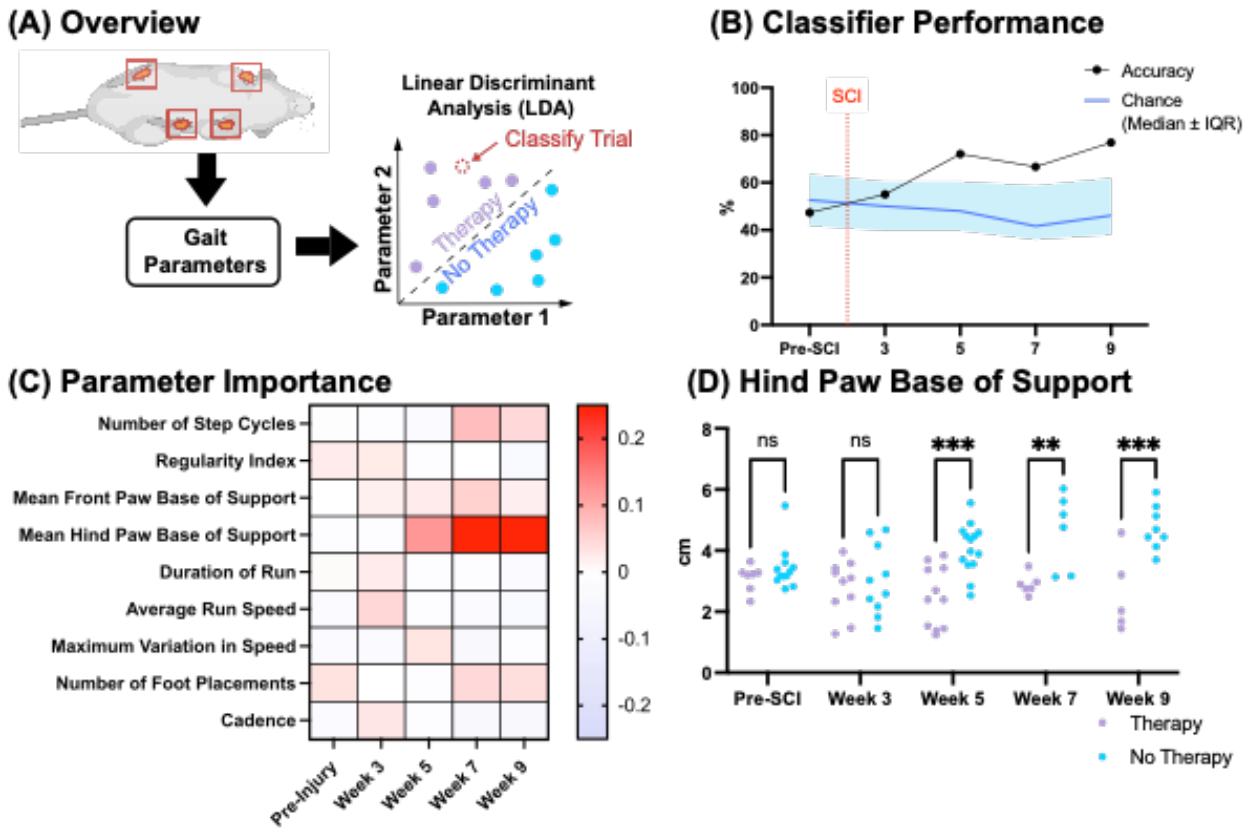

a Multiple gait parameters based on foot placements during walking trials served as inputs to a linear discriminant analysis (LDA) classifier, which defines a linear boundary that best separates trials therapy and no therapy animals. A left-out trial (red) is classified based on this boundary. **b** Classifier performance was evaluated across weeks and compared to a chance distribution based on 1000 iterations of classifications after shuffling group-parameter relationships. IQR = interquartile range. **c** Relative importance of each of the nine gait parameters used was calculated using the ReliefF algorithm, where larger positive values imply greater importance. **d** Mean hind paw base of support over time. Points represent a trial for a single animal. ***p<0.001, **p<0.01, ns = not significant.

Since an LDA approach was able to successfully discriminate the gait of exercised and non-exercised animals at later time points, we determined which parameters best informed this

classification (Fig. 4.1c). The ReliefF algorithm[221] rewards predictors that give different values to neighbors of different classes in multidimensional variable space while also penalizing parameters that give different values to neighbors of the same class. The most important parameter discriminating the gait patterns of the two groups when above-chance classification occurred (i.e., Week 5, 7, and 9) was the mean distance between the hind paws, or the average width between the hind paws when walking. Thus, we evaluated the effect of injury and therapy on hind paw base of support (Fig. 4.1d). As expected, there was a significant interaction between therapy and time [$F(4,78) = 3.803$, $p = 0.0071$, two-way ANOVA]. Animals who did not receive therapy began to widen their best of support relative to Pre-SCI at later weeks [Week 3 ($p = 0.722$), Week 5 ($p = 0.255$), Week 7 ($p = 0.030$), Week 9 ($p = 0.007$)], consistent with other work[222]. In contrast, there was no change observed among animals that received therapy at any time point [Week 3 ($p = 0.926$), Week 5 ($p = 0.6926$), Week 7 ($p =0.988$), Week 9 ($p = 0.792$)].

Adopting a wider base of support represents one strategy to maintain postural stability, reducing the need for more refined joint movements in the face of a perturbation. As non-exercised animals widened their hindlimb base of support over the weeks following spinal cord injury, this result suggests that injured animals must acquire novel compensatory postural strategies when not provided physical rehabilitation therapy after injury.

4.3.2 The hindlimb adopts novel, exercise-dependent locomotor strategies after moderate contusion

To more thoroughly characterize changes in gait after contusion, we collected two-dimensional hindlimb kinematics during treadmill walking for individual step cycles from a subset of

animals (therapy = 4, control = 4) at weeks 2 (therapy: 302 step cycles v. control: 158 step cycles), 5 (374 v. 171 step cycles), and 9 (389 v. 214 step cycles) after injury (Fig. 4.2a). Changes in kinematic parameters were compared between exercised and non-exercised animals using a linear mixed effects model with the individual animal as the random effect.

While pre-injury recordings were not collected due to difficulty for animals to tolerate the harness (see Methods), the gait between the two groups did not differ at Week 2 (toe height, $p = 0.6172$; stride length, $p = 0.1991$); stance phase duration[223], $p = 0.3546$; swing phase duration[223], $p = 0.6671$).

However, all four of these parameters were affected differently for the two groups at later time points (Fig. 4.2b-e) [Interactions of group x week post-injury: Toe Height, $F(2,1660.60) = 20.2106$, $p < 0.0001$; Stride Length, $F(2, 1660.10) = 22.3289$, $p < 0.0001$; Swing Phase Duration, $F(2, 1660.78$, $p = 0.0433$); Stance Phase Duration, $F(2,1660.75)$, $p = 0.0014$]. For non-exercised animals, toe height (Fig. 4.2b) significantly decreased at week 9 [Week 2 v. Week 9: $p = 0.0001$; Week 5 v. Week 9: $p < 0.0001$] whereas exercised animals displayed a significant and stable increase in toe height by week 5 [Week 2 v. 5: $p < 0.0001$; Week 5 v. Week 9: $p = 0.386$]. This was associated with a relative decrease in the stride length (Fig. 4.2c) in the non-exercised animals [Week 2 v. Week 5, $p = 0.3870$; Week 2 v. Week 9, $p = 0.0009$; Week 5 v. Week 9, $p < 0.0001$] and increase in the exercised animals [Week 2 v. Week 5, $p = 1.000$; Week 2 v. Week 9, $p = 0.0071$; Week 5 v. Week 9; $p = 0.0056$].

These positional changes were associated with temporal changes as well. Whereas the stance phase duration (Fig. 4d) of non-exercised animals significantly dropped at later time points [Week 2 v. Week 5, $p = 1.000$; Week 2 v. Week 9, $p = 0.0003$; Week 5 v. Week 9, $p = 0.0010$], it remained largely

Figure 4.2. Effect of therapy on hindlimb kinematics after injury

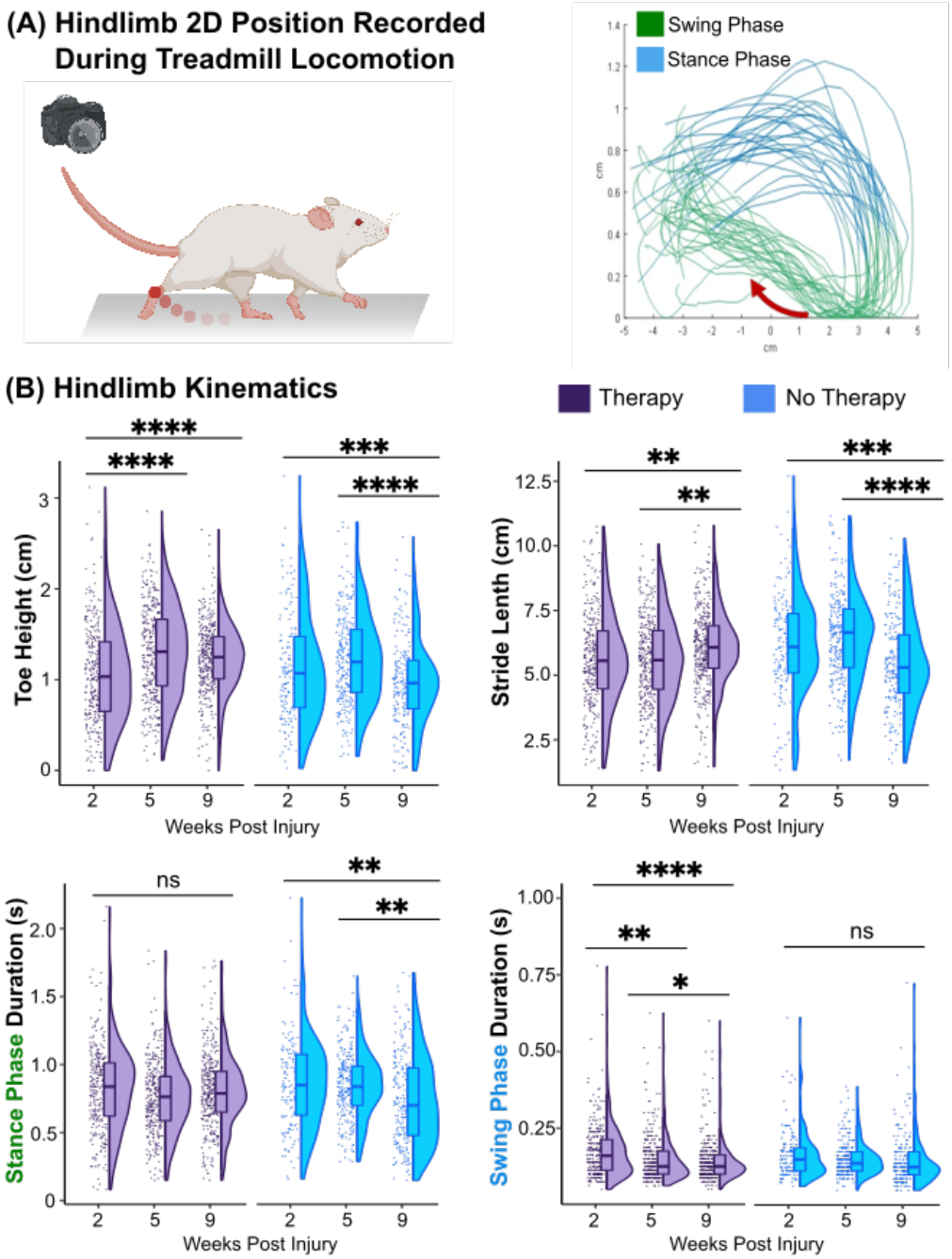

a Behavioral setup in which a camera tracked the 2D position of a marker on the right hindlimb as the rat walked unsupported on a treadmill (left). Exemplar hindlimb trajectories for one animal, divided into the stance (green) and swing (blue) phases of the step cycle (right). **b** Toe height, stride length, stance phase duration, and swing phase duration shown as a function of time for each experimental group. Each point represents a step cycle from a single animal. Statistical significance determined with a linear mixed effects model to control for within-animal effects. ****p < 0.0001; ***p<0.001, **p<0.01, *p<0.05, ns = Not significant.

constant in the exercised animals [Week 2 v. Week 5, p = 0.0854; Week 2 v. Week 9, p = 0.7814; Week 5 v. Week 9, p = 0.7272]. Conversely, the swing phase duration (Fig. 4e) was constant across time for the non-exercised animals [Week 2 v. Week 5, p = 0.2810; Week 2 v. Week 9, p = 0.3554; Week 5 v. Week 9; p = 1.000] but became significantly faster with each subsequent week for the exercised animals [Week 2 v. Week 5, p = 0.0006; Week 2 v. Week 9, p < 0.0001; Week 5 v. Week 9, p = 0.0482].

Therefore, injury reduced the size of the path taken by the hindlimb while also reducing the time the animal maintained contact with the platform. This inability of the non-exercised animals to maintain contact with the treadmill before taking additional steps suggests instability in maintaining weight supported steps (and thus poor postural control strategies). However, therapy led to fewer, larger hindlimb movements with a more confident, faster swing phase as well as a more stabilized stance phase – all continuing to improve with time. These combined data support that exercise is associated with better hindlimb control and robust steps.

4.3.3 Information in M1 about postural perturbations is reduced after moderate injury, but maintained with exercise therapy

So far, we demonstrated that our moderate contusion model has a detrimental effect on postural stability that is attenuated with regular physical rehabilitation. To assess the effect of spinal cord injury and subsequent therapy on cortical encoding of posture and ultimately the associated cortical computations, twelve animals (therapy = 7, control = 5) were implanted with microwire arrays that spanned the primary motor cortex (M1) of one hemisphere (Fig. 4.3a). Prior to injury and then 1-, 5-, and 9-weeks post-injury, we recorded single-unit neural activity in the trunk and hindlimb regions within M1 [Pre-Injury: 362 neurons (91 ± 24) across exercised animals v. 154 neurons (59 ±

25) across non-exercised animals; Week 1: 351 (95 ± 29) v. 241 (90 ± 17) ; Week 5: 343 (99 ± 29) v. 200 (81 ± 16) ; Week 9: 319 (91 ± 26) v. 174 (67 ± 16)] as animals maintained balance while standing unrestrained on a platform that tilted randomly at two different speeds in each direction in the lateral plane.

Figure 4.3. Single neuron tilt discrimination

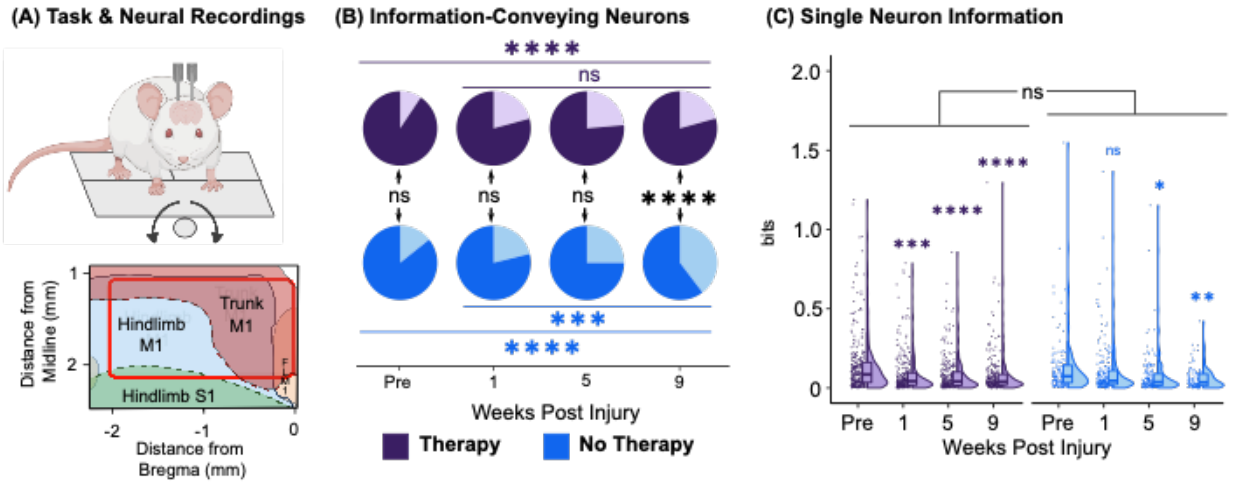

a Rats stood on a platform that tilted clockwise or counterclockwise at two different speeds (top) while single-unit neurons were recorded from the trunk and hindlimb motor cortex (M1, coordinates shown on bottom). **b** Neurons that conveyed greater mutual information about the tilt type than chance were considered "information-conveying" neurons. Ratios of information-conveying neurons were compared across time and therapy groups. Statistical significance determined by chi-square tests. **c** Mutual information based on the ability to discriminate the different perturbation types was quantified for information-conveying neurons described in **b** and compared across time and experimental group. Statistical significance was determined by a linear mixed effects model, controlling for between-animal effects. **b,c** Pre = Pre-Injury, ****p<0.0001, ***p<0.001, **p<0.01, *p<0.05, ns = not significant.

In line with previous work, we observed that M1 neurons conveyed information about the perturbation at all time points post-injury. Information (measured in bits) was determined by calculating the mutual information between a neuron's firing pattern and the type of perturbation during a given trial, and this value was compared to the average information conveyed after shuffling

firing pattern and trial relationships 100 times (i.e., "chance information"). A neuron was considered informative if it conveyed more information than chance (Fig. 4.3b). Prior to injury, 90.6% of neurons in the therapy group and 85.7% of neurons in the control group conveyed information, with no difference observed between groups [$\chi^2(1) = 2.19$, $p = 0.555$]. Injury significantly reduced the proportion of informative neurons in both therapy [$\chi^2(3) = 28.14$, $p < 0.0001$] and control animals [$\chi^2(3) = 31.28$, $p < 0.0001$], with no difference between groups one week after injury [therapy: 79.2%, control: 78.8%, $\chi^2(1) < 0.0001$, $p = 1.000$]. However, whereas information continued to decline in subsequent weeks in the control group [$\chi^2(2) = 18.31$, $p = 0.0002$], no further loss was observed in the exercised animals [$\chi^2(2) = 1.10$, $p = 1.000$]. As a result, significantly more neurons conveyed information than control animals by week 9 (79.3% in therapy animals, 60.3% in control animals, $\chi^2(1) = 19.42$, $p < 0.0001$]. Therefore, while injury significantly reduced the proportion of neurons that modulated their responses for the different perturbations, physical therapy prevented further the additional reduction in the size of the responsive neural pool observed in non-exercised animals.

In addition to quantifying the size of the population of neurons that convey information, the amount of information actually conveyed by those neurons is equally important. Therefore, we evaluated the effect of injury and subsequent therapy on the amount of information conveyed by individual M1 neurons (Fig. 4.3c). Regardless of therapy [$F(1, 10.38) = 0.0439$, $p = 0.8380$], single neuron information was significantly reduced after injury [$F(3,1686.6) = 12.4944$, $p < 0.0001$].

Therefore, on a single neuron level, spinal cord injury leads to a reduction in both the proportion of information-conveying neurons in M1 as well as the amount of information conveyed by those neurons. Exercise prevents further decline in the number of information-carrying neurons

but does not impact the amount of information carried per neuron. This rescue of information carrying neurons was associated with improved postural behavior.

4.3.4 Preserved cortical dynamics after injury support maintained decoding

Given these behavioral changes as well as single neuron mutual information changes we wanted to assess the extent to which we could decode the *intended* posture of the animal based on the activity of neural populations. Therefore, we decoded the instantaneous angle of the tilting based on M1 population activity using a linear Kalman filter[224] (Fig. 4.4a). Prior to injury, M1 was able to decode the angle of the platform with relatively high accuracy (correlation coefficient: 0.51 ± 0.23). Interestingly, decoding accuracies remained comparable to pre-injury accuracies at one (0.54 ± 0.19; t(11) 0.6212, p > 0.999, Bonferroni adjusted), five (0.46 ± 0.16; t(11) = 0.8390, p > 0.999, Bonferroni adjusted), and even nine (0.38 ± 0.19; t(11) = 2.360, p = 0.1134, Bonferroni adjusted) weeks after contusion (Fig. 4.4a). Additionally, exercise therapy had no effect on decoding accuracies after injury [F(1,10) = 2.014, p = 0.1866].

Our behavioral and single neuron analyses demonstrated significant effects after mid-thoracic contusion; therefore, the unaltered ability of neural populations recorded in the hindlimb and trunk regions of the cortex to decode the position of the platform is surprising. The attenuation in mutual information observed in individual M1 neurons after injury that likely arose from damage to both ascending and descending fibers in the mid thoracic spinal cord clearly did not impact the ability of the population to decode. Gallego et al demonstrated long-term stability of dynamics within the somatosensory cortices in monkeys during a reaching task for up to two years despite the steady

Fig 4.4 Preserved cortical encoding supported by maintained neural dynamics

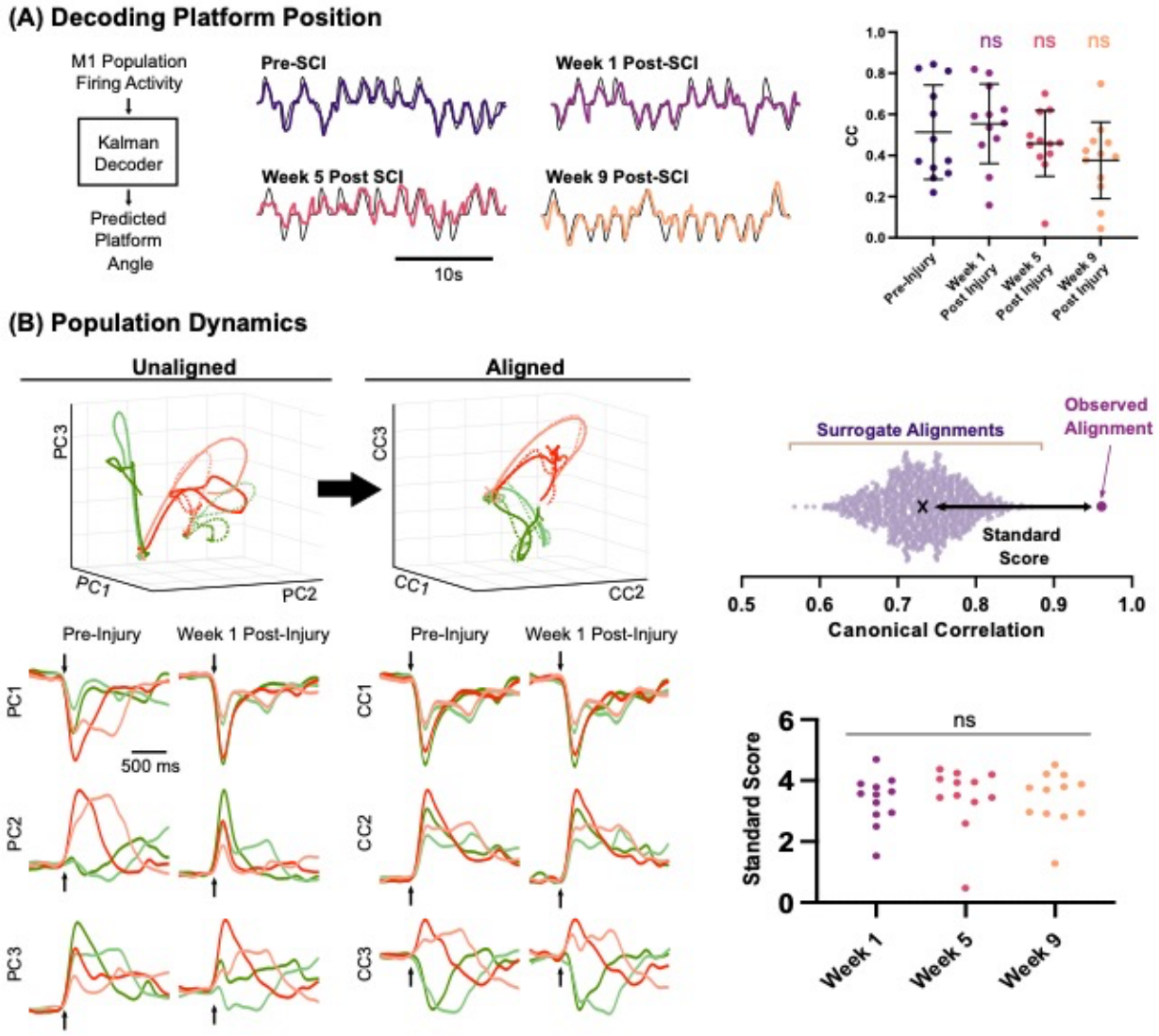

a Firing activity from the hindlimb and trunk M1 were used to predict the angle of the platform on which the rat stood. Exemplar predictions (colored lines) compared to true platform angles (black lines) are shown for one animal (center). Decoding accuracy (CC, correlation coefficient) is shown over time, with each point representing one animal (right). **b** Canonical correlation analysis (CCA) aimed to align pre-injury and post-injury neural trajectories for the four tilt types (red = counterclockwise, green = clockwise, dark = fast, light = slow). Top plots show latent dynamics before and after alignment. (Top) Solid lines show pre-injury trajectories whereas dotted lines show post-injury trajectories. (Bottom) Plots show individual components plotted against time, with arrow denoting start of tilt. PC = principal component, CC = canonical. Experimental canonical correlations were compared to a distribution of 1000 correlations calculated from simulated neural data, and a standard score (i.e., a z-score) was calculated for the true experimental value (right, top). These standard scores were compared across time (right, bottom), with each point representing one animal. **a, b** Statistical significance was determined by repeated measures ANOVA. ns = not significant.

turnover in recorded neurons using canonical correlation analysis (CCA)[219]. They concluded that these stable dynamics support the consistent behavior seen across days. Thus, we hypothesized that maintained cortical decoding of platform position was similarly supported by cortical computations that are maintained even after significant spinal injury.

We used canonical correlation analysis (CCA) to assess the stability of neuronal dynamics post injury by comparing how well post-injury M1 dynamics aligned with those observed pre-injury (Fig. 4.4b). Importantly, alignment on average remained over three standard deviations greater than that achieved by comparisons of the same pre-injury dynamics to 1000 different simulations of post-injury dynamics we constructed using tensor maximum entropy (TME)[225]. The TME method generates a set of surrogate neural activity that preserves the mean and covariance of the original neural data across time, neurons, and conditions but is otherwise random. Interestingly, we observed no changes across weeks post-injury [$F(2,20) = 0.2420$, $p = 0.7874$) or between treatment groups [$F(1,10) = 0.6640$, $p = 0.4341$]. Thus, despite the changes we observed on the individual neuron level, cortical dynamics (and therefore posture-related computations) remain preserved even after spinal cord injury.

4.4 Discussion

Using a rodent model of spinal cord injury with and without physical rehabilitation therapy, we investigated the extent to which significant sensorimotor deficits and well-established plasticity along the entire neural axis could alter the underlying dynamics of the cortex, particularly with respect to those implicated during postural control. Indeed, mid-thoracic contusion injury caused marked motor dysfunction that was associated with a decrease in both the number of cortical neurons

conveying posture-related information as well as the information conveyed by those neurons. This supports previous work in which we observed that the forces animals applied to the tilting platform during the perturbations were both delayed and attenuated after complete transection of the same spinal level[114,116]. These deficits were similarly associated with decreased modulation and responsiveness in the hindlimb sensory and motor cortices. Interestingly, moderate physical rehabilitation through daily exercise therapy appeared to have lessened the severity of both of these behavioral and cortical effects. In contrast, population level encoding remained preserved, with neural ensembles continuing to predict the speed and magnitude of the perturbation on a single-trial basis at every timepoint studied after spinal cord injury. While this could have been explained by successfully developed novel or adaptive computations in response to sustained sensorimotor function, our results here demonstrate that this was most likely explained by the fact that the underlying computations of this cortical area in fact remained highly stable even after injury. Interestingly, these population-level computations in the motor cortex were perturbed neither by injury nor by physical therapy, even when these both led to different levels of motor function and even unique changes to the very neurons making up those populations.

Stability of neural signals in light of changes to the neural system, either as a result of injury or through therapy-mediated neuroplasticity, likely explains why injured individuals are able to so readily learn neuroprosthetic control[226]. Instead of adapting arbitrary, novel computations that differ from existing neural structure and impede learning[227], individuals can utilize pre-existing repertoires to control a brain-machine interface[228]. While stability has been observed in cortical computations during motor tasks in healthy subjects[219], the effect of neurological injury on these able-bodied dynamics has

not directly been studied, especially at the single-neuron level. In two different brain-machine interface tasks where population activity in the hindlimb M1 directly controlled an external device, we observed that animals performed just as well after complete spinal cord transection as they did prior to injury[27,116].

This could have occurred in one of two ways: (1) the cortex could have employed preserved population-level computations, or (2) novel strategies could have been adopted that ultimately perform the same. Multiple pieces of evidence support the former. First, cortical representations of limbs remain remarkably stable following amputation[229,230]. Activation of the hand region in the human primary sensory cortex (S1) evokes sensation in the amputated "phantom" arm – not in the neighboring representations[231], providing an anatomical substrate for maintained dynamics that are robust to altered sensory inputs and motor outputs. Second, the pairwise differences in single-unit neural activity recorded from the postural parietal cortex during different individual finger movements in a tetraplegic subject had similar structure to those gleaned from the fMRI activity of able-bodied individuals[232], suggesting motor representations are maintained even a decade after injury. Third, significant similarities have been observed between the neural dynamics of humans with absent or severely impaired motor function to those characterized in healthy non-human primates[14,91], demonstrating not only conserved cortical function across species but implying preserved dynamics after severe motor neuron disease. Thus, even in the absence of sensory feedback and limb movement, M1 computations remain heavily preserved. This likely relates to the fact that cortical computations during actual and imagined movement are governed by highly similar dynamical features[233].

How can population activity can be stable despite significant changes in single neuron dynamics, such as those that we observed in both therapy and control animals after injury? Such a disconnect has been observed by others in the motor cortex as well as sensory[234,235] and even hippocampal[236] networks. Despite unstable single neuron tuning properties over short periods of time, skilled movement[237] as well as decoding accuracy from frontal and parietal neural populations[238] remain consistent. One possibility is that significant redundancy simply exists within the neural ensemble, such that single-neuron volatility does not perturb population-level dynamics[234,235,238]. Alternatively, significant active compensation can occur to maintain a stable population in a sort of dynamic equilibrium[239]. For example, pharmaceutically suppressing synaptic activity of hippocampal neurons grown in vitro temporarily decreased the population's average firing rate but led to sustained changes in most individual neuron firing rates long after the population stabilized[236]. Analogously, we observed the performance of rats in a brain-machine interface task transiently decrease immediately following a complete spinal cord transection; however, the return to pre-injury performance of our population decoder less than a week later was associated with changes to single neuron firing patterns[27].

Finally, an unaddressed question in brain-machine interface research is the ultimate interplay between BMI use and different forms of neuroplasticity, such as those mediated through interventions like physical rehabilitation therapy[57]. As BMI use itself induces sustained changes in the firing properties of neurons in the cortex as individuals learn to control these devices[159,240], do the changes associated with these two interventions act synergistically (i.e., creating better outcomes than either can alone) or perhaps antagonistically (i.e., working against each other and preventing optimal

outcomes)? Whereas exercise was associated with marked behavioral improvement and maintenance of cortical responsiveness to perturbations, it did not impede cortical decoding performance or even alter the population-level dynamics in the cortex that a brain-machine interface would utilize – suggesting that an antagonistic relationship is less likely. Further work will be needed to investigate the relationship between prolonged therapy and "online" neural control of postural devices (or stimulation to the spinal cord itself to restore muscle movements) to fully tease apart this question.

4.5 Methods

All surgical and experimental procedures were approved by the Institutional Animal Care and Use Committee of the University of California, Davis. Adult female Sprague Dawley rats were used for all experiments.

Spinal Contusion Surgery: Rats received robotically controlled injury delivered at the T10 vertebral level using the Infinite Horizon impactor (Precision Systems and Instrumentation, USA). The impact force was set at 150 kdyn.

Physical Rehabilitation Therapy: Beginning one week post injury, animals underwent 30 minutes of moderate intensity, quadrupedal treadmill training five days a week for eight weeks. If weight supported plantar stepping could not be achieved, the ventral surfaces of the hind paws were gently stroked in a rhythmic manner and plantar placement of the paws onto the treadmill surface was facilitated manually. Minimal body weight support was required by either lateral pelvic support or holding the distal end of the tail for vertical support. Treadmill speed was adjusted throughout a session to allow (8 – 14 m/min).

Automated Gait Analysis: Gait analysis was performed using the CatWalk Automated Gait Analysis System (Noldus Technology). A glass plate enclosed on the top and two sides suspended 1.5 m above the floor serves as a walkway that rats traverse. A green LED light illuminates the plate, which becomes more intense when contact is made with the glass plate. A red LED light illuminates the corridor from the ceiling, generating a silhouette when the animal enters the corridor. A high-speed camera positioned underneath the glass walkway captures each paw and silhouette, and each footprint is manually labelled by the experimenter. The CatWalk XT software generates numerous parameters for qualitative and quantitative gait analyses. The following parameters were assessed for each trial run: duration of the run, average run speed, number of foot placements (steps), number of patterns (i.e., the number of normal stepping patterns, defined below), regularity index (i.e., the number of normal patterns relative to the total number of steps), cadence (i.e., steps per second), maximum variation in the average speed, and the mean base of support separately for the hind paws and forepaws. A normal stepping pattern fell into one of the three categories: cruciate (right forepaw, RF – left forepaw, right hind paw, RH – left hind paw, LH or LF – RF – LH – RH), alternate (RF – RH – LF – LH or LF – RH – RF – LH), or rotate (RF – LF – LH – RH or LF – RF – RH – LH).

Classification of Automated Gait Assessment Runs: For each assessment timepoint (Pre-Injury, Week 3, Week 5, Week 7, and Week 9), a linear discriminant analysis classifier was used to classify runs by therapy group, with each run representing a unique animal's trial. Classifier accuracy was assessed using a leave-one-out approach. Chance accuracy was calculated by shuffling the associations between animal group and gait parameters and re-running the classifier. A chance distribution was calculated based on 1000 iterations of this reshuffling. To determine which gait

parameters best contributed to this classification, the ReliefF algorithm[221] was used. This randomized and iterative algorithm evaluated the parameters based on how well their values discriminated the runs from the other experimental group.

Treadmill Kinematic Recordings: Animals were acclimated to a treadmill after spinal cord injury. Colored markers were applied to the toes of the left hindlimb. A video camera (Cineplex Studios, Plexon Inc.) placed to the side of the treadmill tracked the cartesian coordinates of the markers, acquiring at 80 frames per second. Animals were placed in a harness that ensured a stationary position on the treadmill but provided no weight support or lateral stabilization. A MATLAB script was used to extract toe position data, the following kinematic variables were calculated: maximum toe height, stride length, the duration of the swing phase (the time from toe-off to following foot-strike) and the duration of the stance phase (from foot-strike to following toe-off). Assessments were only collected post-injury as uninjured animals would not tolerate the harness and not engaged in the task.

Tilt Task: Similar to our previous work[114,116,129], animals were positioned on a platform. At random inter-tilt intervals, the platform would tilt in either the left or right direction at one of two speeds to a maximum angle of 16˚ before returning to the neutral position at a constant speed. Tilt order was randomized, and no visual or auditory cue was given prior to tilt onset. 100 trials of each tilt type were collected.

Neural Implants: To record chronically from populations of cortical neurons, we implanted rats with 32-channel (8 x 4 configuration, 250 mm resolution; Microprobes, Gaithersburg, MD, USA) in the infragranular layer (1.3-1.5 mm) of the right hemisphere using standard surgical procedures. The electrode array spanned 0-2mm caudal to bregma and 1.25-2.0 mm lateral to midline, centered

around the trunk and hindlimb representations in the primary motor cortex (M1)[129]. Neural signals were amplified and filtered (Multichannel Neuron Acquisition Processer; Plexon Inc, USA) and then manually sorted into putative single units online (Sort Client; Plexon Inc, USA), with sort quality reassessed prior to each neural recording session. Spike times were collected as the animal completed the tilt task.

Information Analysis: In line with our previous work[114,116], we assessed the amount of information in individual neurons using a peristimulus time histogram (PSTH)-based classifier[241] using the first second of neural firing after tilt onset in 50ms bins. Briefly, Briefly, in a leave-one-out manner, PSTHs are generated from remaining trials for each tilt type. A single trial is then classified as belonging to the tilt type for which PSTH had the smallest Euclidian distance relative to that trial's spiking activity. Mutual information was calculated from classifier's confusion matrix. For four tilt types, mutual information values could range from 0 bits (implying no relation between neural firing patterns and the different tilt types) to 2 bits (based on the Shannon information formula with four equally likely perturbation types). Chance-level information was determined by calculating information conveyed by the same neural activity after shuffling the trials to which it belonged. This was repeated 100 times, and chance-level information was defined as the mean information of these 100 iterations. All information values were corrected relative to chance, and any neurons with information ≤ 0 bits were considered to not convey information.

Decoding Tilt Platform Angle from M1 Activity: To determine how well the neural ensemble activity could predict the angle of the tilting platform, a linear Kalman filter was trained using 80% of the trials. Prediction (and therefore decoding) accuracy was assessed by calculating the

correlation coefficient between the predicted and true platform angles during the remaining 20% of trials.

Determining Stability of Neural Latent Dynamics: Separately for each animal and timepoint, neural activity 500ms before and 1500ms after tilt onset was Gaussian smoothed and then averaged within tilt type to form four PSTHs. Principal components analysis (PCA) was then applied to the concatenated, z-scored PSTHs. To then align the pre-injury dynamics to the dynamics at each timepoint after injury, we used canonical correlation analysis. The first 10 principal components (PCs) from were used from each time point. Alignment was defined as the average of the correlation coefficients from the first three resultant "canonical components" (CCs). Chance alignment was determined by calculating the alignment between pre-injury dynamics and the dynamics from 1000 different instances of surrogate post-injury data (generated using the tensor maximum entropy method). True alignment was compared to this distribution of chance alignments by calculating its standard score (the number of standard deviations of the true value from the mean of the chance alignments).

Statistics: For limb kinematics recording during treadmill walking and for single-neuron information analyses, individual step cycles and neurons were treated as independent samples, respectively. A linear mixed effects model was used to assess the effect of the fixed effects time (weeks post injury) and group (therapy v. non-therapy) on each dependent variable, with the individual animal treated as the random effect. This approximates a repeated-measures ANOVA while accounting for across-animal variability in determining statistical significance. Proportions of information conveying neurons were compared using Chi-Squared tests with Bonferroni corrections

to account for multiple comparisons. We compared decoder accuracy and population stability methods with analyses of variance.

Discussion and Conclusion

5.1 Summary

Despite the simplicity of the tilting task, this work has demonstrated that neural populations in the sensorimotor cortex not only modulate their responses in response to unexpected postural perturbations, but they also undergo complex computations to help the body maintain a stable center of pressure. Individual neurons convey significant information about postural perturbations, even after the complete transection of the mid-thoracic spinal cord. This information is encoded in parallel streams by speed-scaling and direction-dependent neural responses. As expected, the trunk is highly implicated in postural control, with the trunk representation in the motor cortex conveying just as much information about the perturbation as the hindlimb representation. Ground reaction forces, notably those most altered by mediolateral shifts in center of pressure, can be decoded based on the latent dynamics of the motor cortex, with different perturbation directions requiring unique computations that can be scaled with perturbation speed. After injury, the responsiveness of individual neurons to perturbations and the information conveyed by the neurons that respond is attenuated but remains significantly above chance (and can be further enhanced with physical rehabilitation); however, as a population, cortical dynamics are largely preserved. This can be explained by significant redundancy in the cortex and the maintained visual, vestibular inputs, and even somatosensory inputs from forelimb and trunk regions above the injury. Regardless, such preserved dynamics allow for continued decoding of postural metrics even months after spinal cord injury.

Thus, while additional work is critical, we argue that the cortex conveys sufficient, interpretable information to be used for the control of a brain-machine interface to restore postural control (and thus lateral stability) in individuals with spinal cord injury.

5.2 Future directions: closing the loop

While the cortex may convey significant information about postural control, it is unknown if these cortical signals are sufficient to stabilize an individual's center of pressure in response to postural perturbations through cortically-controlled neuroprosthetics. Thus, the most natural follow up study would test the conclusion of this work head-on.

Additionally, instead of controlling some external device (e.g., an exoskeleton), the control of spinal cord stimulators would ultimately allow individuals to control the movement of their own muscles. Fortunately, spinal cord stimulation for the treatment of lower limb paralysis (resulting from neurological conditions such as stroke, amyotrophic lateral sclerosis, or spinal cord injury) has come a long way. It has been long known that circuits in the lumbosacral spinal cord can be activated through electrical stimulation even after SCI, either intraparenchymally through intraspinal microstimulation, in which penetrating electrodes deliver current directly to their targets epidurally, or epidurally, where electrodes sit on the dorsal surface of the spinal cord. Such epidural stimulation recruits proprioceptive afferent fibers[242], activating both central pattern generator networks[243,244] as well as reflex circuits[242,245,246]. Various groups have demonstrated how and when to stimulate the spinal cord to create instantaneous and sustained rhythmic locomotor movements in the legs.

Bridging our work with this spinal stimulation work would allow for an assessment of the feasibility of such a brain-spine interface in the augmentation of at least one aspect postural control after SCI. To do so, one could imagine expanding the dynamical systems approach highlighted in Chapter 2 that related latent cortical dynamics, observed neural firing activity, and recorded ground reaction forces to an additional stimulation term. Systems identification experiments, in which a range of stimulation parameters are applied to the spinal cord as the animal performs the task, would be necessary to build this model. If our hypothesis that the latent state of the cortex conveys the center of pressure of the animal is correct, we could then build a closed-loop control framework that stimulates the spinal cord to correct aberrant cortical dynamics while also righting the animal's motor response.

Of course, a "closed-loop" system trained on restoring appropriate muscle responses to unexpected lateral perturbations is only a step toward full recovery of postural control. Assuming adequate performance on the tilting platform, the next natural question would be to assess this model in the "open field." Given that this transition introduces additional sensory, motor, and cognitive processes, it is important to assess the generalizability of this model – especially as such a paradigm could potentially even restore one aspect of postural control while interfering with other critical motor functions. This and other considerations are discussed further in the Appendix.

Appendix I – Targets beyond the cortex

Developing a translatable postural BMI (or any neuroprosthetic) requires a signal that is not only stable informative, but also readily accessible. The combined work I have presented specifically investigates the extent to which the cortex could serve as this signal. The cortex is an attractive source of signal as it is a large, superficial surgical target, already ubiquitously used in BMI research, and – based on this work – highly informative about postural control before and after spinal cord injury. However, that is not to say that it is *the optimal* neural substrate for extracting the maximal amount of postural information. The neuroanatomical basis of postural control is complex and highly interconnected, with multiple major structures heavily implicated in this critical motor function. While reviewing the neuroanatomy of postural control, I consider the feasibility of using each of these areas to control a neural interface.

Brainstem

While humans and animals with spinal cord injuries can recover postural reflexes mediated by intrinsic spinal cord circuits below the level of injury, the poor timing and inadequate strength of these responses is insufficient to maintain lateral stability[43,45,101,175,247]. This implies that descending information from supraspinal centers is necessary to generate robust, appropriate corrective responses. Reversible lesions to the spinal cord (i.e., through cooling) at T12 in rabbits – removing the influence of supraspinal centers on spinal circuits in rabbits – led to inappropriate postural responses and an inactivation of previously responsive interneurons in the intermediate and ventral laminae of the

spinal cord that were both reversed with rewarming[248]. This, along with similar findings in other spinalization experiments[249,250], suggests that the intrinsic spinal cord circuits are not sufficient for proper postural control without descending signals from supraspinal centers including the vestibular system[46], reticular formation[39–45], red nucleus[251], and even the cortex[48–50]. These supraspinal commands likely provide both tonic signals to increase the excitability of the spinal cord circuits as well as phasic signals to elicit specific situational responses.

The vestibulospinal and reticulospinal tracts of rabbits and rats seem critical for postural control. Lyalka et al. demonstrated this in a series of lesion experiments[45]. Whereas postural control on a tilting platform was recovered after dorsal and lateral hemisections of the spinal cord, it never returned after a ventral hemisection (where the vestibulospinal and reticulospinal tracts can be found in rabbits and rats). Thus, these experiments suggested that the primary supraspinal center for postural control could be found in the brainstem and not the cortex. Indeed, premammillary decerebrated rabbits and cats can generate postural corrections during various postural tasks whereas animals transected more caudally through the midbrain or pons cannot. Even in humans, it appears that the cortex does not contribute to the initial short-latency component of postural responses that immediately follows a postural perturbation[110].

The vestibulospinal tract is of particular interest, as the vestibular system supplies the nervous system with a gravitational frame of reference[252] by providing sensory signals about three-dimensional head rotations and translations. The vestibulospinal tract is more excitable when an individual is sitting rather than lying down[253]. The lateral vestibulospinal tract extends the entire length of the spinal cord, providing inputs to the motoneurons for both forelimb and hindlimb muscles[254]. A

recent study in mice showed that lateral vestibular circuits were critical for fast responses to postural perturbations[255]. Thus, interfacing with the brainstem, notably the vestibulospinal tract, may provide a better signal for postural control, as it is at the confluence of multiple somatosensory, visual, vestibular, cerebellar, and cortical sensory signals before sending descending signals to the spinal cord.

Despite the attractiveness of these brainstem structures from a neuroanatomical and scientific standpoint, the feasibility of implanting recording electrodes to access them is questionable due to the sensitive nature of these areas (e.g., their proximity to respiratory centers). The brainstem has extremely complex anatomy, making any surgery – let alone recording device implantation – at this level incredibly difficult through a limited number of "safe entry zones"[256,257]. Currently, the only FDA-approved brainstem implants are auditory brainstem implants in neurofibromatosis type 2, which are placed relatively superficially within the lateral recess of the fourth ventricle[258]. Despite the difficult anatomy and associated risks in accessing more internal structures, there has been some rodent and monkey work involving recordings from the red nucleus[259] and reticular formation[260] and other brainstem targets[261] in the behaving animal. Should these technologies continue to advance and should the risks of brainstem implantation become comparable to those of cortical implantation, significant information could be gleaned from a brainstem-guided BMI.

Cerebellum

Many motor and sensory signals converge within the cerebellum, allowing for error detection, adaptation, and coordination with respect to perceived body motion in space[110,262]. In tasks where the

standing surface translates to predictable amplitudes, individuals with cerebellar lesions fail to scale the magnitude of their postural response[263,264]. Additionally, damage to the medial cerebellum is associated with a loss of muscle tone in antigravity muscles. Interestingly, lesions to the cerebellum do not seem to affect the postural muscle synergies recruited during surface displacements[265], suggesting that the primary role of the cerebellum in posture is gain control. During a perturbation, in addition to receiving visual[266] and vestibular[267] input, the fastigial nuclei receive spinal and peripheral sensory information via the dorsal spinocerebellar tracts[268], and vestibular signals are relayed to the flocculus and vermis. This convergence of signals allows for the cerebellum to engage in error detection and the development of motor programs, especially for anticipatory postural adjustments.

As an integrator of sensory and motor information, the cerebellum could be a suitable alternative target for a motor BMI. In contrast with the brainstem, interfacing with the cerebellum is significantly more feasible. Cerebellar stimulation has been studied in animal models[269–271] and in humans[272–274] to treat dystonia and other motor outcomes, and various studies delineate how to chronically record cerebellar activity from both the cerebellar cortex and deep nuclei in both humans[275] and animals[276–278]. However, given that the cerebellum projects its postural signals to the cortex and brainstem with no direct descending connections to the spinal cord, understanding the value of information uniquely conveyed by the cerebellum that is not already accessible from other areas is important and should be further studied. Additionally, the effect of spinal cord injury or other neurologic conditions on this information needs further evaluation.

Spinal cord

The spinal cord integrates both descending supraspinal signals and at-level sensory afferents to generate a motor output, while relaying somatosensory information to higher order structures. At a given spinal cord level, the deeper grey matter is organized dorsoventrally, with sensory input fibers entering the spinal cord dorsally and motor output fibers exiting each spinal level ventrally.

It has been known for over a century that the spinal cord itself contains intrinsic circuitry needed to respond to external postural perturbations. Even after complete transection rostral to the lumbosacral spinal cord, adult cats have been shown to demonstrate some level of postural control of the hindlimbs. Coined "postural limb reflexes", these responses can be elicited by epidural electrical stimulation and appear to be driven primarily by somatosensory inputs – especially stretch and load receptors from the ipsilateral limb[47,279]. In a task where rabbits were subjected to unexpected tilts in the lateral plane as the activity of putative spinal cord interneurons were recorded, it was shown that two pools of fairly dispersed interneurons had significant modulation in response to either limb flexion or extension[248,279]. Lifting a hindlimb from the tilting platform (presumably removing its somatosensory input to the spinal cord) reduced the firing rate of these spinal interneurons on the ipsilateral side. Similarly, pyridoxine-induced destruction of large-diameter peripheral sensory nerve fibers in cats led to significantly delayed muscle activity and less robust corrections in response to horizontal translation of their support surface[44]. In contrast, bilateral labyrinthectomy[280] and blindfolding, removing vestibular and visual sensory inputs, did not affect trunk and limb stabilization in this task.

It is less technically challenging to access the dorsal spinal cord than it is the ventral spinal cord, explaining why chronic recordings of the dorsal root ganglia of freely moving animals have been collected since the 1970s, while recording efferent motor information has been more limited. In one study in cats, action potentials could be recorded from the lumbar ventral roots; however, the authors of this study highlighted important limitations. Accurate placement of electrodes in the ventral roots was challenging to achieve, and the percentage of functional electrodes dropped off after implantation[281]. Meanwhile, dorsal root ganglion recordings may be a promising alternative. The dorsal root ganglia are structures that contain the cell bodies of thousands of sensory axons entering the dorsal spinal cord. The signal from the dorsal root ganglia can be decoded to predict limb location, and this signal has even been used to control intramuscular[282] and intraspinal[283] stimulation in anesthetized cats to generate rudimentary walking behaviors (while the head, forelimbs, and trunk were supported).

In addition to the grey matter, the spinal cord also contains multiple descending and ascending pathways. As discussed above, many such pathways originating in the brainstem convey critical information about postural control and represent the final output of supraspinal computations. One group demonstrated the feasibility of recording rubrospinal tract fibers in rats using chronically implanted arrays[284]. Over a four-week period, the signal appeared stable and minimal tissue responses were seen histologically. Additionally, they demonstrated that this signal conveyed significant information about the timing of behavior[285]. This suggest that targeting these tracts as they descend within the spinal cord may serve as an attractive alternative to recording such signals from their less accessible brainstem origins.

Conclusion

In summary, postural perturbations elicit multiple sensory signals – visual, vestibular, proprioceptive, and cutaneous – that are relayed across the neural axis. Reciprocal direct and indirect connections between the cortex, cerebellum, brainstem, and basal ganglia ultimately converge in the spinal cord, modulating basic postural reflexes that ultimately activate particular muscle synergies to provide a correction. Thus, myriad options exist as the signal for a theoretical postural neuroprosthetic, but differences in feasibility and safety require careful consideration. While the brainstem may provide the best signal, accessing these nuclei poses concerns that are much less of a concern in other areas. Additionally, while this work focused on restoring postural control after spinal cord injury, the pathophysiology of the neurological disorder being treated will be an important consideration as well. As recording technologies advance, perhaps large-scale recordings across multiple targets may ultimately balance information gain and implant safety.

Appendix II – Toward a clinical tool

Designing any BMI technology involves many complex components. The combined work of this dissertation primarily addressed the signal that can be acquired and subsequently interpreted from the cortex about postural control. Importantly, given the complexity of fully independent motor control and the novelty of directly addressing postural control therewithin, I chose to focus on one aspect of posture: responding to unexpected perturbations during stance.

Within that niche, this I demonstrated that information about unexpected postural disturbances and subsequent motor responses could be extracted from subsets of neurons recorded in the sensorimotor cortex of rats– an area commonly used in brain-machine interface research but whose role in postural control is often overlooked – both before (Chapter 2) and after spinal cord injury (Chapters 3 and 4). More specifically, I showed that perturbation characteristics and even behavioral responses could be decoded better using motor cortical neurons (whether from the trunk or hindlimb representations) than when using with sensory cortical neurons (Chapter 2). Additionally, I uncovered a possible explanation regarding how individuals can learn to control a brain-machine interface (1) years after injury and (2) without the need for models to be developed prior to injury (Chapter 4). That being said, multiple critical steps remain between the conclusions of this work and eventual clinical application. This section will provide an overview of some of these primary considerations that should be addressed in animal models before translating this technology to human studies.

Assessing Online Performance & Neurostimulation

Before evaluating the generalizability of these results to other tasks, further work should critically evaluate if these findings are robust to "online" experiments[286]. All of the findings described in this dissertation were based on post hoc analyses of recorded data. As a result, while I could make conclusions about how samplings of neurons in the cortex represent different aspects of the task, I could not assess either the necessity of these dynamics or even the sufficiency of these signals to ultimately improve postural control through a BMI.

Therefore, the most natural step would be to assess these models online, where the firing patterns and dynamics of cortical neurons influences the experimental task/outcome itself. One method of assessing this would involve having the decoded platform position (predicted from the cortical dynamics) actually control the instantaneous position of the platform. In this case, would the animal be able to maintain a righted platform position despite occasionally introduced perturbations? Would that animal outperform another animal whose decoded position was based on a "remapped" or "outside manifold" dynamical model (where we intentionally shuffle the relationships between recorded neurons and latent dimensions)? Alternatively, the more translational next step in assessing the robustness of our models for improving postural control would be evaluating if these cortical dynamics are necessary and sufficient to inform *spinal cord stimulation* to elicit corrective behaviors in the spinally injured animal. Multiple methods of spinal cord stimulation exist[287]. Fortunately, epidural stimulation of the dorsal spinal cord is well studied[29–32] and clinically approved. While some have

evaluated how it can be used to restore motor function after neurological injury, expanding this work to also control the muscles of postural control is complex.

First, we would need to decide where to stimulate the spinal cord[26,288]. In a task that primarily requires lateral stability and therefore the control of both trunk muscles as well as flexors and extensors of the leg, we would likely need to place stimulating electrodes on both the left and right spinal cord, and likely in at least three different sites therewithin. While thorough research has demonstrated how to stimulate the spinal cord to enhance locomotor movements, less work has identified the parameters to elicit unilateral leg movements.

After gaining a general idea of where to position our electrodes in the cord, the next step is building a model that relates cortical firing activity, stimulation parameters, perturbation angle (i.e., bodily state), and muscle activity. Unfortunately, such relationships are complex, and we are not privileged with fundamental physics laws or other "first principles" to build a bottom-up model of these interactions. In this situation, a system identification approach is necessary. Systems identification is data-driven, in which we provide a series of inputs (stimulations and perturbations) and model those against the various outputs (cortical firing, cortical dynamics, and recorded behaviors). By varying the type of input provided (e.g., duration, frequency, amplitude) and the electrodes stimulated (both in isolation and in combinations), we can determine the optimal stimulation methods in a state-dependent manner[289]. Through this method, we can also assess how many stimulating electrodes are realistically needed. For example, when tilting to the right, do we simply need to elicit extension of the right leg, or do we need to elicit extension of the right leg and flexion of the left leg? If the former is sufficient to stabilize center of pressure this would remove the need for pair of "flexion-eliciting" electrodes, reducing

the footprint of this technology. As this modeling would need to be conducted on a subject-by-subject basis, it would also allow us to control for different injury severities (and therefore different residual muscle function and activation thresholds) and anatomy.

Additionally, as we would be modeling stimulation to the spinal cord based on the dynamics of the cortex to elicit muscular outputs, an important concern is raised. Electrical stimulation of the nervous system lacks target specificity. When targeting the reflex circuits at a particular level, stimulation can also activate multiple neighboring ascending and descending pathways within the spinal cord, even sending signals to the cortex itself[26]. Thus, stimulation of the spinal cord will likely affect behavior both directly (through direct stimulation of the spinal cord and activation of motor neurons) and indirectly (through altering cortical responses that then provide descending inputs to the cord). This is particularly true when aiming to model clinically-relevant anatomically incomplete injuries. Different candidate models should be assessed, especially in unanesthetized animals.

If the spinally-injured animal is able to maintain its center of pressure better under cortically-controlled spinal stimulation than under random stimulation, tonic stimulation, or some other structured paradigm, it would suggest that the dynamics of the cortex are truly necessary and sufficient to organize coordinated motor responses. This would truly assess the feasibility of using the cortex as a control signal for postural control and allow for next steps to be taken with more confidence.

Beyond the tilt platform

Assuming we demonstrate that cortically-controlled spinal cord stimulation improves behavior on the tilting platform after spinal cord injury, the next important question would be the extent to which this framework generalizes to other motor and locomotor behaviors. Such a question is important for two reasons. First, postural control is not limited to responses to lateral perturbations from stance. Can cortical signals restore postural control during locomotion, climbing stairs, navigating uneven or sloped terrain, or when simply when perturbed in a direction beyond the mediolateral dimension? Second, how does this approach interact with BMIs methods that restore other lost motor function? Does the stimulation needed to elicit unilateral leg flexion and extension for postural control interfere with stimulation paradigms that induce locomotion? Do the cortical dynamics we observed become muddied and less usable with the additional sensory inputs and cortical processes associated with non-stationary bodily states in more natural environments?

The simplest first step to address these questions would be to compare the behaviors of animals in these more complex tasks under "standard" locomotor BMI alone, "postural BMI" alone, and under both. The postural BMI can be recreated using a second systems identification approach where different stimuli are provided to the animal as it freely navigates in the open field or on a treadmill. In addition to addressing the deficiencies of each of these paradigms, this would allow us to discern how these two paradigms interact.

This latter question is important. Animals and humans with neurological conditions tend to not have isolated postural instability; they also have significantly impaired motor function. Individuals with lost lower limb function will realistically need a BMI that restores both locomotion and postural control. Thus, how can these two concepts – restoring locomotion and restoring posture – be

combined in an optimal way? Perhaps during locomotion, a combined BMI actively stimulates the cord to elicit locomotion. Meanwhile, while the postural signals are actively decoded throughout, only corrective postural control signals are delivered to the cord when a significant error signal is detected.

Stimulation Targets

I have discussed stimulation exclusively with respect to the spinal cord; however, one could also consider additional targets. While some may think targeting the muscles or even peripheral nerves themselves would be a reasonable alternative, this method comes with significant drawbacks. First, even simple movements involve multiple muscles. Recreating those movement though peripheral stimulation would involve multiple electrodes (and therefore an extremely large technological footprint and likely multiple invasive implantations) as well as investigations into optimal stimulation protocols to elicit natural movements. In contrast, stimulating the central nervous system (i.e., through spinal cord stimulation) activates muscle *synergies*[290], or groups of muscles that are activated in a concerted fashion to generate particular movements. Identifying relevant postural synergies that can be elicited through spinal cord stimulation would therefore limit the number of electrodes needed and take advantage of inherent functional structure. Of course, further work would need to truly compare the merits of these two forms of stimulation to determine which could offer a more optimal clinical outcome.

However, in a closed-loop system based on cortical dynamics, stimulating the spinal cord to "correct" aberrant cortical dynamics could be considered a rather indirect approach. Alternatively, one

could imagine stimulating the cortex, modulating the very dynamics that we are recording[289]. Bonizzato and Martinez demonstrated that intracortical stimulation in phase coherence with locomotion promoted locomotor control in a hemisection SCI model in the rat[64]. In individuals with incomplete injuries, perhaps such cortical stimulation can improve certain levels of lower limb function by mimicking descending phasic drive to central pattern generators and encouraging activity-dependent plasticity. However, the more targeted control of specific muscle synergies in response to particular postural perturbations will likely pose a more significant challenge that will be further complicated by variability in cortical reorganization and spared white matter tracts across individuals and within individuals over time.

Control Algorithms

Satisfactory BMI control must not only be reliable, but it must also be fast and safe. Even "long latency" postural control mechanisms naturally occur within hundreds of milliseconds. Restoring such processes requires multiple computational steps. During a perturbation, cortical signals must be filtered and processed, the current latent state must be calculated, a decision regarding if and how to stimulate must be made, and stimulation must be delivered quickly enough to elicit a corrective movement to prevent a fall. A BMI device must be developed in a way that its hardware and software components minimize each of these introduced processing lags while also remaining both affordable and compact (see "Reducing the Footprint" below).

Even if such a system can sufficiently minimize lags, it is also critical that a BMI's control algorithm incorporate important technological and physiologic constraints. A computational model cannot require solutions that requires unsafe, unattainable, or other excessively "costly" levels of current to be delivered to the cord. Simple control methods such as linear quadratic regulators cannot accommodate such "hard constraints". While model predictive control (MPC) is an alternative algorithm that can handle these bounds (and has additional benefits discussed in the "Learning and Plasticity" section below), this method carries its own limitations that would likely increase computational lags. MPC requires constant updating at multiple time horizons to find the optimal control action at different timepoints. When testing different BMI configurations, it is therefore important to quantitatively compare the performance of these different algorithms.

Additional Considerations

Invasive v. Noninvasive Signal Acquisition. In our rat model, we recorded high-frequency activity from intracranial electrodes and manually sorted that activity from each recording channel to individual putative neurons. It is a fact that the signal that can be obtained from sorted single units is unparalleled. However, it is important to consider the disadvantages of this approach and fair alternatives. Any intracranial recording device requires surgery; however, once implanted, current electrode technologies are vulnerable to natural immune responses. As traumatic spinal cord injury is often an injury of the young, improving electrode performance is critical in order to avoid multiple surgeries to replace these devices. Additionally, obtaining single unit recordings requires significant

surgical and technological expertise, leading to ethical questions of accessibility and scalability. Fortunately, it has been shown that brain machine interfaces can operate well using "unsorted" multiunit activity[291,292]. However, given the risks of surgery, further work should determine if noninvasive approaches (i.e., electroencephalography) can sufficiently extract similar levels of postural information from the cortex (and therefore control a BMI just as well as one based on invasive recordings). If not, one could argue that the benefits of restoring reliable, independent movement significantly outweigh the risks of implantation surgery.

Improved Decoder Performance. In this dissertation, we employed rather simple decoding methods to predict behavior and neural dynamics. Such linear models are simplistic but relatively interpretable. This is a significant advantage from a basic science perspective, as it allows us to gain insight into how the brain represents different states and can generate behaviors. Additionally, given how young BMI technology is, developing an understanding or intuition of how these anatomical circuits and stimulation paradigms work is necessary to advance the field in a well-informed manner. However, such models also limit true decoding potential as they come with certain constraints. For example, our linear dynamical systems approach can only model the *linear* dynamics of population activity – even though population dynamics are highly nonlinear. For a clinical tool, the importance of consistently reliable performance significantly outweighs the importance of scientific interpretability. In line with this mindset, multiple groups are developing highly complex decoders based on nonlinear approaches, machine learning, and artificial neural networks[96]. If the end goal is developing an optimal decoder, these approaches will likely lead to more successful performance than linear models. If BMI technologies based on these advanced models outperform those based on linear approaches or even less

complicated "open loop" spinal cord stimulators, the clinical merit of these algorithms should be seriously considered – even if their algorithms live within a "black box."

Replacing Lost Somatosensory Feedback. All motor actions are companied by sensory feedback. While motor signals can control various devices, robust motor control requires the individual to understand the sensory repercussions of those motor commands. While individuals can partially compensate for the loss of somatosensory feedback by relying on visual feedback, it has been shown that BMI control is heavily augmented when sensory feedback is replicated[293–295].

With respect to improving postural stability, this may be less of concern, as visual and vestibular feedback and unaffected somatosensory fibers all provide information to the cortex about the body's position in space. Regardless, it has been shown that somatosensory afferents are critical for robust corrections[109,182,296], so further work investigating how to reintroduce lost sensory information from below the injury to the cortex will ultimately develop better BMI control.

Learning and Plasticity. If a closed-loop BMI system models the relationship between neural activity and behavior, such a system must be capable of adapting to changes observed on various timescales. For example, some degree of functional recovery – either spontaneously or through other therapeutic means such as physical rehabilitation – will alter both motor abilities and the sensory inputs delivered to the cortex. Additionally, as a closed-loop BMI artificially defines a functional relationship between neural activity and stimulated movement[297,298], significant neuroplasticity is expected over the course of BMI learning and long-term BMI use. For example, BMI use is associated with changes in modulation of M1 neurons[160,240], with such changes directly relating to improved BMI performance [160,299]. Certain control methods such as model predictive control can actually account for

such changes. As model predictive control calculates an optimal outputs iteratively with time, it can handle "migration" of a nonlinear system away from initial relationships. Finally, given the various forms of plasticity related to injury, rehabilitation, and BMI control, it is important that we evaluate how to optimize how these mechanisms lead to better outcomes.

Reducing the footprint. As discussed earlier, the motor deficits seen after spinal cord injury and other neurological diseases extend beyond isolated postural instability. Depending on the level of the lesion, lower limb function can be impaired with or without upper limb dysfunction. A largely BMI-driven approach to these conditions would therefore require recordings from multiple cortical locations and stimulators across large areas of cord. Additionally, the computations involved in signal acquisition, processing, and stimulation must be housed in a device that must be battery-operated and portable enough to free the individual from a laboratory setting or even small enough to be implanted subcutaneously, such as in current deep brain stimulator protocols. From a clinical perspective, improving the biocompatibility of these devices and reducing the instances of percutaneous connections is critical to maximize device longevity and patient independence and minimize risks of infection and other complications.

Summary

In conclusion, my dissertation demonstrated the various signals that can be decoded from the sensorimotor cortex about postural control both before and after different extents of spinal cord injury. The ultimate goal of this line of this work, however, is to develop a translational tool to

improve postural stability. Advancing brain machine interface technology to restore this motor function (in addition to the multiple other complex functions impaired by neurological injury) requires many clear steps to get from where we are today in decoding signals, developing devices, identifying stimulation targets, and optimizing stimulation paradigms. Given the advances of neuroengineering approaches over the last few decades, I hope that such a technology can become a reality in the near future through the concerted efforts of clinicians, scientists, and various stakeholders.

References

1. Ditunno, P. L., Patrick, M., Stineman, M. & Ditunno, J. F. Who wants to walk? Preferences for recovery after SCI: A longitudinal and cross-sectional study. *Spinal Cord* (2008). doi:10.1038/sj.sc.3102172
2. Hicks, A. L. *et al.* Long-term body-weight-supported treadmill training and subsequent follow-up in persons with chronic SCI: Effects on functional walking ability and measures of subjective well-being. *Spinal Cord* (2005). doi:10.1038/sj.sc.3101710
3. Cardenas, D. D., Hoffman, J. M., Kirshblum, S. & McKinley, W. Etiology and incidence of rehospitalization after traumatic spinal cord injury: A multicenter analysis. *Arch. Phys. Med. Rehabil.* (2004). doi:10.1016/j.apmr.2004.03.016
4. Bundy, D. T. *et al.* Contralesional Brain-Computer Interface Control of a Powered Exoskeleton for Motor Recovery in Chronic Stroke Survivors. *Stroke* (2017). doi:10.1161/STROKEAHA.116.016304
5. Heck, C. N. *et al.* Two-year seizure reduction in adults with medically intractable partial onset epilepsy treated with responsive neurostimulation: Final results of the RNS System Pivotal trial. *Epilepsia* (2014). doi:10.1111/epi.12534
6. Parastarfeizabadi, M. & Kouzani, A. Z. Advances in closed-loop deep brain stimulation devices. *Journal of neuroengineering and rehabilitation* (2017). doi:10.1186/s12984-017-0295-1
7. Shanechi, M. M. Brain–machine interfaces from motor to mood. *Nat. Neurosci.* (2019). doi:10.1038/s41593-019-0488-y
8. EVARTS, E. V. RELATION OF DISCHARGE FREQUENCY TO CONDUCTION VELOCITY IN PYRAMIDAL TRACT NEURONS. *J. Neurophysiol.* (1965). doi:10.1152/jn.1965.28.2.216
9. Evarts, E. V. Pyramidal tract activity associated with a conditioned hand movement in the monkey. *J. Neurophysiol.* (1966). doi:10.1152/jn.1966.29.6.1011
10. Evarts, E. V. Relation of pyramidal tract activity to force exerted during voluntary movement. *J. Neurophysiol.* (1968). doi:10.1152/jn.1968.31.1.14
11. Georgopoulos, A. P., Schwartz, A. B. & Kettner, R. E. Neuronal population coding of movement direction. *Science (80-.).* (1986). doi:10.1126/science.3749885
12. Nicolelis, M. A. L. Actions from thoughts. *Nature* (2001). doi:10.1038/35053191
13. Chapin, J. K., Moxon, K. A., Markowitz, R. S. & Nicolelis, M. A. L. Real-time control of a robot arm using simultaneously recorded neurons in the motor cortex. *Nat. Neurosci.* (1999). doi:10.1038/10223
14. Hochberg, L. R. *et al.* Neuronal ensemble control of prosthetic devices by a human with tetraplegia. *Nature* (2006). doi:10.1038/nature04970
15. Ethier, C., Oby, E. R., Bauman, M. J. & Miller, L. E. Restoration of grasp following paralysis through brain-controlled stimulation of muscles. *Nature* (2012). doi:10.1038/nature10987
16. Collinger, J. L. *et al.* High-performance neuroprosthetic control by an individual with tetraplegia. *Lancet* (2013). doi:10.1016/S0140-6736(12)61816-9

17. Hochberg, L. R. *et al.* Reach and grasp by people with tetraplegia using a neurally controlled robotic arm. *Nature* (2012). doi:10.1038/nature11076
18. Bouton, C. E. *et al.* Restoring cortical control of functional movement in a human with quadriplegia. *Nature* (2016). doi:10.1038/nature17435
19. Shanechi, M. M., Hu, R. C. & Williams, Z. M. A cortical-spinal prosthesis for targeted limb movement in paralysed primate avatars. *Nat. Commun.* (2014). doi:10.1038/ncomms4237
20. Zimmermann, J. B. & Jackson, A. Closed-loop control of spinal cord stimulation to restore hand function after paralysis. *Front. Neurosci.* (2014). doi:10.3389/fnins.2014.00087
21. Ethier, C., Gallego, J. A. & Miller, L. E. Brain-controlled neuromuscular stimulation to drive neural plasticity and functional recovery. *Current Opinion in Neurobiology* (2015). doi:10.1016/j.conb.2015.03.007
22. Nishimura, Y., Perlmutter, S. I. & Fetz, E. E. Restoration of upper limb movement via artificial corticospinal and musculospinal connections in a monkey with spinal cord injury. *Front. Neural Circuits* (2013). doi:10.3389/fncir.2013.00057
23. Moritz, C. T., Perlmutter, S. I. & Fetz, E. E. Direct control of paralysed muscles by cortical neurons. *Nature* (2008). doi:10.1038/nature07418
24. Ajiboye, A. B. *et al.* Restoration of reaching and grasping movements through brain-controlled muscle stimulation in a person with tetraplegia: a proof-of-concept demonstration. *Lancet* (2017). doi:10.1016/S0140-6736(17)30601-3
25. Fitzsimmons, N. A., Lebedev, M. A., Peikon, I. D. & Nicolelis, M. A. L. Extracting kinematic parameters for monkey bipedal walking from cortical neuronal ensemble activity. *Front. Integr. Neurosci.* (2009). doi:10.3389/neuro.07.003.2009
26. Manohar, A., Flint, R. D., Knudsen, E. & Moxon, K. A. Decoding Hindlimb Movement for a Brain Machine Interface after a Complete Spinal Transection. *PLoS One* (2012). doi:10.1371/journal.pone.0052173
27. Knudsen, E. B. & Moxon, K. A. Restoration of hindlimb movements after complete spinal cord injury using brain-controlled functional electrical stimulation. *Front. Neurosci.* (2017). doi:10.3389/fnins.2017.00715
28. Bonizzato, M. *et al.* Brain-controlled modulation of spinal circuits improves recovery from spinal cord injury. *Nat. Commun.* (2018). doi:10.1038/s41467-018-05282-6
29. Van Den Brand, R. *et al.* Restoring voluntary control of locomotion after paralyzing spinal cord injury. *Science (80-.).* (2012). doi:10.1126/science.1217416
30. Harkema, S. S. J. *et al.* Effect of epidural stimulation of the lumbosacral spinal cord on voluntary movement, standing, and assisted stepping after motor complete paraplegia: a case study. *Lancet* **377**, 1938–47 (2011).
31. Courtine, G. *et al.* Transformation of nonfunctional spinal circuits into functional states after the loss of brain input. *Nat. Neurosci.* (2009). doi:10.1038/nn.2401
32. Lyalka, V. F. *et al.* Facilitation of postural limb reflexes in spinal rabbits by serotonergic agonist administration, epidural electrical stimulation, and postural training. *J. Neurophysiol.* (2011). doi:10.1152/jn.00115.2011
33. Rosin, B. *et al.* Closed-loop deep brain stimulation is superior in ameliorating parkinsonism.

Neuron (2011). doi:10.1016/j.neuron.2011.08.023
34. Tass, P. A. *et al.* Coordinated reset has sustained aftereffects in Parkinsonian monkeys. *Ann. Neurol.* (2012). doi:10.1002/ana.23663
35. Brocker, D. T. *et al.* Improved efficacy of temporally non-regular deep brain stimulation in Parkinson's disease. *Exp. Neurol.* (2013). doi:10.1016/j.expneurol.2012.09.008
36. Paz, J. T. *et al.* Closed-loop optogenetic control of thalamus as a tool for interrupting seizures after cortical injury. *Nat. Neurosci.* (2013). doi:10.1038/nn.3269
37. Wenger, N. *et al.* Closed-loop neuromodulation of spinal sensorimotor circuits controls refined locomotion after complete spinal cord injury. *Sci. Transl. Med.* (2014). doi:10.1126/scitranslmed.3008325
38. Field-Fote, E. C., Yang, J. F., Basso, D. M. & Gorassini, M. A. Supraspinal Control Predicts Locomotor Function and Forecasts Responsiveness to Training after Spinal Cord Injury. *J. Neurotrauma* (2017). doi:10.1089/neu.2016.4565
39. Afelt, Z. Functional significance of ventral descending tracts of the spinal cord in the cat. *Acta Neurobiol. Exp. (Wars).* (1974).
40. Gorska, T., Bem, T. & Majczynski, H. Locomotion in cats with ventral spinal lesions: Support patterns and duration of support phases during unrestrained walking. in *Acta Neurobiologiae Experimentalis* (1990).
41. Górska, T., Bem, T., Majczyński, H. & Zmysłowski, W. Unrestrained walking in cats with partial spinal lesions. *Brain Res. Bull.* (1993). doi:10.1016/0361-9230(93)90183-C
42. Bem, T., Górska, T., Majczyński, H. & Zmysłowski, W. Different patterns of fore-hindlimb coordination during overground locomotion in cats with ventral and lateral spinal lesions. *Exp. Brain Res.* (1995). doi:10.1007/BF00229856
43. Brustein, E. & Rossignol, S. Recovery of locomotion after ventral and ventrolateral spinal lesions in the cat. I. Deficits and adaptive mechanisms. *J. Neurophysiol.* (1998). doi:10.1152/jn.1998.80.3.1245
44. Stapley, P. J., Ting, L. H., Hulliger, M. & Macpherson, J. M. Automatic postural responses are delayed by pyridoxine-induced somatosensory loss. *J. Neurosci.* (2002). doi:10.1523/jneurosci.22-14-05803.2002
45. Lyalka, V. F. *et al.* Impairment and recovery of postural control in rabbits with spinal cord lesions. *J. Neurophysiol.* (2005). doi:10.1152/jn.00538.2005
46. Matsuyama, K. & Drew, T. Vestibulospinal and reticulospinal neuronal activity during locomotion in the intact cat. II. Walking on an inclined plane. *J. Neurophysiol.* (2000). doi:10.1152/jn.2000.84.5.2257
47. Musienko, P. E., Zelenin, P. V., Orlovsky, G. N. & Deliagina, T. G. Facilitation of postural limb reflexes with epidural stimulation in spinal rabbits. *J. Neurophysiol.* (2010). doi:10.1152/jn.00575.2009
48. Beloozerova, I. N. *et al.* Activity of different classes of neurons of the motor cortex during postural corrections. *J. Neurosci.* (2003). doi:10.1523/jneurosci.23-21-07844.2003
49. Karayannidou, A. *et al.* Influences of sensory input from the limbs on feline corticospinal neurons during postural responses. *J. Physiol.* (2008). doi:10.1113/jphysiol.2007.144840

50. Karayannidou, A. *et al.* Activity of pyramidal tract neurons in the cat during standing and walking on an inclined plane. *J. Physiol.* (2009). doi:10.1113/jphysiol.2009.170183
51. Song, W., Ramakrishnan, A., Udoekwere, U. I. & Giszter, S. F. Multiple Types of Movement-Related Information Encoded in Hindlimb/Trunk Cortex in Rats and Potentially Available for Brain-Machine Interface Controls. *IEEE Trans. Biomed. Eng.* (2009). doi:10.1109/TBME.2009.2026284
52. Mushahwar, V. K., Guevremont, L. & Saigal, R. Could cortical signals control intraspinal stimulators? A theoretical evaluation. in *IEEE Transactions on Neural Systems and Rehabilitation Engineering* (2006). doi:10.1109/TNSRE.2006.875532
53. Capogrosso, M. *et al.* A brain-spine interface alleviating gait deficits after spinal cord injury in primates. *Nature* (2016). doi:10.1038/nature20118
54. Donati, A. R. C. *et al.* Long-Term Training with a Brain-Machine Interface-Based Gait Protocol Induces Partial Neurological Recovery in Paraplegic Patients. *Sci. Rep.* (2016). doi:10.1038/srep30383
55. Moraud, E. M. *et al.* Closed-loop control of trunk posture improves locomotion through the regulation of leg proprioceptive feedback after spinal cord injury. *Sci. Rep.* (2018). doi:10.1038/s41598-017-18293-y
56. Cheung, V. C. K. *et al.* Muscle synergy patterns as physiological markers of motor cortical damage. *Proc. Natl. Acad. Sci. U. S. A.* (2012). doi:10.1073/pnas.1212056109
57. Ganzer, P. D., Manohar, A., Shumsky, J. S. & Moxon, K. A. Therapy induces widespread reorganization of motor cortex after complete spinal transection that supports motor recovery. *Exp. Neurol.* (2016). doi:10.1016/j.expneurol.2016.01.022
58. Kao, T., Shumsky, J. S., Murray, M. & Moxon, K. A. Exercise induces cortical plasticity after neonatal spinal cord injury in the rat. *J. Neurosci.* (2009). doi:10.1523/JNEUROSCI.2474-08.2009
59. Ganzer, P. D., Moxon, K. A., Knudsen, E. B. & Shumsky, J. S. Serotonergic pharmacotherapy promotes cortical reorganization after spinal cord injury. *Exp. Neurol.* (2013). doi:10.1016/j.expneurol.2012.12.004
60. Graziano, A., Foffani, G., Knudsen, E. B., Shumsky, J. & Moxon, K. A. Passive Exercise of the Hind Limbs after Complete Thoracic Transection of the Spinal Cord Promotes Cortical Reorganization. *PLoS One* (2013). doi:10.1371/journal.pone.0054350
61. Oza, C. S. & Giszter, S. F. Plasticity and alterations of trunk motor cortex following spinal cord injury and non-stepping robot and treadmill training. *Exp. Neurol.* (2014). doi:10.1016/j.expneurol.2014.03.012
62. Foffani, G., Shumsky, J., Knudsen, E. B., Ganzer, P. D. & Moxon, K. A. Interactive Effects between Exercise and Serotonergic Pharmacotherapy on Cortical Reorganization after Spinal Cord Injury. *Neurorehabil. Neural Repair* (2016). doi:10.1177/1545968315600523
63. Asboth, L. *et al.* Cortico-reticulo-spinal circuit reorganization enables functional recovery after severe spinal cord contusion. *Nat. Neurosci.* (2018). doi:10.1038/s41593-018-0093-5
64. Bonizzato, M. & Martinez, M. An intracortical neuroprosthesis immediately alleviates walking deficits and improves recovery of leg control after spinal cord injury. *Sci. Transl. Med.* (2021).

doi:10.1126/scitranslmed.abb4422
65. Manohar, A., Foffani, G., Ganzer, P. D., Bethea, J. R. & Moxon, K. A. Cortex-dependent recovery of unassisted hindlimb locomotion after complete spinal cord injury in adult rats. *Elife* (2017). doi:10.7554/eLife.23532
66. Yang, W. *et al.* The Effect of Brain–Computer Interface Training on Rehabilitation of Upper Limb Dysfunction After Stroke: A Meta-Analysis of Randomized Controlled Trials. *Frontiers in Neuroscience* (2022). doi:10.3389/fnins.2021.766879
67. Alam, M., Rodrigues, W., Pham, B. N. & Thakor, N. V. Brain-machine interface facilitated neurorehabilitation via spinal stimulation after spinal cord injury: Recent progress and future perspectives. *Brain Research* (2016). doi:10.1016/j.brainres.2016.05.039
68. Omrani, M., Kaufman, M. T., Hatsopoulos, N. G. & Cheney, P. D. Perspectives on classical controversies about the motor cortex. *Journal of Neurophysiology* (2017). doi:10.1152/jn.00795.2016
69. Georgopoulos, A. P. & Carpenter, A. F. Coding of movements in the motor cortex. *Current Opinion in Neurobiology* (2015). doi:10.1016/j.conb.2015.01.012
70. Georgopoulos, A. P., Kalaska, J. F., Caminiti, R. & Massey, J. T. On the relations between the direction of two-dimensional arm movements and cell discharge in primate motor cortex. *J. Neurosci.* (1982). doi:10.1523/jneurosci.02-11-01527.1982
71. Humphrey, D. R., Schmidt, E. M. & Thompson, W. D. Predicting measures of motor performance from multiple cortical spike trains. *Science (80-.).* (1970). doi:10.1126/science.170.3959.758
72. Churchland, M. M. & Shenoy, K. V. Temporal complexity and heterogeneity of single-neuron activity in premotor and motor cortex. *J. Neurophysiol.* (2007). doi:10.1152/jn.00095.2007
73. Caminiti, R., Johnson, P. B. & Urbano, A. Making arm movements within different parts of space: Dynamic aspects in the primate motor cortex. *J. Neurosci.* (1990). doi:10.1523/jneurosci.10-07-02039.1990
74. Scott, S. H. Inconvenient Truths about neural processing in primary motor cortex. in *Journal of Physiology* (2008). doi:10.1113/jphysiol.2007.146068
75. Fetz, E. E. Are movement parameters recognizably coded in the activity of single neurons? in *Movement Control* (2010). doi:10.1017/cbo9780511529788.008
76. Hebb, D. O. Organization of behavior. New York: Wiley. *J. Clin. Psychol.* (1950).
77. Churchland, M. M. *et al.* Stimulus onset quenches neural variability: A widespread cortical phenomenon. *Nat. Neurosci.* (2010). doi:10.1038/nn.2501
78. Yu, B. M. *et al.* Gaussian-process factor analysis for low-dimensional single-trial analysis of neural population activity. *J. Neurophysiol.* (2009). doi:10.1152/jn.90941.2008
79. Kaufman, M. T., Churchland, M. M., Ryu, S. I. & Shenoy, K. V. Cortical activity in the null space: Permitting preparation without movement. *Nat. Neurosci.* (2014). doi:10.1038/nn.3643
80. Kao, J. C. *et al.* Single-trial dynamics of motor cortex and their applications to brain-machine interfaces. *Nat. Commun.* (2015). doi:10.1038/ncomms8759
81. Buesing, L., MacKe, J. H. & Sahani, M. Learning stable, regularised latent models of neural population dynamics. *Netw. Comput. Neural Syst.* (2012).

doi:10.3109/0954898X.2012.677095
82. Pandarinath, C. *et al.* Inferring single-trial neural population dynamics using sequential auto-encoders. *Nat. Methods* (2018). doi:10.1038/s41592-018-0109-9
83. Afshar, A. *et al.* Single-trial neural correlates of arm movement preparation. *Neuron* (2011). doi:10.1016/j.neuron.2011.05.047
84. Sani, O. G., Abbaspourazad, H., Wong, Y. T., Pesaran, B. & Shanechi, M. M. Modeling behaviorally relevant neural dynamics enabled by preferential subspace identification. *Nat. Neurosci.* (2021). doi:10.1038/s41593-020-00733-0
85. Gallego, J. A., Perich, M. G., Miller, L. E. & Solla, S. A. Neural Manifolds for the Control of Movement. *Neuron* (2017). doi:10.1016/j.neuron.2017.05.025
86. Shenoy, K. V., Sahani, M. & Churchland, M. M. Cortical control of arm movements: A dynamical systems perspective. *Annual Review of Neuroscience* (2013). doi:10.1146/annurev-neuro-062111-150509
87. Briggman, K. L. & Kristan, W. B. Multifunctional pattern-generating circuits. *Annual Review of Neuroscience* (2008). doi:10.1146/annurev.neuro.31.060407.125552
88. Petreska, B. *et al.* Dynamical segmentation of single trials from population neural data. in *Advances in Neural Information Processing Systems 24: 25th Annual Conference on Neural Information Processing Systems 2011, NIPS 2011* (2011).
89. Rokni, U. & Sompolinsky, H. How the brain generates movement. *Neural Comput.* (2012). doi:10.1162/NECO_a_00223
90. Churchland, M. M. *et al.* Neural population dynamics during reaching. *Nature* (2012). doi:10.1038/nature11129
91. Pandarinath, C. *et al.* Neural population dynamics in human motor cortex during movements in people with ALS. *Elife* (2015). doi:10.7554/eLife.07436
92. Michaels, J. A., Dann, B. & Scherberger, H. Neural Population Dynamics during Reaching Are Better Explained by a Dynamical System than Representational Tuning. *PLoS Comput. Biol.* (2016). doi:10.1371/journal.pcbi.1005175
93. Cunningham, J. P. & Yu, B. M. Dimensionality reduction for large-scale neural recordings. *Nature Neuroscience* (2014). doi:10.1038/nn.3776
94. Kao, J. C., Ryu, S. I. & Shenoy, K. V. Leveraging neural dynamics to extend functional lifetime of brain-machine interfaces. *Sci. Rep.* (2017). doi:10.1038/s41598-017-06029-x
95. Ghahramani, Z. & Hinton, G. H. *Parameter estimation for linear dynamical systems. Technical Report CRG-TR-96-2, Dept. Comp. Sci., Univ. Toronto* (1996).
96. Linderman, S. W. *et al.* Bayesian learning and inference in recurrent switching linear dynamical systems. in *Proceedings of the 20th International Conference on Artificial Intelligence and Statistics, AISTATS 2017* (2017).
97. Alizadeh, A., Dyck, S. M. & Karimi-Abdolrezaee, S. Traumatic spinal cord injury: An overview of pathophysiology, models and acute injury mechanisms. *Front. Neurol.* (2019). doi:10.3389/fneur.2019.00282
98. Metz, G. A. S. *et al.* Validation of the weight-drop contusion model in rats: A comparative study of human spinal cord injury. *J. Neurotrauma* (2000). doi:10.1089/neu.2000.17.1

99. Köhler, M. & Moyà-Solà, S. Ape-like or hominid-like? The positional behavior of Oreopithecus bambolii reconsidered. *Proc. Natl. Acad. Sci.* **94**, 11747–11750 (1997).
100. Jahn, K. *et al.* Imaging human supraspinal locomotor centers in brainstem and cerebellum. *Neuroimage* (2008). doi:10.1016/j.neuroimage.2007.09.047
101. Dunbar, D. C., Horak, F. B., Macpherson, J. M. & Rushmer, D. S. Neural control of quadrupedal and bipedal stance: Implications for the evolution of erect posture. *Am. J. Phys. Anthropol.* (1986). doi:10.1002/ajpa.1330690111
102. Zehr, E. P. *et al.* Enhancement of arm and leg locomotor coupling with augmented cutaneous feedback from the hand. *J. Neurophysiol.* (2007). doi:10.1152/jn.00562.2007
103. Behrman, A. L. & Harkema, S. J. Locomotor training after human spinal cord injury: A series of case studies. *Phys. Ther.* (2000). doi:10.1093/ptj/80.7.688
104. Kawashima, N., Nozaki, D., Abe, M. O. & Nakazawa, K. Shaping appropriate locomotive motor output through interlimb neural pathway within spinal cord in humans. *J. Neurophysiol.* (2008). doi:10.1152/jn.00020.2008
105. Takakusaki, K. Functional Neuroanatomy for Posture and Gait Control. *J. Mov. Disord.* (2017). doi:10.14802/jmd.16062
106. Deliagina, T. G., Beloozerova, I. N., Orlovsky, G. N. & Zelenin, P. V. Contribution of supraspinal systems to generation of automatic postural responses. *Front. Integr. Neurosci.* (2014). doi:10.3389/fnint.2014.00076
107. Schepens, B., Stapley, P. & Drew, T. Neurons in the pontomedullary reticular formation signal posture and movement both as an integrated behavior and independently. *J. Neurophysiol.* (2008). doi:10.1152/jn.01381.2007
108. Stapley, P. J. & Drew, T. The pontomedullary reticular formation contributes to the compensatory postural responses observed following removal of the support surface in the standing cat. *J. Neurophysiol.* (2009). doi:10.1152/jn.91013.2008
109. Honeycutt, C. F. & Nichols, T. R. The decerebrate cat generates the essential features of the force constraint strategy. *J. Neurophysiol.* (2010). doi:10.1152/jn.00764.2009
110. Jacobs, J. V. & Horak, F. B. Cortical control of postural responses. in *Journal of Neural Transmission* (2007). doi:10.1007/s00702-007-0657-0
111. Woollacott, M. & Shumway-Cook, A. Attention and the control of posture and gait: A review of an emerging area of research. *Gait and Posture* (2002). doi:10.1016/S0966-6362(01)00156-4
112. Maki, B. E. & McIlroy, W. E. Cognitive demands and cortical control of human balance-recovery reactions. in *Journal of Neural Transmission* (2007). doi:10.1007/s00702-007-0764-y
113. Varghese, J. P., McIlroy, R. E. & Barnett-Cowan, M. Perturbation-evoked potentials: Significance and application in balance control research. *Neuroscience and Biobehavioral Reviews* (2017). doi:10.1016/j.neubiorev.2017.10.022
114. Dougherty, J. B., Disse, G. D., Bridges, N. R. & Moxon, K. A. Effect of spinal cord injury on neural encoding of spontaneous postural perturbations in the hindlimb sensorimotor cortex. *J. Neurophysiol.* (2021). doi:10.1152/jn.00727.2020
115. Beloozerova, I. N., Sirota, M. G., Orlovsky, G. N. & Deliagina, T. G. Activity of pyramidal tract neurons in the cat during postural corrections. *J. Neurophysiol.* (2005).

doi:10.1152/jn.00577.2004
116. Bridges, N. R., Meyers, M., Garcia, J., Shewokis, P. A. & Moxon, K. A. A rodent brain-machine interface paradigm to study the impact of paraplegia on BMI performance. *J. Neurosci. Methods* (2018). doi:10.1016/j.jneumeth.2018.05.015
117. Giszter, S., Davies, M. R., Ramakrishnan, A., Udoekwere, U. I. & Kargo, W. J. Trunk sensorimotor cortex is essential for autonomous weight-supported locomotion in adult rats spinalized as P1/P2 neonates. *J. Neurophysiol.* (2008). doi:10.1152/jn.00866.2007
118. Hilton, B. J. *et al.* Re-establishment of cortical motor output maps and spontaneous functional recovery via spared dorsolaterally projecting corticospinal neurons after dorsal column spinal cord injury in adult mice. *J. Neurosci.* (2016). doi:10.1523/JNEUROSCI.3386-15.2016
119. Brown, A. R. & Martinez, M. Chronic inactivation of the contralesional hindlimb motor cortex after thoracic spinal cord hemisection impedes locomotor recovery in the rat. *Exp. Neurol.* (2021). doi:10.1016/j.expneurol.2021.113775
120. Stamenkovic, A. & Stapley, P. J. Trunk muscles contribute as functional groups to directionality of reaching during stance. *Exp. Brain Res.* (2016). doi:10.1007/s00221-015-4536-x
121. Ghamkhar, L. & Kahlaee, A. H. The effect of trunk muscle fatigue on postural control of upright stance: A systematic review. *Gait and Posture* (2019). doi:10.1016/j.gaitpost.2019.06.010
122. Oddsson, L. & Thorstensson, A. Fast voluntary trunk flexion movements in standing: Motor patterns. *Acta Physiol. Scand.* (1987). doi:10.1111/j.1748-1716.1987.tb08044.x
123. Sasaki, A., Milosevic, M., Sekiguchi, H. & Nakazawa, K. Evidence for existence of trunk-limb neural interaction in the corticospinal pathway. *Neurosci. Lett.* (2018). doi:10.1016/j.neulet.2018.01.011
124. Churchland, M. M., Yu, B. M., Sahani, M. & Shenoy, K. V. Techniques for extracting single-trial activity patterns from large-scale neural recordings. *Current Opinion in Neurobiology* (2007). doi:10.1016/j.conb.2007.11.001
125. Melbaum, S. *et al.* Conserved structures of neural activity in sensorimotor cortex of freely moving rats allow cross-subject decoding. *Nat. Commun.* **13**, 7420 (2022).
126. Mimica, B., Dunn, B. A., Tombaz, T., Srikanth Bojja, V. P. T. N. & Whitlock, J. R. Efficient cortical coding of 3D posture in freely behaving rats. *Science (80-.).* (2018). doi:10.1126/science.aau2013
127. DiGiovanna, J. *et al.* Engagement of the rat hindlimb motor cortex across natural locomotor behaviors. *J. Neurosci.* (2016). doi:10.1523/JNEUROSCI.4343-15.2016
128. Jiang, X., Saggar, H., Ryu, S. I., Shenoy, K. V. & Kao, J. C. Structure in Neural Activity during Observed and Executed Movements Is Shared at the Neural Population Level, Not in Single Neurons. *Cell Rep.* (2020). doi:10.1016/j.celrep.2020.108006
129. Nandakumar, B., Blumenthal, G. H., Pauzin, F. P. & Moxon, K. A. Hindlimb Somatosensory Information Influences Trunk Sensory and Motor Cortices to Support Trunk Stabilization. *Cereb. Cortex* (2021). doi:10.1093/cercor/bhab150
130. Chapin, J. K. & Woodward, D. J. Somatic sensory transmission to the cortex during

movement: Phasic modulation over the locomotor step cycle. *Exp. Neurol.* (1982). doi:10.1016/0014-4886(82)90083-8
131. Eguibar, J. R., Quevedo, J., Jiménez, I. & Rudomin, P. Selective cortical control of information flow through different intraspinal collaterals of the same muscle afferent fiber. *Brain Res.* (1994). doi:10.1016/0006-8993(94)90042-6
132. Seki, K. & Fetz, E. E. Gating of sensory input at spinal and cortical levels during preparation and execution of voluntary movement. *J. Neurosci.* (2012). doi:10.1523/JNEUROSCI.4958-11.2012
133. Staines, W. R., Brooke, J. D. & Mcllroy, W. E. Task-relevant selective modulation of somatosensory afferent paths from the lower limb. *Neuroreport* (2000). doi:10.1097/00001756-200006050-00024
134. Schneider, D. M., Nelson, A. & Mooney, R. A synaptic and circuit basis for corollary discharge in the auditory cortex. *Nature* (2014). doi:10.1038/nature13724
135. Stavisky, S. D. *et al.* Neural ensemble dynamics in dorsal motor cortex during speech in people with paralysis. *Elife* (2019). doi:10.7554/eLife.46015
136. Rana, M., Yani, M. S., Asavasopon, S., Fisher, B. E. & Kutch, J. J. Brain connectivity associated with muscle synergies in humans. *J. Neurosci.* (2015). doi:10.1523/JNEUROSCI.1971-15.2015
137. Dietz, V., Quintern, J. & Berger, W. Cerebral evoked potentials associated with the compensatory reactions following stance and gait perturbation. *Neurosci. Lett.* (1984). doi:10.1016/0304-3940(84)90483-X
138. Kalidindi, H. T. *et al.* Rotational dynamics in motor cortex are consistent with a feedback controller. *Elife* (2021). doi:10.7554/eLife.67256
139. Wang, J., Narain, D., Hosseini, E. A. & Jazayeri, M. Flexible timing by temporal scaling of cortical responses. *Nat. Neurosci.* (2018). doi:10.1038/s41593-017-0028-6
140. Mello, G. B. M., Soares, S. & Paton, J. J. A scalable population code for time in the striatum. *Curr. Biol.* (2015). doi:10.1016/j.cub.2015.02.036
141. Goudar, V. & Buonomano, D. V. Encoding sensory and motor patterns as time-invariant trajectories in recurrent neural networks. *Elife* (2018). doi:10.7554/eLife.31134
142. Saxena, S., Russo, A. A., Cunningham, J. & Churchland, M. M. Motor cortex activity across movement speeds is predicted by network-level strategies for generating muscle activity. *Elife* **11**, e67620 (2022).
143. Golub, M. D., Yu, B. M., Schwartz, A. B. & Chase, S. M. Motor cortical control of movement speed with implications for brain-machine interface control. *J. Neurophysiol.* (2014). doi:10.1152/jn.00391.2013
144. Chvatal, S. A. & Ting, L. H. Common muscle synergies for balance and walking. *Front. Comput. Neurosci.* (2013). doi:10.3389/fncom.2013.00048
145. Chvatal, S. A., Torres-Oviedo, G., Safavynia, S. A. & Ting, L. H. Common muscle synergies for control of center of mass and force in nonstepping and stepping postural behaviors. *J. Neurophysiol.* (2011). doi:10.1152/jn.00549.2010
146. Giszter, S. F. & Hart, C. B. Motor primitives and synergies in the spinal cord and after injury-the current state of play. *Ann. N. Y. Acad. Sci.* (2013). doi:10.1111/nyas.12065

147. Torres-Oviedo, G., Macpherson, J. M. & Ting, L. H. Muscle synergy organization is robust across a variety of postural perturbations. *J. Neurophysiol.* (2006). doi:10.1152/jn.00810.2005
148. Ames, K. C. & Churchland, M. M. Motor cortex signals for each arm are mixed across hemispheres and neurons yet partitioned within the population response. *Elife* (2019). doi:10.7554/eLife.46159
149. Varghese, J. P., Beyer, K. B., Williams, L., Miyasike-daSilva, V. & McIlroy, W. E. Standing still: Is there a role for the cortex? *Neurosci. Lett.* (2015). doi:10.1016/j.neulet.2015.01.055
150. Varghese, J. P., Staines, W. R. & McIlroy, W. E. Activity in Functional Cortical Networks Temporally Associated with Postural Instability. *Neuroscience* (2019). doi:10.1016/j.neuroscience.2019.01.008
151. Adkin, A. L., Quant, S., Maki, B. E. & McIlroy, W. E. Cortical responses associated with predictable and unpredictable compensatory balance reactions. *Exp. Brain Res.* (2006). doi:10.1007/s00221-005-0310-9
152. Payne, A. M., Ting, L. H. & Hajcak, G. Do sensorimotor perturbations to standing balance elicit an error-related negativity? *Psychophysiology* (2019). doi:10.1111/psyp.13359
153. Quant, S., Adkin, A. L., Staines, W. R. & McIlroy, W. E. Cortical activation following a balance disturbance. *Exp. Brain Res.* (2004). doi:10.1007/s00221-003-1744-6
154. Staines, W. R., McIlroy, W. E. & Brooke, J. D. Cortical representation of whole-body movement is modulated by proprioceptive discharge in humans. *Exp. Brain Res.* (2001). doi:10.1007/s002210100691
155. Horak, F. B. & Nashner, L. M. Central programming of postural movements: Adaptation to altered support-surface configurations. *J. Neurophysiol.* (1986). doi:10.1152/jn.1986.55.6.1369
156. Gollhofer, A., Horstmann, G. A., Berger, W. & Dietz, V. Compensation of translational and rotational perturbations in human posture: Stabilization of the centre of gravity. *Neurosci. Lett.* (1989). doi:10.1016/0304-3940(89)90014-1
157. Carpenter, M. G., Allum, J. H. J. & Honegger, F. Directional sensitivity of stretch reflexes and balance corrections for normal subjects in the roll and pitch planes. *Exp. Brain Res.* (1999). doi:10.1007/s002210050940
158. Ramanathan, D. S. *et al.* Low-frequency cortical activity is a neuromodulatory target that tracks recovery after stroke. *Nat. Med.* (2018). doi:10.1038/s41591-018-0058-y
159. Ganguly, K., Dimitrov, D. F., Wallis, J. D. & Carmena, J. M. Reversible large-scale modification of cortical networks during neuroprosthetic control. *Nat. Neurosci.* (2011). doi:10.1038/nn.2797
160. Ganguly, K. & Carmena, J. M. Emergence of a stable cortical map for neuroprosthetic control. *PLoS Biol.* (2009). doi:10.1371/journal.pbio.1000153
161. Zhou, X., Tien, R. N., Ravikumar, S. & Chase, S. M. Distinct types of neural reorganization during long-term learning. *J. Neurophysiol.* (2019). doi:10.1152/jn.00466.2018
162. Foffani, G. & Moxon, K. A. PSTH-based classification of sensory stimuli using ensembles of single neurons. *J. Neurosci. Methods* (2004). doi:10.1016/j.jneumeth.2003.12.011
163. Horak, F. B. & Macpherson, J. M. Postural Orientation and Equilibrium. in *Comprehensive Physiology* (1996). doi:10.1002/cphy.cp120107

164. Orlovsky, G. N., Deliagina, T. G. & Grillner, S. Neuronal Control of Locomotion: From Mollusc to Man (Oxford Neuroscience S): 9780198524052: Medicine & Health Science Books @ Amazon.com. *Oxford University Press* (1999).
165. Massion, J. & Dufosse, M. Coordination Between Posture and Movement: Why and How? *Physiology* (1988). doi:10.1152/physiologyonline.1988.3.3.88
166. Barbeau, H., Ladouceur, M., Mirbagheri, M. M. & Kearney, R. E. The effect of locomotor training combined with functional electrical stimulation in chronic spinal cord injured subjects: Walking and reflex studies. *Brain Research Reviews* (2002). doi:10.1016/S0165-0173(02)00210-2
167. Fung, J. & Macpherson, J. M. Attributes of quiet stance in the chronic spinal cat. *J. Neurophysiol.* (1999). doi:10.1152/jn.1999.82.6.3056
168. Macpherson, J. M. & Fung, J. Weight support and balance during perturbed stance in the chronic spinal cat. *J. Neurophysiol.* (1999). doi:10.1152/jn.1999.82.6.3066
169. Rossignol, S., Bouyer, L., Barthélemy, D., Langlet, C. & Leblond, H. Recovery of locomotion in the cat following spinal cord lesions. *Brain Research Reviews* (2002). doi:10.1016/S0165-0173(02)00208-4
170. Rossignol, S., Drew, T., Brustein, E. & Jiang, W. Locomotor performance and adaptation after partial or complete spinal cord lesions in the cat. *Prog. Brain Res.* (1999). doi:10.1016/s0079-6123(08)62870-8
171. Giuliani, C. A. & Smith, J. L. Development and characteristics of airstepping in chronic spinal cats. *J. Neurosci.* (1985). doi:10.1523/jneurosci.05-05-01276.1985
172. Kellog, W. N., Deese, J. & Pronko, N. H. On the behavior of the lumbo-spinal dog. *J. Exp. Psychol.* (1946). doi:10.1037/h0060016
173. Edgerton, V. R. *et al.* Retraining the injured spinal cord. *Journal of Physiology* (2001). doi:10.1111/j.1469-7793.2001.0015b.x
174. Edgerton, V. R., Tillakaratne, N. J. K., Bigbee, A. J., De Leon, R. D. & Roy, R. R. Plasticity of the spinal neural circuitry after injury. *Annual Review of Neuroscience* (2004). doi:10.1146/annurev.neuro.27.070203.144308
175. Pratt, C. A., Fung, J. & Macpherson, J. M. Stance control in the chronic spinal cat. *J. Neurophysiol.* (1994). doi:10.1152/jn.1994.71.5.1981
176. De Leon, R. D., Tamaki, H., Hodgson, J. A., Roy, R. R. & Edgerton, V. R. Hindlimb locomotor and postural training modulates glycinergic inhibition in the spinal cord of the adult spinal cat. *J. Neurophysiol.* (1999). doi:10.1152/jn.1999.82.1.359
177. Chvatal, S. A., Macpherson, J. M., Torres-Oviedo, G. & Ting, L. H. Absence of postural muscle synergies for balance after spinal cord transection. *J. Neurophysiol.* (2013). doi:10.1152/jn.00038.2013
178. Macpherson, J. M., Fung, J. & Jacobs, R. Postural orientation, equilibrium, and the spinal cord. *Advances in neurology* (1997).
179. Lyalka, V. F., Orlovsky, G. N. & Deliagina, T. G. Impairment of postural control in rabbits with extensive spinal lesions. *J. Neurophysiol.* (2009). doi:10.1152/jn.00009.2008
180. Jiang, W. & Drew, T. Effects of bilateral lesions of the dorsolateral funiculi and dorsal columns

at the level of the low thoracic spinal cord on the control of locomotion in the adult cat. I. Treadmill walking. *J. Neurophysiol.* (1996). doi:10.1152/jn.1996.76.2.849
181. Beloozerova, I. N. *et al.* Activity of different classes of neurons of the motor cortex during postural corrections. *J. Neurosci.* **23**, 7844–53 (2003).
182. Beloozerova, I. N. *et al.* Postural Control in the Rabbit Maintaining Balance on the Tilting Platform. *J. Neurophysiol.* (2003). doi:10.1152/jn.00590.2003
183. Deliagina, T. G., Sirota, M. G., Zelenin, P. V., Orlovsky, G. N. & Beloozerova, I. N. Interlimb postural coordination in the standing cat. *J. Physiol.* (2006). doi:10.1113/jphysiol.2006.104893
184. Musienko, P. E., Zelenin, P. V., Lyalka, V. F., Orlovsky, G. N. & Deliagina, T. G. Postural performance in decerebrated rabbit. *Behav. Brain Res.* (2008). doi:10.1016/j.bbr.2008.02.011
185. Ganzer, P. D., Beringer, C. R., Shumsky, J. S., Nwaobasi, C. & Moxon, K. A. Serotonin receptor and dendritic plasticity in the spinal cord mediated by chronic serotonergic pharmacotherapy combined with exercise following complete SCI in the adult rat. *Exp. Neurol.* (2018). doi:10.1016/j.expneurol.2018.03.006
186. Ghosh, A. *et al.* Functional and anatomical reorganization of the sensory-motor cortex after incomplete spinal cord injury in adult rats. *J. Neurosci.* (2009). doi:10.1523/JNEUROSCI.1828-09.2009
187. Harkema, S. *et al.* Effect of epidural stimulation of the lumbosacral spinal cord on voluntary movement, standing, and assisted stepping after motor complete paraplegia: A case study. *Lancet* (2011). doi:10.1016/S0140-6736(11)60547-3
188. Lavrov, I. *et al.* Facilitation of stepping with epidural stimulation in spinal rats: Role of sensory input. *J. Neurosci.* (2008). doi:10.1523/JNEUROSCI.1069-08.2008
189. Shah, P. K. *et al.* Unique spatiotemporal neuromodulation of the lumbosacral circuitry shapes locomotor success after spinal cord injury. *J. Neurotrauma* **33**, 1709–1723 (2016).
190. Kilkenny, C., Browne, W., Cuthill, I. C., Emerson, M. & Altman, D. G. Editorial: Animal research: Reporting in vivo experiments-The ARRIVE Guidelines. *Journal of Cerebral Blood Flow and Metabolism* (2011). doi:10.1038/jcbfm.2010.220
191. Knudsen, E. B., Flint, R. D. & Moxon, K. A. Encoding of temporal intervals in the rat hindlimb sensorimotor cortex. *Front. Syst. Neurosci.* (2012). doi:10.3389/fnsys.2012.00067
192. Leergaard, T. B. *et al.* Three-dimensional topography of corticopontine projections from rat sensorimotor cortex: Comparisons with corticostriatal projections reveal diverse integrative organization. *J. Comp. Neurol.* (2004). doi:10.1002/cne.20289
193. Moxon, K. A., Hale, L. L., Aguilar, J. & Foffani, G. Responses of infragranular neurons in the rat primary somatosensory cortex to forepaw and hindpaw tactile stimuli. *Neuroscience* (2008). doi:10.1016/j.neuroscience.2008.08.009
194. Kao, T., Shumsky, J. S., Knudsen, E. B., Murray, M. & Moxon, K. A. Functional role of exercise-induced cortical organization of sensorimotor cortex after spinal transection. *J. Neurophysiol.* (2011). doi:10.1152/jn.01017.2010
195. Antri, M., Orsal, D. & Barthe, J. Y. Locomotor recovery in the chronic spinal rat: Effects of long-term treatment with a 5-HT2 agonist. in *European Journal of Neuroscience* (2002). doi:10.1046/j.1460-9568.2002.02088.x

196. Barbeau, H. & Rossignol, S. The effects of serotonergic drugs on the locomotor pattern and on cutaneous reflexes of the adult chronic spinal cat. *Brain Res.* (1990). doi:10.1016/0006-8993(90)90435-E
197. Ichiyama, R. M., Gerasimenko, Y. P., Zhong, H., Roy, R. R. & Edgerton, V. R. Hindlimb stepping movements in complete spinal rats induced by epidural spinal cord stimulation. *Neurosci. Lett.* (2005). doi:10.1016/j.neulet.2005.04.049
198. Lavrov, I. *et al.* Plasticity of spinal cord reflexes after a complete transection in adult rats: Relationship to stepping ability. *J. Neurophysiol.* (2006). doi:10.1152/jn.00325.2006
199. Sławińska, U., Majczyński, H., Dai, Y. & Jordan, L. M. The upright posture improves plantar stepping and alters responses to serotonergic drugs in spinal rats. *J. Physiol.* (2012). doi:10.1113/jphysiol.2011.224931
200. Rath, M. *et al.* Trunk Stability Enabled by Noninvasive Spinal Electrical Stimulation after Spinal Cord Injury. *J. Neurotrauma* **35**, 2540–2553 (2018).
201. Adkins, D. A. L., Boychuk, J., Remple, M. S. & Kleim, J. A. Motor training induces experience-specific patterns of plasticity across motor cortex and spinal cord. *Journal of Applied Physiology* (2006). doi:10.1152/japplphysiol.00515.2006
202. Dietz, V., Horstmann, G. A. & Berger, W. Interlimb coordination of leg-muscle activation during perturbation of stance in humans. *J. Neurophysiol.* (1989). doi:10.1152/jn.1989.62.3.680
203. Dietz, V., Quintern, J., Berger, W. & Schenck, E. Cerebral potentials and leg muscle e.m.g. responses associated with stance perturbation. *Exp. Brain Res.* (1985). doi:10.1007/BF00236540
204. Fujio, K., Obata, H., Kitamura, T., Kawashima, N. & Nakazawa, K. Corticospinal excitability is modulated as a function of postural perturbation predictability. *Front. Hum. Neurosci.* (2018). doi:10.3389/fnhum.2018.00068
205. Jacobs, J. V *et al.* Changes in the activity of the cerebral cortex relate to postural response modification when warned of a perturbation. *Clin. Neurophysiol.* **119**, 1431–42 (2008).
206. Allen, G. I., Azzena, G. B. & Ohno, T. Somatotopically organized inputs from fore- and hindlimb areas of sensorimotor cortex to cerebellar Purkyně cells. *Exp. Brain Res.* (1974). doi:10.1007/BF00238316
207. Azzena, G. B., Mameli, O. & Tolu, E. Convergence of central and peripheral signals on vestibular cells. *Acta Otolaryngol.* (1983). doi:10.3109/00016488309130942
208. Landgren, S. & Silfvenius, H. Nucleus Z, the medullary relay in the projection path to the cerebral cortex of group I muscle afferents from the cat's hind limb. *J. Physiol.* (1971). doi:10.1113/jphysiol.1971.sp009633
209. Sakamoto, T., Porter, L. L. & Asanuma, H. Long-lasting potentiation of synaptic potentials in the motor cortex produced by stimulation of the sensory cortex in the cat: a basis of motor learning. *Brain Res.* (1987). doi:10.1016/0006-8993(87)91029-8
210. Ashe, J. & Georgopoulos, A. P. Movement parameters and neural activity in motor cortex and area 5. *Cereb. Cortex* (1994). doi:10.1093/cercor/4.6.590
211. Moran, D. W. & Schwartz, A. B. Motor Cortical Representation of Speed and Direction

During Reaching Motor Cortical Representation of Speed and Direction During Reaching. *J Neurophysiol* **82**, 2676–2692 (1999).
212. Pinto, D. J., Brumberg, J. C. & Simons, D. J. Circuit dynamics and coding strategies in rodent somatosensory cortex. *J. Neurophysiol.* (2000). doi:10.1152/jn.2000.83.3.1158
213. Ganzer, P. D. *et al.* Closed-loop neuromodulation restores network connectivity and motor control after spinal cord injury. *Elife* (2018). doi:10.7554/eLife.32058
214. Krucoff, M. O., Rahimpour, S., Slutzky, M. W., Edgerton, V. R. & Turner, D. A. Enhancing Nervous System Recovery through Neurobiologics, Neural Interface Training, and Neurorehabilitation. *Front. Neurosci.* **10**, 584 (2016).
215. Sayenko, D. G. *et al.* Vestibulospinal and Corticospinal Modulation of Lumbosacral Network Excitability in Human Subjects. *Front. Physiol.* **9**, 1746 (2018).
216. Taccola, G. *et al.* Acute neuromodulation restores spinally-induced motor responses after severe spinal cord injury. *Exp. Neurol.* **327**, 113246 (2020).
217. Taccola, G., Sayenko, D., Gad, P., Gerasimenko, Y. & Edgerton, V. R. And yet it moves: Recovery of volitional control after spinal cord injury. *Prog. Neurobiol.* **160**, 64–81 (2018).
218. Kim, S. P. *et al.* Point-and-click cursor control with an intracortical neural interface system by humans with tetraplegia. *IEEE Trans. Neural Syst. Rehabil. Eng.* (2011). doi:10.1109/TNSRE.2011.2107750
219. Gallego, J. A., Perich, M. G., Chowdhury, R. H., Solla, S. A. & Miller, L. E. Long-term stability of cortical population dynamics underlying consistent behavior. *Nat. Neurosci.* (2020). doi:10.1038/s41593-019-0555-4
220. Basso, D. M., Beattie, M. S. & Bresnahan, J. C. A Sensitive and Reliable Locomotor Rating Scale for Open Field Testing in Rats. *J. Neurotrauma* (1995). doi:10.1089/neu.1995.12.1
221. Kononenko, I. Estimating Attributes: Analysis and Extensions of RELIEF. in *European Conference on Machine Learning* (1994).
222. Hamers, F. P. T., Lankhorst, A. J., Van Laar, T. J., Veldhuis, W. B. & Gispen, W. H. Automated quantitative gait analysis during overground locomotion in the rat: Its application to spinal cord contusion and transection injuries. *J. Neurotrauma* (2001). doi:10.1089/08977150150502613
223. Rigosa, J. *et al.* Decoding bipedal locomotion from the rat sensorimotor cortex. *J. Neural Eng.* (2015). doi:10.1088/1741-2560/12/5/056014
224. Wu, W. *et al.* Neural decoding of cursor motion using a Kalman filter. in *Advances in Neural Information Processing Systems* (2003).
225. Elsayed, G. F. & Cunningham, J. P. Structure in neural population recordings: An expected byproduct of simpler phenomena? *Nat. Neurosci.* (2017). doi:10.1038/nn.4617
226. Andersen, R. A. & Aflalo, T. Preserved cortical somatotopic and motor representations in tetraplegic humans. *Curr. Opin. Neurobiol.* **74**, 102547 (2022).
227. Sadtler, P. T. *et al.* Neural constraints on learning. *Nature* (2014). doi:10.1038/nature13665
228. Hwang, E. J., Bailey, P. M. & Andersen, R. A. Volitional control of neural activity relies on the natural motor repertoire. *Curr. Biol.* (2013). doi:10.1016/j.cub.2013.01.027
229. Makin, T. R. & Bensmaia, S. J. Stability of Sensory Topographies in Adult Cortex. *Trends in*

Cognitive Sciences (2017). doi:10.1016/j.tics.2017.01.002
230. Makin, T. R. *et al.* Phantom pain is associated with preserved structure and function in the former hand area. *Nat. Commun.* (2013). doi:10.1038/ncomms2571
231. Flesher, S. N. *et al.* Intracortical microstimulation of human somatosensory cortex. *Sci. Transl. Med.* (2016). doi:10.1126/scitranslmed.aaf8083
232. Guan, C. *et al.* Stability of motor representations after paralysis. *Elife* **11**, e74478 (2022).
233. Dekleva, B. M. *et al.* Motor cortex retains and reorients neural dynamics during motor imagery. *bioRxiv* 2023.01.17.524394 (2023). doi:10.1101/2023.01.17.524394
234. Montijn, J. S., Meijer, G. T., Lansink, C. S. & Pennartz, C. M. A. Population-Level Neural Codes Are Robust to Single-Neuron Variability from a Multidimensional Coding Perspective. *Cell Rep.* (2016). doi:10.1016/j.celrep.2016.07.065
235. Chambers, A. R., Aschauer, D. F., Eppler, J.-B., Kaschube, M. & Rumpel, S. A stable sensory map emerges from a dynamic equilibrium of neurons with unstable tuning properties. *Cereb. Cortex* bhac445 (2022). doi:10.1093/cercor/bhac445
236. Slomowitz, E. *et al.* Interplay between population firing stability and single neuron dynamics in hippocampal networks. *Elife* (2015). doi:10.7554/eLife.04378
237. Rokni, U., Richardson, A. G., Bizzi, E. & Seung, H. S. Motor Learning with Unstable Neural Representations. *Neuron* (2007). doi:10.1016/j.neuron.2007.04.030
238. Carmena, J. M., Lebedev, M. A., Henriquez, C. S. & Nicolelis, M. A. L. Stable ensemble performance with single-neuron variability during reaching movements in primates. *J. Neurosci.* (2005). doi:10.1523/JNEUROSCI.2772-05.2005
239. Barrett, D. G. T., Denève, S. & Machens, C. K. Optimal compensation for neuron loss. *Elife* (2016). doi:10.7554/eLife.12454
240. Carmena, J. M. *et al.* Learning to control a brain-machine interface for reaching and grasping by primates. *PLoS Biol.* (2003). doi:10.1371/journal.pbio.0000042
241. Foffani, G. & Moxon, K. A. PSTH-based classification of sensory stimuli using ensembles of single neurons. *J. Neurosci. Methods* **135**, 107–120 (2004).
242. Capogrosso, M. *et al.* A computational model for epidural electrical stimulation of spinal sensorimotor circuits. *J. Neurosci.* (2013). doi:10.1523/JNEUROSCI.1688-13.2013
243. McCrea, D. A. Spinal circuitry of sensorimotor control of locomotion. *Journal of Physiology* (2001). doi:10.1111/j.1469-7793.2001.0041b.x
244. Gerasimenko, Y. *et al.* Novel and direct access to the human locomotor spinal circuitry. *J. Neurosci.* (2010). doi:10.1523/JNEUROSCI.4751-09.2010
245. Minassian, K. *et al.* Stepping-like movements in humans with complete spinal cord injury induced by epidural stimulation of the lumbar cord: Electromyographic study of compound muscle action potentials. *Spinal Cord* (2004). doi:10.1038/sj.sc.3101615
246. Lavrov, I. *et al.* Epidural stimulation induced modulation of spinal locomotor networks in adult spinal rats. *J. Neurosci.* (2008). doi:10.1523/JNEUROSCI.0080-08.2008
247. Grillner, S. & Shik, M. L. On the Descending Control of the Lumbosacral Spinal Cord from the "Mesencephalic Locomotor Region". *Acta Physiol. Scand.* (1973). doi:10.1111/j.1748-1716.1973.tb05396.x

248. Zelenin, P. V., Lyalka, V. F., Hsu, L. J., Orlovsky, G. N. & Deliagina, T. G. Effects of reversible spinalization on individual spinal neurons. *J. Neurosci.* (2013). doi:10.1523/JNEUROSCI.2394-13.2013
249. Sherrington, C. S. Flexion-reflex of the limb, crossed extension-reflex, and reflex stepping and standing. *J. Physiol.* (1910). doi:10.1113/jphysiol.1910.sp001362
250. Rudolf Magnus (1873–1927) physiology of posture. *JAMA J. Am. Med. Assoc.* (1968). doi:10.1001/jama.1968.03140370091023
251. Zelenin, P. V., Beloozerova, I. N., Sirota, M. G., Orlovsky, G. N. & Deliagina, T. G. Activity of red nucleus neurons in the cat during postural corrections. *J. Neurosci.* (2010). doi:10.1523/JNEUROSCI.2991-10.2010
252. Horak, F. B., Buchanan, J., Creath, R. & Jeka, J. Vestibulospinal control of posture. in *Advances in Experimental Medicine and Biology* (2002). doi:10.1007/978-1-4615-0713-0_17
253. Tanaka, H. *et al.* Posture influences on vestibulospinal tract excitability. *Exp. Brain Res.* (2021). doi:10.1007/s00221-021-06033-8
254. Nyberg-Hansen, R. & Mascitti, T. A. Sites and mode of termination of fibers of the vestibulospinal tract in the cat. An experimental study with silver impregnation methods. *J. Comp. Neurol.* (1964). doi:10.1002/cne.901220307
255. Murray, A. J., Croce, K., Belton, T., Akay, T. & Jessell, T. M. Balance Control Mediated by Vestibular Circuits Directing Limb Extension or Antagonist Muscle Co-activation. *Cell Rep.* (2018). doi:10.1016/j.celrep.2018.01.009
256. Cucu, A. I. *et al.* The brainstem and its neurosurgical history. *Neurosurgical Review* (2021). doi:10.1007/s10143-021-01496-3
257. Párraga, R. G. *et al.* Microsurgical anatomy and internal architecture of the brainstem in 3D images: Surgical considerations. *J. Neurosurg.* (2016). doi:10.3171/2015.4.JNS132778
258. Edgerton, B. J., House, W. F. & Hitselberger, W. Hearing by cochlear nucleus stimulation in humans. *Ann. Otol. Rhinol. Laryngol.* (1982).
259. Brockett, A. T., Hricz, N. W., Tennyson, S. S., Bryden, D. W. & Roesch, M. R. Neural Signals in Red Nucleus during Reactive and Proactive Adjustments in Behavior. *J. Neurosci.* (2020). doi:10.1523/JNEUROSCI.2775-19.2020
260. Márton, G. *et al.* A silicon-based microelectrode array with a microdrive for monitoring brainstem regions of freely moving rats. *J. Neural Eng.* (2016). doi:10.1088/1741-2560/13/2/026025
261. Pomberger, T. & Hage, S. R. Semi-chronic laminar recordings in the brainstem of behaving marmoset monkeys. *J. Neurosci. Methods* (2019). doi:10.1016/j.jneumeth.2018.10.026
262. Shaikh, A. G., Meng, H. & Angelaki, D. E. Multiple reference frames for motion in the primate cerebellum. *J. Neurosci.* (2004). doi:10.1523/JNEUROSCI.0109-04.2004
263. Horak, F. B. & Diener, H. C. Cerebellar control of postural scaling and central set in stance. *J. Neurophysiol.* (1994). doi:10.1152/jn.1994.72.2.479
264. Timmann, D. & Horak, F. B. Prediction and set-dependent scaling of early postural responses in cerebellar patients. *Brain* (1997). doi:10.1093/brain/120.2.327
265. Mummel, P. *et al.* Postural responses to changing task conditions in patients with cerebellar

lesions. *J. Neurol. Neurosurg. Psychiatry* (1998). doi:10.1136/jnnp.65.5.734
266. Büttner, U. *et al.* Multimodal signal integration in vestibular neurons of the primate fastigial nucleus. in *Annals of the New York Academy of Sciences* (2003). doi:10.1196/annals.1303.021
267. McCall, A. A., Miller, D. J., Catanzaro, M. F., Cotter, L. A. & Yates, B. J. Hindlimb movement modulates the activity of rostral fastigial nucleus neurons that process vestibular input. *Exp. Brain Res.* (2015). doi:10.1007/s00221-015-4311-z
268. Stecina, K., Fedirchuk, B. & Hultborn, H. Information to cerebellum on spinal motor networks mediated by the dorsal spinocerebellar tract. *Journal of Physiology* (2013). doi:10.1113/jphysiol.2012.249110
269. White, J. J. & Sillitoe, R. V. Genetic silencing of olivocerebellar synapses causes dystonia-like behaviour in mice. *Nat. Commun.* (2017). doi:10.1038/ncomms14912
270. Cooperrider, J. *et al.* Chronic deep cerebellar stimulation promotes long-term potentiation, microstructural plasticity, and reorganization of perilesional cortical representation in a rodent model. *J. Neurosci.* (2014). doi:10.1523/JNEUROSCI.0953-14.2014
271. Machado, A. G., Baker, K. B., Schuster, D., Butler, R. S. & Rezai, A. Chronic electrical stimulation of the contralesional lateral cerebellar nucleus enhances recovery of motor function after cerebral ischemia in rats. *Brain Res.* (2009). doi:10.1016/j.brainres.2009.05.007
272. Galanda, M., Mistina, L. & Zoltan, O. Behavioural responses to cerebellar stimulation in cerebral palsy. *Acta Neurochir. Suppl. (Wien).* (1989). doi:10.1007/978-3-7091-9029-6_8
273. Werhahn, K. J., Taylor, J., Ridding, M., Meyer, B. U. & Rothwell, J. C. Effect of transcranial magnetic stimulation over the cerebellum on the excitability of human motor cortex. *Electroencephalogr. Clin. Neurophysiol. - Electromyogr. Mot. Control* (1996). doi:10.1016/0013-4694(95)00213-8
274. Cooper, I. S. Chronic Cerebellar Stimulation in Epilepsy. *Arch. Neurol.* (1976). doi:10.1001/archneur.1976.00500080037006
275. Slaughter, D. G., Nashold, B. S. & Somjen, G. G. Electrical recording with micro- and macroelectrodes from the cerebellum of man. *J. Neurosurg.* (1970). doi:10.3171/jns.1970.33.5.0524
276. Wolfe, J. W., Rawlings, C. A. & Llinás, R. R. A procedure for chronic microelectrode recording from cerebellar cortex in the awake cat and monkey. *Physiol. Behav.* (1973). doi:10.1016/0031-9384(73)90068-1
277. Christie, J. M. & Gaffield, M. A. The cerebellum encodes and influences the initiation and termination of discontinuous movements. *bioRxiv* (2021).
278. Vos, B. P., Wijnants, M., Taeymans, S. & De Schutter, E. Miniature carrier with six independently moveable electrodes for recording of multiple single-units in the cerebellar cortex of awake rats. in *Journal of Neuroscience Methods* (1999). doi:10.1016/S0165-0270(99)00122-3
279. Hsu, L. J., Zelenin, P. V., Orlovsky, G. N. & Deliagina, T. G. Effects of galvanic vestibular stimulation on postural limb reflexes and neurons of spinal postural network. *J. Neurophysiol.* (2012). doi:10.1152/jn.00041.2012
280. Inglis, J. T. & MacPherson, J. M. Bilateral labyrinthectomy in the cat: Effects on the postural

response to translation. *J. Neurophysiol.* (1995). doi:10.1152/jn.1995.73.3.1181
281. Debnath, S., Bauman, M. J., Fisher, L. E., Weber, D. J. & Gaunt, R. A. Microelectrode array recordings from the ventral roots in chronically implanted cats. *Front. Neurol.* (2014). doi:10.3389/fneur.2014.00104
282. Bauman, M. J., Bruns, T. M., Wagenaar, J. B., Gaunt, R. A. & Weber, D. J. Online feedback control of functional electrical stimulation using dorsal root ganglia recordings. in *Proceedings of the Annual International Conference of the IEEE Engineering in Medicine and Biology Society, EMBS* (2011). doi:10.1109/IEMBS.2011.6091831
283. Holinski, B. J., Everaert, D. G., Mushahwar, V. K. & Stein, R. B. Real-time control of walking using recordings from dorsal root ganglia. *J. Neural Eng.* (2013). doi:10.1088/1741-2560/10/5/056008
284. Prasad, A. & Sahin, M. Chronic recordings from the rat spinal cord descending tracts with microwires. in *Proceedings of the Annual International Conference of the IEEE Engineering in Medicine and Biology Society, EMBS* (2011). doi:10.1109/IEMBS.2011.6090821
285. Prasad, A. & Sahin, M. Characterization of neural activity recorded from the descending tracts of the rat spinal cord. *Front. Neurosci.* (2010). doi:10.3389/fnins.2010.00021
286. Vidaurre, C., Sannelli, C., Müller, K. R. & Blankertz, B. Machine-learning-based coadaptive calibration for Brain-computer interfaces. *Neural Computation* (2011). doi:10.1162/NECO_a_00089
287. Mondello, S. E., Kasten, M. R., Horner, P. J. & Moritz, C. T. Therapeutic intraspinal stimulation to generate activity and promote long-term recovery. *Front. Neurosci.* **8**, 1–7 (2014).
288. Dougherty, J. B., Goodman, J. M., Knudsen, E. B. & Moxon, K. A. Controlled unilateral isometric force generated by epidural spinal cord stimulation in the rat hindlimb. *IEEE Trans. Neural Syst. Rehabil. Eng.* (2012). doi:10.1109/TNSRE.2012.2190424
289. Yang, Y., Connolly, A. T. & Shanechi, M. M. A control-theoretic system identification framework and a real-time closed-loop clinical simulation testbed for electrical brain stimulation. *J. Neural Eng.* (2018). doi:10.1088/1741-2552/aad1a8
290. Wenger, N. *et al.* Spatiotemporal neuromodulation therapies engaging muscle synergies improve motor control after spinal cord injury. *Nat. Med.* (2016). doi:10.1038/nm.4025
291. Trautmann, E. M. *et al.* Accurate Estimation of Neural Population Dynamics without Spike Sorting. *Neuron* (2019). doi:10.1016/j.neuron.2019.05.003
292. Flint, R. D., Wright, Z. A., Scheid, M. R. & Slutzky, M. W. Long term, stable brain machine interface performance using local field potentials and multiunit spikes. *J. Neural Eng.* (2013). doi:10.1088/1741-2560/10/5/056005
293. Yeom, H. G., Kim, J. S. & Chung, C. K. High-accuracy brain-machine interfaces using feedback information. *PLoS One* (2014). doi:10.1371/journal.pone.0103539
294. Velliste, M., Perel, S., Spalding, M. C., Whitford, A. S. & Schwartz, A. B. Cortical control of a prosthetic arm for self-feeding. *Nature* (2008). doi:10.1038/nature06996
295. Flesher, S. N. *et al.* A brain-computer interface that evokes tactile sensations improves robotic arm control. *Science (80-.).* (2021). doi:10.1126/science.abd0380

296. Ozdemir, R. A., Goel, R., Reschke, M. F., Wood, S. J. & Paloski, W. H. Critical Role of Somatosensation in Postural Control Following Spaceflight: Vestibularly Deficient Astronauts Are Not Able to Maintain Upright Stance During Compromised Somatosensation. *Front. Physiol.* (2018). doi:10.3389/fphys.2018.01680
297. Fetz, E. E. Volitional control of neural activity: Implications for brain-computer interfaces. in *Journal of Physiology* (2007). doi:10.1113/jphysiol.2006.127142
298. Francis, J. T. & Song, W. Neuroplasticity of the sensorimotor cortex during learning. *Neural Plast.* (2011). doi:10.1155/2011/310737
299. Wessberg, J. *et al.* Real-time prediction of hand trajectory by ensembles of cortical neurons in primates. *Nature* (2000). doi:10.1038/35042582